

อนุภาคนาโนจากอนุพันธ์ซินนามेतของพอลิไวนิลแอลกอฮอล์



นางสาวชุลีพร ลวดทอง

สถาบันวิทยบริการ จุฬาลงกรณ์มหาวิทยาลัย

วิทยานิพนธ์นี้เป็นส่วนหนึ่งของการศึกษาตามหลักสูตรปริญญาวิทยาศาสตรมหาบัณฑิต

สาขาวิชาเคมี ภาควิชาเคมี

คณะวิทยาศาสตร์ จุฬาลงกรณ์มหาวิทยาลัย

ปีการศึกษา 2550

ลิขสิทธิ์ของจุฬาลงกรณ์มหาวิทยาลัย

NANOPARTICLES FROM CINNAMATE DERIVATIVES
OF POLY(VINYL ALCOHOL)



Miss Chuleeporn Luadthong

สถาบันวิทยบริการ
จุฬาลงกรณ์มหาวิทยาลัย

A Thesis Submitted in Partial Fulfillment of the Requirements

for the Degree of Master of Science Program in Chemistry

Department of Chemistry

Faculty of Science

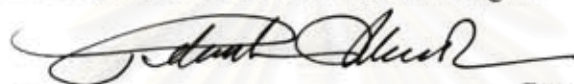
Chulalongkorn University

Academic year 2007

Copyright of Chulalongkorn University

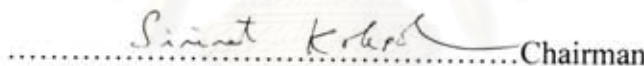
Thesis Title NANOPARTICLES FROM CINNAMATE DERIVATIVES OF
 POLY(VINYL ALCOHOL)
By Miss Chuleeporn Luadthong
Field of Study Chemistry
Thesis Advisor Associate Professor Supason Wanichwecharungruang, Ph.D.

Accepted by the Faculty of Science, Chulalongkorn University in Partial
Fulfillment of the Requirements for the Master's Degree

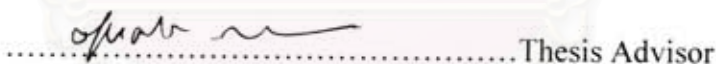


.....Dean of the Faculty of Science
(Professor Piamsak Menasveta, Ph.D.)

THESIS COMMITTEE



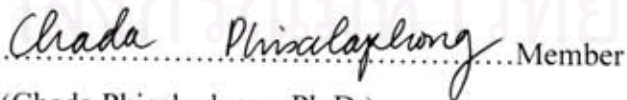
.....Chairman
(Associate Professor Sirirat Kokpol, Ph.D.)



.....Thesis Advisor
(Associate Professor Supason Wanichwecharungruang, Ph.D.)



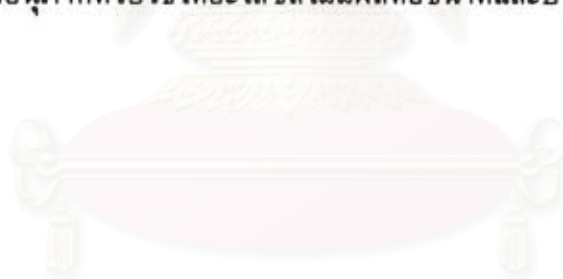
.....Member
(Associate Professor Nuanphun Chantarasiri, Ph.D.)



.....Member
(Chada Phisalaphong, Ph.D.)

ชูลีพร ลวดทอง : อนุภาคนาโนจากอนุพันธ์ซินนามेटของพอลิไวนิลแอลกอฮอล์
(NANOPARTICLES FROM CINNAMATE DERIVATIVES OF
POLY(VINYL ALCOHOL) อ. ที่ปรึกษา : รศ. ดร. ศุภศร วณิชเวชารุ่งเรือง, 92
หน้า

ได้ทำการศึกษาเกี่ยวกับปัจจัยที่มีผลต่อการเกิดและลักษณะของอนุภาคที่เกิดขึ้นเตรียมสารพอลิ(ไวนิลแอลกอฮอล์-โค-ไวนิลซินนามेट), พอลิ(ไวนิลแอลกอฮอล์-โค-ไวนิล-4-เมททอกซีซินนามेट), พอลิ(ไวนิลแอลกอฮอล์-โค-ไวนิล-2,4-ไดเมททอกซีซินนามेट) และ พอลิ(ไวนิลแอลกอฮอล์-โค-ไวนิล-2,4,5-ไตรเมททอกซีซินนามेट) จากปฏิกิริยาเอสเทอร์ฟิเคชัน สารอนุพันธ์ซินนามेटของพอลิไวนิลแอลกอฮอล์สามารถเกิดการประกอบตัวเองขึ้นเป็นอนุภาคโดยผ่านกระบวนการไดอะไลซิส จากการทดลองพบว่าเปอร์เซ็นต์การแทนที่ของอนุพันธ์ซินนามेटในโพลีเมอร์พอลิไวนิลแอลกอฮอล์มีผลสวนทางต่อขนาดอนุภาค แต่แปรผันตรงต่อค่าประจุบนพื้นผิวของอนุภาค ขนาดของอนุภาคลดลงเมื่อความเข้มข้นของพอลิเมอร์ที่สังเคราะห์ลดลง ในขั้นตอนการประกอบตัวเองขึ้นเป็นอนุภาค อย่างไรก็ตามน้ำหนักโมเลกุลของสายโซ่ไวนิลแอลกอฮอล์ โครงสร้างของกรดซินนามิกที่ติดบนสายโซ่พอลิไวนิลแอลกอฮอล์และตัวทำละลายที่ใช้ในการเตรียมอนุภาคด้วยวิธีไดอะไลซิสไม่มีผลต่อขนาดและประจุบนพื้นผิวของอนุภาค



สถาบันวิทยบริการ จุฬาลงกรณ์มหาวิทยาลัย

ภาควิชา.....เคมี..... ลายมือชื่อนิสิต.....ชูลีพร ลวดทอง.....
สาขาวิชา.....เคมี..... ลายมืออาจารย์ที่ปรึกษา.....
ปีการศึกษา.....2550.....

4872273723: MAJOR CHEMISTRY

KEY WORD: Amphiphilic copolymer / Substituted PV(OH) nanoparticles

CHULEEPORN LUADTHONG: NANOPARTICLES FROM CINNAMATE DERIVATIVES OF POLY(VINYL ALCOHOL). THESIS ADVISOR: ASSOC. PROF. SUPASON WANICHWECHARUNGRUANG, Ph.D., 92 PP.

The factors affecting nanoparticle formation and particle's morphology were studied. Amphiphilic poly(vinylalcohol-co-vinylcinnamate), poly(vinylalcohol-co-vinyl-4-methoxycinnamate), poly(vinylalcohol-co-vinyl-2,4-dimethoxycinnamate) and poly(vinylalcohol-co-vinyl-2,4,5-trimethoxycinnamate) were prepared using esterification reaction. Poly(vinylalcohol-co-vinylcinnamate) derivatives were able to self-assemble into nanoparticles through dialysis method. It was found that the degree of substitution (DS) of cinnamoyl moieties on PV(OH) backbone inversely correlated with particle's sizes, but directly correlated with surface-charges of the particles. Particles's sizes also decreased with the decrease in polymer concentration during self-assembly process. However, molecular weight of PV(OH) backbone, cinnamic acid structure grafted onto PV(OH) backbone and the solvent selected to prepare the obtained particles by dialysis method had no effect on the particle's sizes and surface charges of the particles.

สถาบันวิทยบริการ
จุฬาลงกรณ์มหาวิทยาลัย

Department.....Chemistry..... Student's signature..... *Chuleeporn Luadthong*.....
Field of study.....Chemistry..... Advisor's signature..... *[Signature]*.....
Academic year....2007.....

ACKNOWLEDGEMENTS

I have many people to thank for their help and encouragement for this project. First of all, I would like to express my deeply – say many thanks to my beloved advisor, Associate Professor Dr. Supason Wanichweacharungruang, for all her valuable suggestions, guidance, and encouragement all throughout my study.

I am also grateful to the other members of my committee, Associate Professor Dr. Sirirat Kokpol, Associate Professor Dr. Nuanphan Chantarasiri and Dr. Chada Phisalaphong for their comments, technical guidelines, and advice given to me for the completion of my thesis work.

Moreover, I also special acknowledge all members of research group for the good working environment, helpful, opinion, and encouragement.

Most importantly, I would like to express my deepest gratitude to my parent and relatives for their love, continued help, support, encouragement and endless patience they always give me. Without all of them as mentioned, this thesis would not be possible.



สถาบันวิทยบริการ
จุฬาลงกรณ์มหาวิทยาลัย

CONTENTS

	Page
Abstract in Thai.....	iv
Abstract in English.....	v
Acknowledgements.....	vi
List of Schemes.....	ix
List of Figures.....	ix
List of Table.....	xiv
List of Abbreviations.....	xv
CHAPTER I INTRODUCTION.....	1
1.1 Polymeric nanoparticles.....	1
1.2 Poly(vinyl alcohol).....	4
1.3 Cinnamic acid derivative.....	7
1.4 Literature Review.....	8
CHAPTER II EXPERIMENTAL.....	13
2.1 Materials and Chemicals.....	13
2.2 Instruments and Equipments.....	13
2.3 Synthesis of <i>trans</i> -substituted cinnamic acids.....	14
2.4 Synthesis of poly(vinylalcohol-co-vinylcinnamate) derivative.....	16
2.5 Preparation of the substituted polymeric nanoparticles.....	21
2.6 General procedure for molar absorptivity measurements.....	21
CHAPTER III RESULT AND DISCUSSION.....	22
3.1 Synthesis of <i>trans</i> -substituted cinnamic acid derivatives.....	22
3.2 Synthesis of poly(vinylalcohol-co-vinylcinnamate).....	22
3.3 Synthesis of poly(vinylalcohol-co-vinyl-4-methoxycinnamate).....	32
3.4 Synthesis of poly(vinylalcohol-co-vinyl-2,4-dimethoxycinnamate).....	42
3.5 Synthesis of poly(vinylalcohol-co-vinyl-2,4,5-trimethoxycinnamate)...	44
3.6 Effects of solvent used in the self-assembly process.....	50
3.7 Effects of anti-solvent used in the self-assembly process.....	51
3.8 Nanoparticles Stability in various pH of phosphate buffer solution.....	52

CHAPTER IV CONCLUSIONS.....	55
REFERENCES.....	57
APPENDICES.....	63
VITA.....	92



สถาบันวิทยบริการ
จุฬาลงกรณ์มหาวิทยาลัย

List of Schemes

Schemes	Page
Scheme 2.1 Synthetic pathway of <i>trans</i> -substituted cinnamic acids.....	14
Scheme 2.2 Synthetic pathway of poly(vinylalcohol-co-vinylcinnamate) derivatives.....	17

List of Figures

Figures	Page
Figure 1.1 Schematic representation of the intestinal epithelium with a view of a Peyer's patch and detail of the follicle associated epithelium.....	3
Figure 1.2 Synthesis of poly(vinyl alcohol).....	5
Figure 1.3 Scanning electron micrograph of the PV(OH) hydrogel nanoparticles.....	8
Figure 1.4 Scanning electron micrograph of PLGA-PV(OH) composite microsphere (a) the internal structure and distribution of the PV(OH) nanoparticle inside (b).....	9
Figure 1.5 Transmission electron micrograph of poly(2-sulfobutyl-vinylalcohol)- <i>g</i> -poly(lactide-co-glycolides) nanoparticles.....	9
Figure 1.6 Scanning electron micrograph of free PLGA nanoparticles loaded with dexamethasone (a) PLGA nanoparticles entrapped into the dextran-PV(OH) hydrogel (b).....	10
Figure 1.7 Scanning electron micrograph of the PV(OH)-DNA nanoparticles.....	11
Figure 1.8 Scanning electron micrograph of the polyvinylalcohol substituted with oleylamine.....	11
Figure 1.9 Scanning electron micrograph of PV(OH)-graft-poly(lactide-co-glycolide) nanoparticles.....	12

Figure 2.1 Structure and nomenclature of the synthesized substituted cinnamic acids.....	15
Figure 3.1 UV absorption spectra of 200 ppm (in DMSO) of PV(OH) (124000 Dalton) (a) and 10 ppm (in DMSO) of poly(vinylalcohol-co-vinyl cinnamate) PA1 (b), PA2 (c) and PA3 (d).....	25
Figure 3.2 Morphology of poly(vinyl alcohol) (Mw 124,000-186,000), PV(OH)124K , PA1 particles, PA2 particles and PA3 particles. All images were obtained by SEM except that of PA1 particles which was obtained by TEM.....	26
Figure 3.3 Size distribution (a), Average of hydrodynamic diameter (b) and Zeta-potential of various degree of substituted of poly(vinylalcohol-co-vinylcinnamate) nanoparticles.....	28
Figure 3.4 Scanning electron micrographs of PA3 nanoparticles prepared from concentrations of 6 ppm (a), 60 ppm (b), 600 ppm (c), 6,000 ppm (d), 12,000 ppm (e).....	30
Figure 3.5 Schematic representation of particles at lower polymers concentration (a) and higher polymers concentration (b).....	31
Figure 3.6 UV absorption spectra of poly(vinylalcohol-co-vinyl-4-methoxy cinnamate):200 ppm (in DMSO) of PB1 (a) and 20 ppm (in DMSO) of PB2 (b), PB3 (c) and PB4 (d).....	34
Figure 3.7 Morphology of PB1 particles, PB2 particles, PB3 particles and PB4 particles. PB1 and PB2 images were obtained by SEM except that of PB1 particles and PB2 particles which were obtained by TEM.....	36
Figure 3.8 Morphology of loosely packed particles of poly(vinylalcohol-co-vinyl-4-methoxycinnamate) (a,b) and red blood cell (c).....	37
Figure 3.9 Size distribution (a), Average of hydrodynamic diameter (b) and Zeta-potential of various degree of substituted of poly(vinylalcohol-co-vinyl-4-methoxycinnamate) nanoparticles.....	38
Figure 3.10 Scanning electron micrographs of PB3 nanoparticles prepared from concentrations of 6 ppm (a), 60 ppm (b), 600 ppm (c), 6,000 ppm (d), 12,000 ppm (e).....	40

Figure 3.11 Scanning electron micrographs of PB4 nanoparticles prepared from concentrations of 6 ppm (a), 60 ppm (b), 600 ppm (c), 6,000 ppm (d), 12,000 ppm (e).....	41
Figure 3.12 UV absorption spectrum of 20 ppm (in DMSO) of poly(vinylalcohol-co-vinyl-2,4-dimethoxycinnamate) polymer.....	43
Figure 3.13 Scanning electron micrograph of poly(vinylalcohol-co-vinyl-2,4-dimethoxycinnamate) nanoparticles (PC).....	43
Figure 3.14 UV absorption spectrum of 20 ppm (in DMSO) of poly(vinylalcohol-co-vinyl-2,4,5-trimethoxycinnamate) polymer.....	45
Figure 3.15 Scanning electron micrographs of poly(vinylalcohol-co-vinyl-2,4,5-trimethoxycinnamate) nanoparticles (PD).....	45
Figure 3.16 Size distribution (a) and Zeta-potential (b) of various <i>trans</i> -substituted cinnamic acid derivatives of poly(vinylalcohol-co-vinylcinnamate) nanoparticles.....	46
Figure 3.17 Scanning electron micrographs of poly(vinylalcohol-co-vinylcinnamate) prepared from PV(OH)50,000 Daltons (P_xB) and PV(OH)10,000 Daltons (P_yB).....	49
Figure 3.18 Size distribution (a), Average of hydrodynamic diameter (b) and Zeta-potential of various Molecular weight of PV(OH) of poly(vinylalcohol-co-vinyl-4-methoxycinnamate) nanoparticles.....	50
Figure 3.19 Scanning electron micrographs of poly(vinylalcohol-co-vinyl-4-methoxycinnamate) nanoparticles (PB4) prepared from DMF (a) and DMSO (b) using as the solvent.....	51
Figure 3.20 Scanning electron micrographs of PB4 prepared from water (Milli-Q [®]) (a) and Hexane (b) using as the anti solvent.....	52
Figure 3.21 Pictures of the colloidal stability and aggregation behavior in various pH of phosphate buffer solution (no buffer, pH 4, pH 7 and pH 10) of 600 ppm (a) and 200 ppm (b) of PB4 nanoparticle suspensions.....	53
Figure 3.22 Scanning electron micrographs of aggregated nanoparticles of 600 ppm of PA7 in various pH of phosphate buffer solution. (a) No buffer (b) pH 4 (c) pH 7 and (d) pH 10.....	54

Figure A1 IR (a) and ¹ H-NMR spectrum (b) of 2,4-dimethoxycinnamic acid (2,4-DMC) in DMSO- <i>d</i> ₆	64
Figure A2 IR (a) and ¹ H-NMR spectrum (b) of 2,4,5-trimethoxycinnamic acid (2,4,5-TMC) in CDCl ₃	65
Figure A3 IR (a) and ¹ H-NMR spectrum (b) of poly(vinyl alcohol) (PV(OH)124,000 Daltons) in DMSO- <i>d</i> ₆	66
Figure A4 ¹ H-NMR spectrum of poly(vinyl alcohol) (PV(OH)50,000 Daltons) in DMSO- <i>d</i> ₆	67
Figure A5 ¹ H-NMR spectrum (b) of poly(vinyl alcohol) (PV(OH)10,000 Daltons) in DMSO- <i>d</i> ₆	68
Figure A6 IR (a) and ¹ H-NMR spectrum (b) of Poly(vinylalcohol-co-vinyl cinnamate), DS 0.04 (PA1) in DMSO- <i>d</i> ₆	69
Figure A7 IR (a) and ¹ H-NMR spectrum (b) of Poly(vinylalcohol-co-vinyl cinnamate), DS 0.14 (PA2) in DMSO- <i>d</i> ₆	70
Figure A8 IR (a) and ¹ H-NMR spectrum (b) of Poly(vinylalcohol-co-vinyl cinnamate), DS 0.25 (PA3) in DMSO- <i>d</i> ₆	71
Figure A9 IR (a) and ¹ H-NMR spectrum (b) of Poly(vinylalcohol-co-vinyl-4- methoxycinnamate), DS 0.01 (PB1) in DMSO- <i>d</i> ₆	72
Figure A10 IR (a) and ¹ H-NMR spectrum (b) of Poly(vinylalcohol-co-vinyl-4- methoxycinnamate), DS 0.09 (PB2) in DMSO- <i>d</i> ₆	73
Figure A11 IR (a) and ¹ H-NMR spectrum (b) of Poly(vinylalcohol-co-vinyl-4- methoxycinnamate), DS 0.27 (PB3) in DMSO- <i>d</i> ₆	74
Figure A12 IR (a) and ¹ H-NMR spectrum (b) of Poly(vinylalcohol-co-vinyl-4- methoxycinnamate), DS 0.44 (PB4) in DMSO- <i>d</i> ₆	75
Figure A13 IR (a) and ¹ H-NMR spectrum (b) of Poly(vinylalcohol-co-vinyl-2,4- dimethoxycinnamate), DS 0.46 (PC) in DMSO- <i>d</i> ₆	76
Figure A14 IR (a) and ¹ H-NMR spectrum (b) of Poly(vinylalcohol-co-vinyl-2,4,5- trimethoxycinnamate), DS 0.53 (PD) in DMSO- <i>d</i> ₆	77
Figure A15 IR (a) and ¹ H-NMR spectrum (b) of Poly(vinylalcohol-co-vinyl-4- methoxycinnamate) (Mw 50,000 Daltons, DS 0.28) (P_xB) in DMSO- <i>d</i> ₆	78

Figure A16 IR (a) and ¹ H-NMR spectrum (b) of Poly(vinylalcohol-co-vinyl-4-methoxycinnamate) (Mw 10,000 Daltons, DS 0.28) (P_yB) in DMSO- <i>d</i> ₆	79
Figure A17 Thermogram of Poly(vinylalcohol-co-vinylcinnamate) Mw 124,000-186,000 (PV(OH) 124,000 Daltons).....	80
Figure A18 Thermogram of Poly(vinylalcohol-co-vinylcinnamate), DS 0.04 (PA1).....	81
Figure A19 Thermogram of Poly(vinylalcohol-co-vinylcinnamate), DS 0.14 (PA2).....	82
Figure A20 Thermogram of Poly(vinylalcohol-co-vinylcinnamate), DS 0.25 (PA3).....	83
Figure A21 Thermogram of Poly(vinylalcohol-co-vinyl-4-methoxycinnamate), DS 0.01 (PB1).....	84
Figure A22 Thermogram of Poly(vinylalcohol-co-vinyl-4-methoxycinnamate), DS 0.09 (PB2).....	85
Figure A23 Thermogram of Poly(vinylalcohol-co-vinyl-4-methoxycinnamate), DS 0.27 (PB3).....	86
Figure A24 Thermogram of Poly(vinylalcohol-co-vinyl-4-methoxycinnamate), DS 0.44 (PB4).....	87
Figure A25 Thermogram of Poly(vinylalcohol-co-vinyl-2,4-dimethoxycinnamate), DS 0.46 (PC).....	88
Figure A26 Thermogram of Poly(vinylalcohol-co-vinyl-2,4,5-trimethoxycinnamate), DS 0.53 (PD).....	89
Figure A27 Thermogram of Poly(vinylalcohol-co-vinyl-4-methoxycinnamate) (Mw 50,000 Daltons, DS 0.28) (P₅B).....	90
Figure A28 Thermogram of Poly(vinylalcohol-co-vinyl-4-methoxycinnamate) (Mw 10,000 Daltons, DS 0.46) (P₉B).....	91

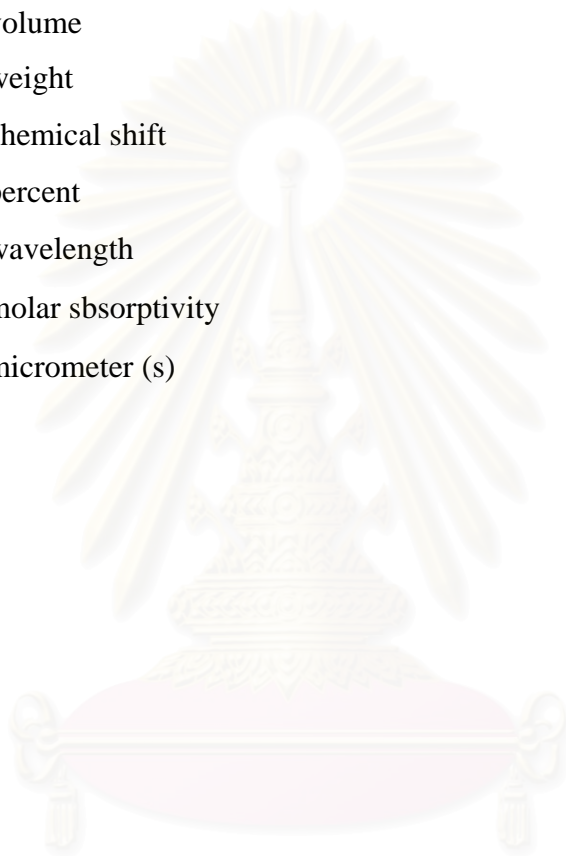
List of Tables

Table	Page
Table 2.1 Condition used during the syntheses of obtained PV(OH).....	16
Table 3.1 Structure and physicochemical properties of the poly(vinylalcohol-co-vinylcinnamate) derivatives.....	24
Table 3.2 The hydrodynamic diameters determined from dynamic light scattering technique and Zeta-potential of DS 0.04 (PA1), DS 0.14 (PA2) and DS 0.25 (PA3) of the poly(vinylalcohol-co-vinyl cinnamate) nanoparticulate suspensions, respectively.....	28
Table 3.3 Structure and physicochemical properties of the poly(vinylalcohol-co-vinyl-4-methoxycinnamate) derivatives.....	33
Table 3.4 The hydrodynamic diameters determined from dynamic light scattering technique and Zeta-potential of DS 0.01 (PB1), DS 0.09 (PB2), DS 0.27 (PB3) and DS 0.25 (PA4) of the poly(vinylalcohol-co-vinyl-4-methoxycinnamate) nanoparticulate suspensions, respectively.....	38
Table 3.5 Structure and physicochemical properties of the poly(vinylalcohol-co-vinyl-2,4-dimethoxycinnamate) compound.....	42
Table 3.6 Structure and physicochemical properties of the poly(vinylalcohol-co-vinyl-2,4,5-trimethoxycinnamate) compound.....	44
Table 3.7 Structure and physicochemical properties of the poly(vinylalcohol-co-vinyl-4-methoxycinnamate) prepared from PV(OH)50,000 Daltons (P_xB), PV(OH)10,000 Daltons (P_yB) and PV(OH)124,000 Daltons (PB3, PB4).....	48
Table 3.8 The hydrodynamic diameters determined from dynamic light scattering technique and Zeta-potential of the poly(vinylalcohol-co-vinyl-4-methoxycinnamate) nanoparticulate suspensions prepared from PV(OH)50,000 Daltons (P_xB), PV(OH)10,000 Daltons (P_yB) and PV(OH)124,000 Daltons (PB3, PB4).....	49

List of Abbrevitions

br	broad
°C	degree Celsius
CDCl ₃	deuterated chloroform
cm ⁻¹	unit of wavenumber (IR)
d	doublet (NMR)
DLS	dynamic light scatterin
DMF	dimethyl formamide
DMSO	dimethyl sulfoxide
DMSO- <i>d</i> ₆	deuterated dimethyl sulfoxide
DSC	differential scanning calorimetry
DS	degree of substitution
FT-IR	Fourier transform infrared spectrophotometer
g	gram (s)
h	hour
IR	infrared
J	coupling constant
KBr	potassium bromide
NMR	nuclear magnetic resonance
m	multiplet (NMR)
min	minute (s)
ml	milliliter (s)
mmol	millimole
mV	millivoltage
Mw	molecular weight
nm	nanometer (s)
NMR	nuclear agnetic resonance
PDI	polydisperse index
ppm	parts of million
s	singlet (NMR)
SEM	scanning electron microscopy

t	triplet (NMR)
TEM	transmission electron microscopy
T_g	glass transition temperature
T_m	melting temperature
UV	ultraviolet
v	volume
w	weight
δ	chemical shift
%	percent
λ	wavelength
ϵ	molar absorptivity
μm	micrometer (s)



สถาบันวิทยบริการ
จุฬาลงกรณ์มหาวิทยาลัย

CHAPTER I

INTRODUCTION

1.1 Polymeric nanoparticles

Throughout various fields of science and technology, a push towards the use of nano-scale technology is well underway. Nanotechnology has the potential to produce low-cost, self-replicating systems that could revolutionize the scientific landscape [1]. One area where nano-scale work is already well underway is within the field of cosmetic and drug delivery. In cosmetic and drug delivery, nanoparticles are fabricated in order to entrap and deliver specific pharmaceutical agents to various locations within the body.

Traditional drug delivery methods include oral and intravenous routes of administration. These methods are still the most widely used today, yet each has its disadvantages. Oral delivery via tablets or capsules is largely inefficient due to exposure of the pharmaceutical agent to the metabolic processes of the body [2]. Therefore, a larger than necessary dose is often required and the maximum effectiveness of the drug is limited. Traditional intravenous (IV) administration is much more problematic. Specificity for IV injectable drugs is often low, necessitating large amounts of a drug be injected into a patient, creating a high concentration of the drug in the blood stream that could potentially lead to toxic side effects [3]. Nanoparticle drug delivery, utilizing degradable and absorbable polymers, provides a more efficient, less risky solution to many drug delivery challenges.

Recently, polymeric nanoparticles (PNPs) have been the object of growing scientific attention. They have emerged as potential carriers because of their ability to delivery a wide range of drugs to varying areas of the body for sustained periods of time [4-6]. Nanoparticles are generally defined as colloidal particles ranging in size from 10-100 nm whereas microparticles are particles larger than 1 μm . Based on the method used for their formation, they could be either nanospheres (or nanoparticles),

which are essentially monolithic systems having a solid matrix, or nanocapsules, which have a hollow interior that is filled with a compound of interest and is surrounded by a polymeric shell. Natural polymers (proteins, collagen and polysaccharides) have not been widely used for this purpose since they vary in purity, and often require crosslinking that could denature the embedded drug. Consequently, synthetic polymers have received significantly more attention in this field. The most widely used polymers for nanoparticles have been poly(lactic acid) (PLA) [5,6], poly(glycolic acid) (PGA) [7], poly(vinyl alcohol) (PV(OH)) [8,9] and co-polymers, poly(lactide-co-glycolide) (PLGA) [10,11,12], poly(vinyl alcohol)-graft-poly(lactide-co-glycolide) (PV(OH)-g-PLGA) [13]. These polymers have shown good biocompatibility and resorbability through natural pathways.

During the 1980s and 1990s several drug delivery systems were developed to improve the efficiency of drugs and minimize toxic side effects [14]. The early nanoparticles and microparticles were mainly formulated from poly(alkylcyanoacrylate). Initial promise of microparticles was dampened by the fact that there was a size limit for the particles to cross the intestinal lumen into the lymphatic system following oral delivery. Likewise, the therapeutic effect of drug-loaded nanoparticles was relatively poor due rapid clearance of the particles by phagocytosis post intravenous administration. In recent years this problem has been solved by the addition of surface modifications to nanoparticles.

Another class of nano-sized vehicles that have been used in drug delivery applications is liposomes. These vesicles, prepared from lipids, have been used as potential drug carriers because of the protection they can offer drugs contained in their core. However, liposomes possess a low encapsulation efficiency, poor storage stability, and rapid leakage of water-soluble drugs in the blood [15]. As such, their ability to control the release of many drugs may not be good. Recently, biodegradable polymeric nanoparticles have shown their advantage over liposomes by their increased stability and the unique ability to create a controlled release.

In recent years, significant researches have been done using nanoparticles as oral drug delivery vehicles. In this application, the major interest is in lymphatic uptake of the nanoparticles by the Peyer's patches in the GALT (gut associated lymphoid tissue). The intestinal epithelium with a view of a Peyer's patch shows in

Figure 1.1 Peyer's patches are characterized by M cells that overlie the lymphoid tissue and are specialized for endocytosis and transport into intraepithelial spaces and adjacent lymphoid tissue [16]. Nanoparticles bind the apical membrane of the M cells, followed by a rapid internalization and a 'shuttling' to the lymphocytes [17]. The size and surface charge of the nanoparticles are crucial for the uptake. There have been many reports as to the optimum size for Peyer's Patch uptake ranging from less than 1 μm to less than 5 μm [18,19]. It has been shown that microparticles remain in the Peyer's patches while nanoparticles are disseminated systemically [20]. This application of nanoparticles in oral delivery holds tremendous promise for the development of oral vaccines and in cancer therapy.

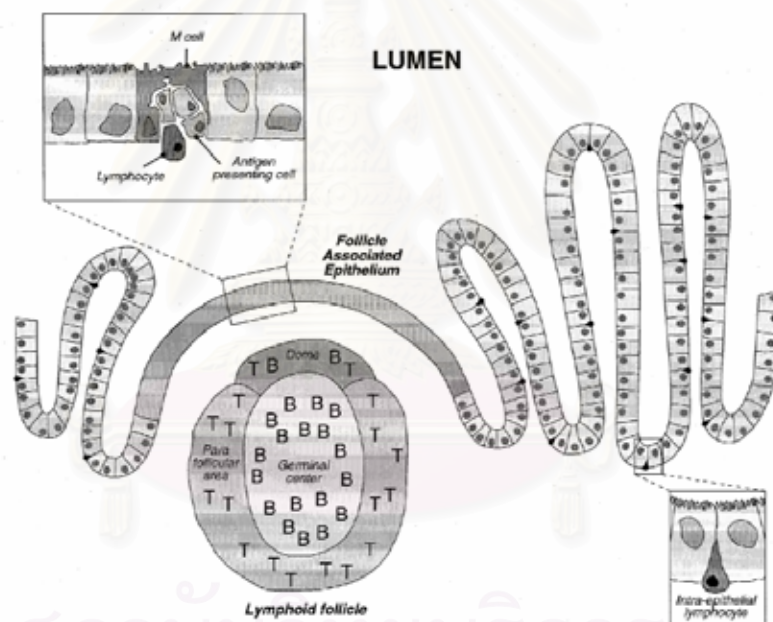


Figure 1.1 Schematic representation of the intestinal epithelium with a view of a Peyer's patch and detail of the follicle associated epithelium [16].

Nanoparticles have a further advantage over larger microparticles, because they are better suited for intravenous delivery. The diameter of the smallest blood capillaries is 5-6 μm . The size of particles being distributed into the bloodstream must be significantly smaller than 5 μm , without forming aggregates, to ensure that the particles do not form an embolism. The transdermal route, in particular, is improved in the presence of carriers entrapped in the intercorneocyte spaces (30-100 nm) on the

skin surface [19], thus providing release of the loaded drug as long as the corneum has been renewed.

Polymeric nanoparticles (PNPs) have the potential to completely transform drug delivery technology. PNPs represent a significant improvement over traditional oral and intravenous methods of administration in terms of efficiency and effectiveness. Also, PNPs can have engineered specificity, allowing them to deliver a higher concentration of pharmaceutical agent to a desired location. This feature makes PNPs ideal candidates for cancer therapy, delivery of vaccines, and delivery of targeted antibiotics. Moreover, PNPs can be easily incorporated into other activities related to drug delivery, such as tissue engineering, and into drug delivery for species other than humans. Then, PNPs were prepared from the obtained polymers.

Amphiphilic polymer, consisting of both hydrophilic and hydrophobic parts, is able to self-assemble into micro/nanostructures when placed in a solvent that is selective for either the hydrophilic or hydrophobic part. In this work amphiphilic polymer was prepared from grafting some hydrophobic moieties (cinnamic acid derivative) onto the hydrophilic polymer backbone (poly(vinyl alcohol)).

1.2 Poly(vinyl alcohol)

Poly(vinyl alcohol) (synonyms: vinyl alcohol polymer, PV(OH), ethenol homo polymer) is highly hydrophilic synthetic polymers used since the early 1930s. PV(OH) was selected as a starting material in this work due to its biocompatibility, biodegradability non-toxicity, non-carcinogenicity and the possibility for chemical modification at the hydroxyl groups. PV(OH) is also well accepted pharmaceutically safe polymer to both human and the environment. The United States Food and Drug Administration (**FDA**) have approved that polyvinyl alcohol is Substances Generally Recognized as Safe (**GRAS**), through scientific procedures, for use in aqueous film coating formulations applied to dietary supplement products (i.e., tablets or capsules), where the coating formulation is up to four percent (by weight) of the tablet or capsule, and polyvinyl alcohol is up to 45 percent (by weight) of the coating formulation. In addition, it is used as an indirect food additive in products that are in contact with food, as a diluent in color additive mixtures for coloring shell eggs, and

for use in several medical applications, including in coatings applied to pharmaceutical tablets.

The physical characteristics of PV(OH) are dependent on its method of preparation. PV(OH) is obtained from the hydrolysis or partial hydrolysis of polyvinylacetate which is made by the polymerization of vinyl acetate monomer (Figure 1.2). PV(OH) is generally classified into two groups, fully hydrolyzed (A) and partially hydrolyzed (B).

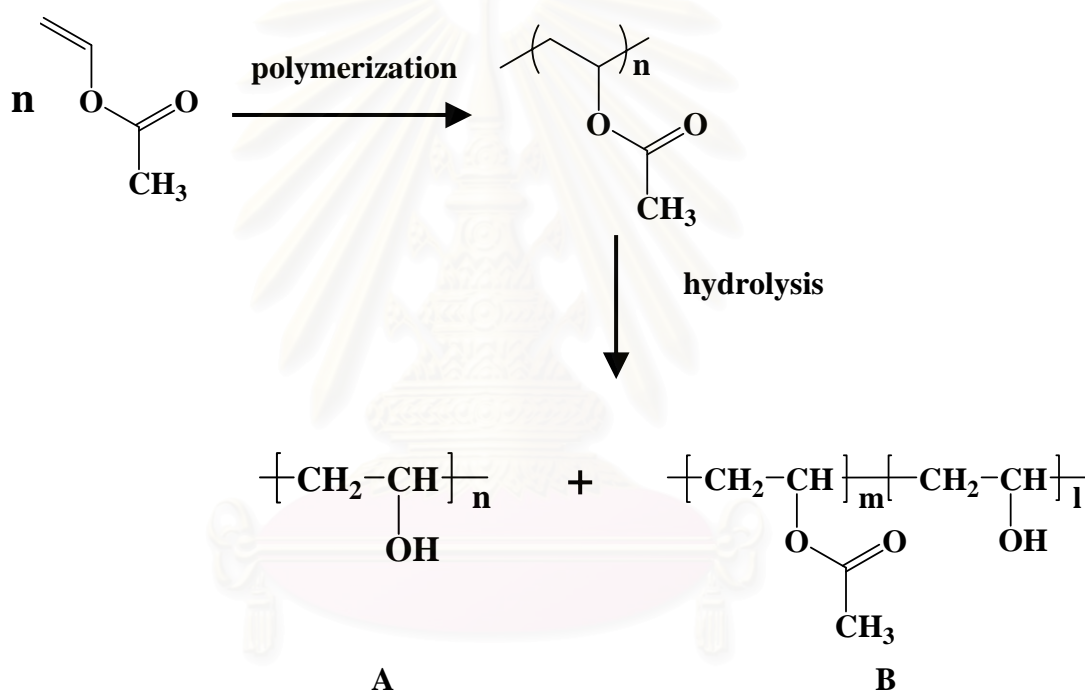


Figure 1.2 Synthesis of poly(vinyl alcohol)

Varying the length of the initial vinyl acetate polymer and the degree of hydrolysis under alkaline or acidic conditions, yields PV(OH) products of different molecular weights (20,000-400,000), solubility, flexibility, tensile strength and adhesiveness. Various properties are measured to characterize PV(OH). They include pH, viscosity, loss on drying, melting point, refractive index, heavy metals and residue on ignition. These properties vary with molecular weight and % hydrolysis and they are used for differentiating various grades of PV(OH).

The safety of PV(OH) makes this polymer very popular on various application worldwide. It was applied in pharmaceutical, medical, cosmetic and food products. Examples of products containing PV(OH) are resins, lacquers, surgical threads and contact lens fluids.

PV(OH) is used in the textile industries as a sizing and finishing agent. PV(OH) can also be incorporated into a water-soluble fabric in the manufacture of degradable protective apparel, laundry bags for hospitals, rags, sponges, sheets, covers, as well as physiological hygiene products.

PV(OH) is also widely used in the manufacture of paper products as a sizing and coating agent. It provides stiffness to these products making it useful in tube winding, carton sealing and board lamination.

PV(OH) is used as a thickening agent for latex paint and common household white glue or in other adhesive mixtures such as remoistenable labels and seals, as well as gypsum-based cements such as is used for ceramic tiles.

PV(OH) is used as an indirect food additive in products which are in contact with food and has also been approved for use in packaging meat products by the Meat Inspection Division of the USDA and approved for use in packaging poultry products by the Poultry Division of the USDA.

As an industrial and commercial product, PV(OH) is valued for its solubility and biodegradability, which contributes to its very low environmental impact. Several microorganisms ubiquitous to artificial and natural environments such as septic systems, landfills, compost and soil have been identified which are able to degrade PV(OH) through enzymatic processes. A combination of oxidase and hydrolase enzyme activities degrade PV(OH) into acetic acid but both the percent hydrolysis and its solubility affect the rate of PV(OH) biodegradation.

PV(OH) is safe as used in cosmetic formulations. The emulsifying binding and thickening properties of PV(OH) make it useful for cosmetic applications. Cold creams, cleansing creams, shaving creams, eye make-up and facial masks may be formulated using PV(OH).

PV(OH) is approved for use in several medical applications including transdermal patches, the preparation of jellies that dry rapidly when applied to the skin and in immediate and sustained release tablet formulations. Cross-linked

polyvinyl alcohol microspheres are also used for controlled release of oral drugs. Ophthalmic solutions, such as synthetic tears, may also contain PV(OH) because it provides good dispersion and coating properties [21]. PV(OH) is included in the FDA Inactive Ingredient Guide for ophthalmic preparations and oral tablets.

In the drug delivery area, most researchers are exploring the potential use of PV(OH) as an emulsifier to prepare nanoparticles with the solvent extraction/evaporation method [22] and dialysis method [23]. Usually PV(OH) is viewed as a steric stabilizer in emulsion polymerization. Recently, PV(OH) was also used as a starting material to prepare hydrogel [8] or amphiphilic polymeric micro/nanoparticles [22,36].

1.3 Cinnamic acid derivative

Cinnamic acid is a highly valuable class of fine chemicals with applications in polymer formulations, medication, pesticide, sensitive resin and plastics as well as general organic synthesis. It is well-known as a photosensitive compound and is widely used as a component of functional polymers, such as liquid crystal polymers and photoreactive resins made of poly(vinyl alcohol) immobilized with cinnamoyl groups [24,25,26]. Cinnamic acid and its derivatives including esters and carboxylic functional derivatives are used as important components in flavours, perfumes, synthetic indigo and pharmaceuticals.

4-Methoxycinnamic acid exhibited a hepatoprotective activity in rat hepatocytes from toxicity induced by carbon tetrachloride (CCl₄) [27]. 4-Methoxycinnamic acid had inhibitory effects on the diphenolase activity of mushroom tyrosinase and the inhibition was reversible [28]. 4-Methoxycinnamic acid showed the highest microbial α -glucosidase inhibitory activity [29]. Esters of 4-methoxycinnamic acid have been used widely in the cosmetic industry as stable UVB filter.

2,4-Dimethoxycinnamic acid and 2,4,5-trimethoxycinnamic acid were firstly synthesized by Thitinun Monhaphol [30]. They showed excellent UV absorption ability. Both compounds are non-toxic and photostable [30]. Esters of both cinnamic acids and their close structural analogues have emerged as new sunscreens of the cinnamate class [31].

In this work, cinnamic acid, 4-methoxycinnamic acid, 2,4-dimethoxycinnamic acid and 2,4,5-trimethoxycinnamic acid were chosen as hydrophobic substitute to be grafted onto the PV(OH) chain. Their UV-absorption property should impart into the obtained grafted polymers. Thus, nanoparticles prepared from these UV-absorption polymers should possess some UV screening properties.

1.4 Literature reviews

In 1998, Wu and coworker prepared poly(vinyl alcohol) hydrogel nanoparticles (675 ± 42.7 nm diameter) by using a water-in-oil emulsion technology plus cyclic freezing-thawing process (Figure 1.3). Encapsulation of the bovine serum albumin (BSA) into the particles was also carried out. It was demonstrated that BSA is stable in the PV(OH) hydrogel nanoparticles. The particles also showed prolonged released characteristics [8].



Figure 1.3 Scanning electron micrograph of the PV(OH) hydrogel nanoparticles.

In 1999, Wu and coworker loaded the bovine serum albumin (BSA) into the PV(OH) nanoparticles, then encapsulated the BSA-containing nanoparticles into PLGA microspheres by a phase separation method (Figure 1.4). The PLGA-PV(OH) composite microspheres are spherical in shape with nonporous surface and possess prolonged BSA release characteristic (two months). The particle size is ~ 71.5 - 282.7 μm . [33].

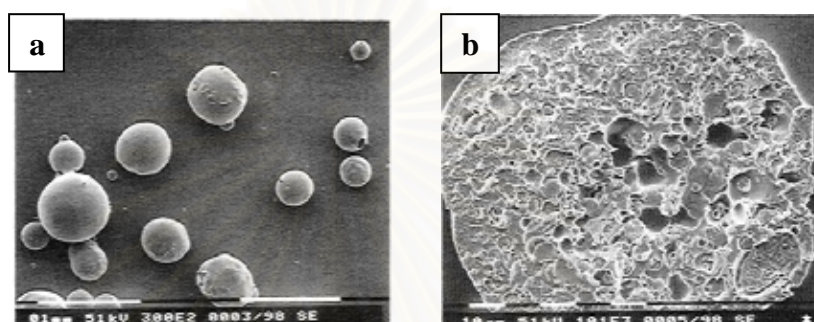


Figure 1.4 Scanning electron micrograph of PLGA-PV(OH) composite microspheres (a) the internal structure and distribution of the PV(OH) nanoparticle inside (b).

In 2000, Kissel and coworker synthesized poly(2-sulfobutyl-vinyl alcohol)-*g*-poly(lactide-co-glycolides) with various degrees of substitution. They introduced negatively charged sulfobutyl groups onto the PV(OH) backbone before grafting this product onto poly(lactide-co-glycolides) chains. The obtained polymers were induced into nanoparticles by solvent displacement technique (Figure 1.5). The particles' mean diameters (Z-average) were ~ 100 - 500 nm, depending on polymer composition. The zeta-potential value increased with the substitution degree of sulfobutyl onto PV(OH) backbone [34].

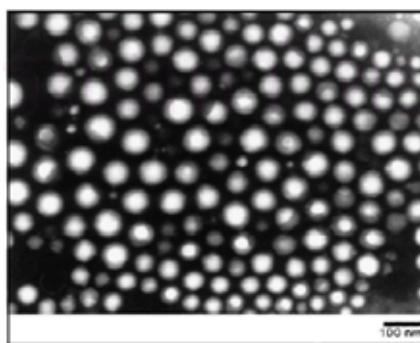


Figure 1.5 Transmission electron micrograph of poly(2-sulfobutyl-vinyl alcohol)-*g*-poly(lactide-co-glycolides) nanoparticles.

In 2001, Kissel and coworker loaded tetanus toxoid (TT) into biodegradable poly(2-sulfobutyl-vinylalcohol)-graft-poly(lactide-co-glycolides) nanospheres by an adsorption process. They studied effects of solvents on particle sizes. The average diameters of nanoparticles are ~100 nm, 500 nm and > 1 μm , depending on the solvent used [35].

In 2002, Luppi and coworker prepared nanocarriers from poly(vinylalcohol-co-vinylolate), at a substitution degree of 4.8%. The obtained nanocarrier showed particle size in the range of 200-300 nm and demonstrated enhanced retinyl palmitate transcutaneous permeation [36].

In 2002, Cascone and coworker prepared biodegradable poly(lactide-co-glycolide) (PLGA) nanoparticles loaded with dexamethasone, that could then be entrapped into the dextran-PV(OH) hydrogel (Figure 1.6). This study showed that dextran-PV(OH) hydrogels could be used as hydrophilic matrices for controlled release of the drug loaded in PLGA nanoparticles [37].

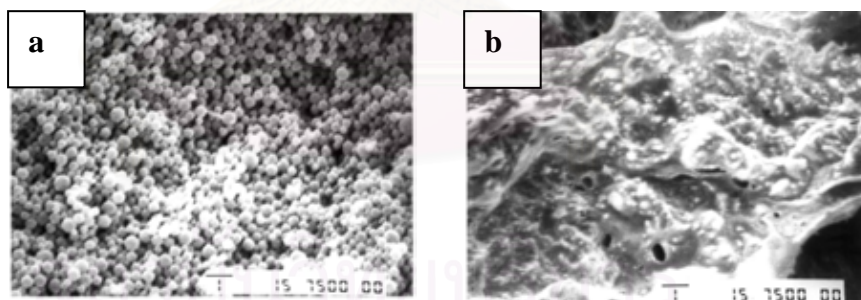


Figure 1.6 Scanning electron micrograph of free PLGA nanoparticles loaded with dexamethasone (a) PLGA nanoparticles entrapped into the dextran-PV(OH) hydrogel (b).

In 2004, Kishida and coworker prepared PV(OH)-DNA nanoparticles using PV(OH) with different molecular weights, degrees of saponifications and concentrations, using ultra high pressure technology i.e., under 10,000 atmosphere (981 MPa) condition at 40⁰C for 10 min (Figure 1.7). The resulting nanoparticles showed average diameter ~200 nm. The molecular weight of PV(OH) had the effect on particle size. The obtained PV(OH)-DNA nanoparticles showed high gene transfer into cell [9].

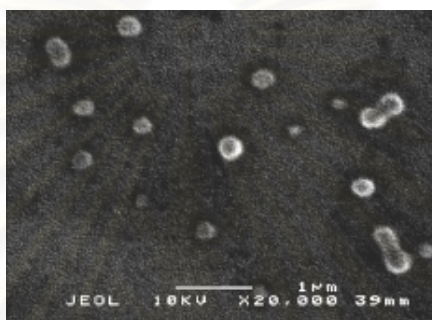


Figure 1.7 Scanning electron micrograph of the PV(OH)-DNA nanoparticles.

In 2005, Orienti and coworker grafted oleyl amine onto PV(OH) at a substitution degree of 1.5% and prepared polymeric micelles from the grafted product (Figure 1.8). An entrapment of all-trans-retinoic acid (ATRA) was then carried out by spray-drying method. The average diameters of nanoparticles was ~100-500 nm, depending on the polymer concentration used [22].

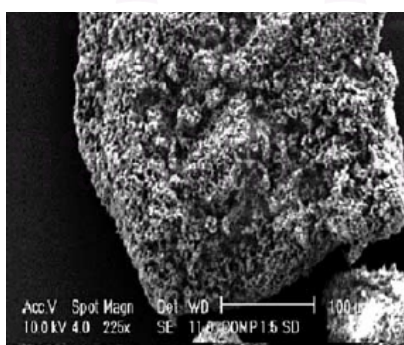


Figure 1.8 Scanning electron micrograph of the polyvinylalcohol substituted with oleylamine.

In 2007, Kissel and coworker prepared PV(OH)-graft-poly(lactide-co-glycolide) with varying PLGA chain length. The obtained polymers were induced into nanoparticles by solvent displacement method (Figure 1.9). The average diameters of nanoparticles was < 180 nm in diameter. The Paclitaxel (anticancer) drugs could be loaded into nanoparticles without affecting the nanoparticle size [13].

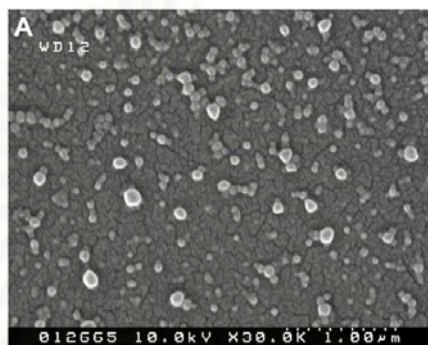


Figure 1.9 Scanning electron micrograph of PV(OH)-graft-poly(lactide-co-glycolide) nanoparticles.

1.5 Research goal

The objectives of this research can be summarized as follows:

1. To synthesize poly(vinylalcohol-co-vinylcinnamate) derivatives with: various molecular weights of the PV(OH) backbone, various degrees of substitution of *trans*-substituted cinnamic acids and various types of *trans*-substituted cinnamic acid derivatives (cinnamic acid, 4-methoxycinnamic acid, 2,4-dimethoxycinnamic acid and 2,4,5-trimethoxycinnamic acid).
2. To carry out the self-assembly of the obtained PV(OH) derivatives via dialysis method.

CHAPTER II

EXPERIMENTAL

2.1 Materials and Chemicals

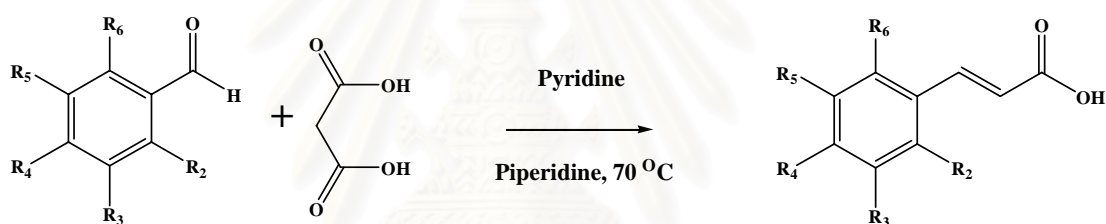
Poly(vinyl alcohol), Mw 124,000-186,000, 87-89% deacetylated (**PV(OH) 124,000 Daltons**); poly(vinyl alcohol), Mw 35,000-50,000, 87-89% deacetylated (**PV(OH)50,000 Daltons**); poly(vinyl alcohol), Mw 9,000-10,000, 80% deacetylated (**PV(OH)10,000 Daltons**) and dialysis membranes with a molecular weight cutoff of 12,400 Daltons (size 76 mm. x 49 mm) were purchased from Aldrich Chemical Company (Steinheim, Germany). Cinnamic acid (CA) was purchased from Fluka Chemical Company (Buchs, Switzerland). 4-Methoxycinnamic acid (4-MCA), 2,4-dimethoxybenzaldehyde and 2,4,5-trimethoxybenzaldehyde were purchased from Acros Organics (Geel, Belgium). 4-Dimethylaminopyridine (DMAP) was purchased from Merck (Damstadt, Germany). Sodium carbonate anhydrous was purchased from Carlo Erba Reagent (Milan, Italy). Pyridine and benzene was purchased from J.T. Baker Inc. (New Jersey, USA). Dimethyl formamide (DMF) and dimethyl sulfoxide (DMSO) were purchased from Labscan (Dublin, Ireland). Thionyl chloride was obtained from the Department of chemistry, Faculty of science, Chulalongkorn University (old stock) and it was double distilled before use.

2.2 Instruments and Equipments

FT-IR analysis was carried out using a Nicolet Fourier transform Infrared spectrophotometer: Impact 410 (Nicolet Instruments Technologies, Inc., Madison, WI, USA). ^1H - and ^{13}C -NMR analyses were carried out using a Varian Mercury spectrometer which operated at 400.00 MHz for ^1H and 100.00 MHz for ^{13}C nuclei (Varian Company, Palo Alto, CA, USA) in deuterated chloroform (CDCl_3) or deuterated dimethylsulfoxide ($\text{DMSO}-d_6$) with tetramethylsilane (TMS) as an internal reference. UV analysis was done with the aid of UV 2500 UV-Vis spectrophotometer (Shimadzu Corporation, Kyoto, Japan), using a quartz cell with 1 cm pathlength. Thin layer chromatography (TLC) was performed on aluminum sheets precoated with silica

gel (Meck Kieselgel 60 F₂₅₄) (Merck KgaA, Darmstadt, Germany). Thermogram of each sample was obtained by differential scanning calorimetry: DSC 204 (Netzsch Group, Selb, Germany). The measurements were carried out at temperatures of 0-380 °C under nitrogen at a scanning rate of 10 °C/min. Transmission Electron Microscopy (TEM) was carried out using JEM-2100 (Jeol, Ltd., Japan) and Scanning Electron Microscopy (SEM) was performed on JEM-6400 (Jeol, Ltd., Japan). The particle size and zeta-potential analysis were performed without prefiltering by Mastersizer S and Zetasizer nanoseries (Malvern Instruments, Worcestershire, UK), respectively.

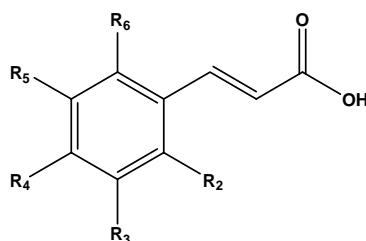
2.3 Synthesis of *trans*-substituted cinnamic acids



Scheme 2.1 Synthetic pathway of *trans*-substituted cinnamic acids.

2,4-Dimethoxycinnamic acid and 2,4,5-trimethoxycinnamic acid were synthesized using Knoevenagel-Doebner condensation [31,38] between benzaldehyde and malonic acid (scheme 2.1). Briefly, 2,4-dimethoxybenzaldehyde (8.26 g, 0.05 mole) or 2,4,5-trimethoxybenzaldehyde (9.81 g, 0.05 mole) were dissolved in pyridine (48.3 ml, 0.6 mole). Then, malonic acid (5.2 g, 0.05 mole) and piperidine (2.47 ml, 25.25 mmole) were added. The reaction mixture was heated at 85 °C for 6-8 h. After the mixture had been cooled, cold 10% aqueous HCl were added. The solid was separated by suction filtration, washed with cold water and recrystallized with a mixture of water:ethanol (volume ratio 1:2).

Both cinnamic acids were characterized by NMR, IR and UV spectroscopy (see in appendix A1-A2). Their structures are shown in Figure 2.1.



Compound	R ₂	R ₃	R ₄	R ₅	R ₆
2,4-dimethoxycinnamic acid (2,4-DMC)	OCH ₃	H	OCH ₃	H	H
2,4,5-trimethoxycinnamic acid (2,4,5-TMC)	OCH ₃	H	OCH ₃	OCH ₃	H

Figure 2.1 Structure and nomenclature of the synthesized substituted cinnamic acids.

2,4-Dimethoxycinnamic acid (2,4-DMC): light yellow solid. yield: 84%. T_m : 156-162 °C. FT-IR (KBr, cm^{-1}): 3465 (COO-H, stretching), 3001, 2933, and 2835 (H-C=C, stretching), 1673 (C=O, stretching) and 1598, 1463 and 755 (aromatic ring). $^1\text{H-NMR}$ (400 MHz, CDCl_3 , δ , ppm): 10.55 (s, 1H, COOH), 7.76 (d, $J=16.4$ Hz, 1H, Ar-CH=), 7.59 (d, $J=7.8$ Hz, 1H, Ar-H), 6.68 (s, 1H, Ar-H), 6.57 (d, $J=7.8$ Hz, 1H, Ar-H), 6.36 (d, $J=16.4$ Hz, 1H, =CH-COOH) and 3.85, 3.50 (s, 2x3H, 2xOCH₃). UV-vis (DMSO) λ_{max} , nm (ϵ , $\text{M}^{-1}\text{cm}^{-1}$): 289 (10795) and 327 (13108).

2,4,5-Trimethoxycinnamic acid (2,4,5-TMC): yellow solid. yield: 89%. T_m : 165-167 °C. FT-IR (KBr, cm^{-1}): 3483 (COO-H), 3009, 2935 and 2823 (H-C=C, stretching), 1685 (C=O, stretching) and 1600, 1463 and 755 (aromatic ring). $^1\text{H-NMR}$ (400 MHz, CDCl_3 , δ , ppm): 10.55 (s, 1H, COOH), 8.30 (d, $J=16.0$ Hz, 1H, Ar-CH=), 6.73 and 7.49 (s, 2H, Ar-H), 6.61 (d, $J=15.5$ Hz, 1H, =CH-COOH) and 4.17, 4.12 and 4.10 (s, 9H, 3xOCH₃). UV-vis (DMSO) λ_{max} , nm (ϵ , $\text{M}^{-1}\text{cm}^{-1}$): 282 (12000) and 350 (13000).

2.4 Synthesis of poly(vinylalcohol-co-vinylcinnamate) derivative

Table 2.1 Condition used during the syntheses of obtained PV(OH).

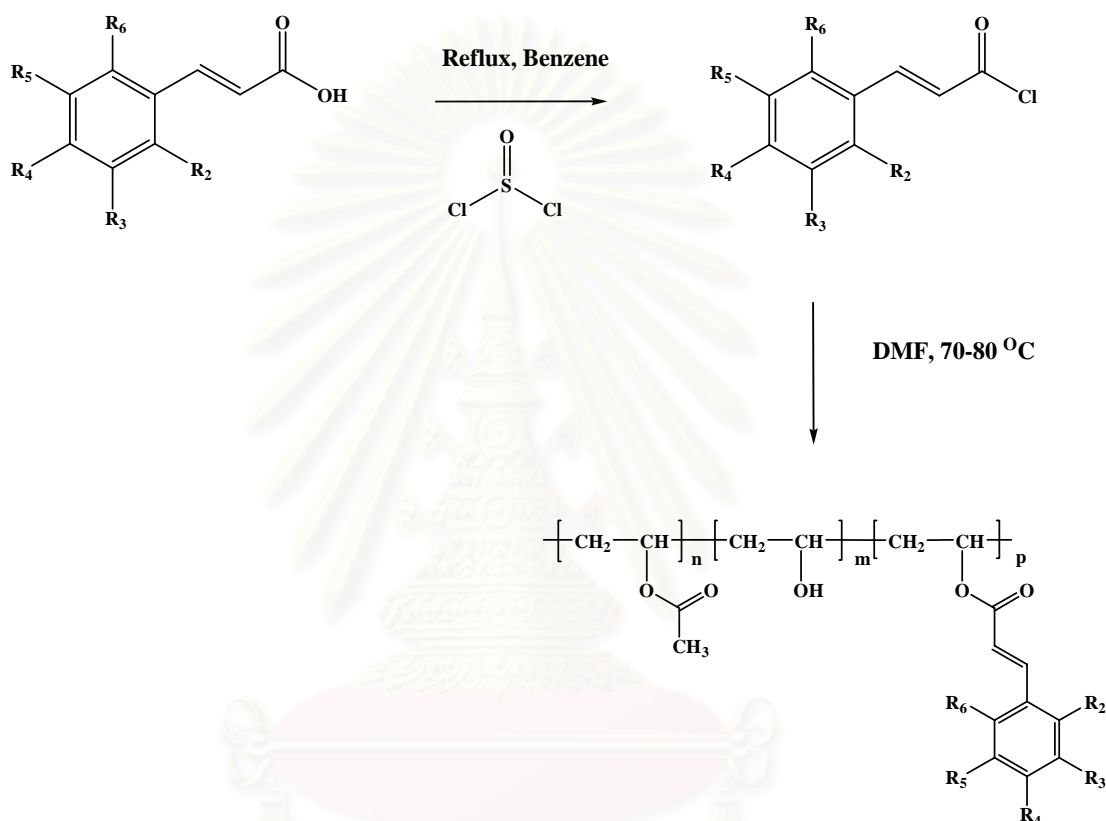
Compound	Mw of PV(OH)	<i>Trans</i> -substitued cinnamic acid derivative	Amounts of <i>trans</i> -cinnamic acid derivative	
PA1	PV(OH)124,000 Daltons	CA	0.40 g, 2.7 mmole	
PA2			4.00 g, 27 mmole	
PA3			8.00 g, 54 mmole	
PB1		PV(OH)124,000 Daltons	4-MCA	0.48 g, 2.7 mmole
PB2				1.44 g, 8.1 mmole
PB3				4.81 g, 27 mmole
PB4				9.62 g, 54 mmole
PC	2,4-DMC		5.65 g, 27 mmole	
PD	2,4,5-TMC	6.49 g, 27 mmole		
P₅B	PV(OH)50,000 Daltons	4-MCA	4.81 g, 27 mmole	
P₉B	PV(OH)10,000 Daltons		4.81 g, 27 mmole	

The poly(vinylalcohol-co-vinylcinnamate) derivatives were synthesized using classical esterification reaction between *trans*-substitued cinnamoyl chloride and PV(OH) (scheme 2.2).

First, the *trans*-substitued cinnamoyl chloride was prepared by reacting *trans*-substitued cinnamic acid (see Table 2.1) with thionyl chloride (2.5-flod) in a presence of pyridine (2 drops), in 40 ml dry benzene [39]. The mixture was refluxed overnight. Then, the solvent and the excess thionyl chloride were removed by rotary evaporation under reduced pressure. Finally, benzene addition (5 ml) and evaporation were performed to remove the last traces of thionyl chloride.

Second, poly(vinylalcohol-co-vinylcinnamate) derivatives were prepared. PV(OH) (1.19 g, 27 mmole of monomeric unit) were dissolved in 70 ml of heated anhydrous DMF. Then, pyridine (2.18 ml, 27 mmole) was added. The obtained clear solution was then poured into a round botton flask containing the freshly prepared

trans-substituted cinnamoyl chloride. The mixture was stirred at 80-90 °C for 1-2 h. The substituted polymer was separated by precipitation with 1.0% w/v aq. Na₂CO₃. The precipitate was washed with distilled water. The obtained solid was dried under vacuum to constant weight.



Scheme 2.2 Synthetic pathway of poly(vinylalcohol-co-vinylcinnamate) derivatives.

Poly(vinylalcohol-co-vinylcinnamate) products

PA1: white solid. DS: 3.5. T_g: 71.6 °C. FT-IR (KBr, cm⁻¹): 3377 (OH), 2939 (-C-H, stretching), 1710 (C=O, stretching), 1636, 1575 (C=C, stretching), 1434 (-CH₂-, bending) and 1262, 1186, 1095 (C-O, stretching). ¹H-NMR (400 MHz, DMSO-*d*₆, δ, ppm): 7.71 (br, 1H, Ar-CH=), 7.63 (br, 2H, Ar-H), 7.39 (br, 3H, Ar-H), 6.62 (br, 1H, =CH-COOR), 4.66, 4.45 and 4.21 (s, 21H, -OH), 3.89 (br, 3H, -CH-OCOCH₃), 3.83 (br, 21H, -CH-OH), and 2.30-0.80 (br, 8H of CH₃-CO and 50H of -CH-CH₂-CH- of PV(OH) backbone). UV-vis (DMSO) λ_{max}, nm (ε, M⁻¹cm⁻¹, per monomeric unit): 279 (1364).

PA2: yellow solid. DS: 13.6. T_g : 72.8 °C. FT-IR (KBr, cm^{-1}): 3472 (OH), 3063, 3023 (=C-H, stretching), 2929 (-C-H, stretching), 1720 (C=O, stretching), 1636, 1575 (C=C, stretching), 1441 (-CH₂-, bending) and 1312, 1248, 1174 (C-O, stretching). ¹H-NMR (400 MHz, DMSO-*d*₆, δ , ppm): 8.17 (br, 1H, Ar-CH=), 7.65 (br, 2H, Ar-H), 7.41 (br, 3H, Ar-H), 6.58 (br, 1H, =CH-COOR), 5.5-4.1 (br, 5H, -OH), 4.0-3.5 (br, 6H, of -CH-OH and -CH-OCOCH₃) and 2.30-0.80 (br, 2H of CH₃-CO and 14H of -CH-CH₂-CH- of PV(OH) backbone). UV-vis (DMSO) λ_{max} , nm (ϵ , M⁻¹cm⁻¹, per monomeric unit): 282 (2544).

PA3: yellow solid. DS: 24.7. T_g : 73.1 °C. FT-IR (KBr, cm^{-1}): 3484 (OH), 3061, 3023 (=C-H, stretching), 2927 (-C-H, stretching), 1715 (C=O, stretching), 1633, 1575 (C=C, stretching), 1441 (-CH₂-, bending) and 1312, 1250, 1173 (C-O, stretching). ¹H-NMR (400 MHz, DMSO-*d*₆, δ , ppm): 8.12 (br, 1H, Ar-CH=), 7.64 (br, 2H, Ar-H), 7.37 (br, 3H, Ar-H), 6.55 (br, 1H, =CH-COOR), 5.5-4.5 (br, 3H, -OH), 4.2-3.8 (br, 3H, of -CH-OH and -CH-OCOCH₃) and 2.30-0.80 (br, 1H of CH₃-CO and 8H of -CH-CH₂-CH- of PV(OH) backbone). UV-vis (DMSO) λ_{max} , nm (ϵ , M⁻¹cm⁻¹, per monomeric unit): 280 (4814).

Poly(vinylalcohol-co-vinyl-4-methoxycinnamate) products

PB1: white solid. DS: 0.5. T_g : 63.8 °C. FT-IR (KBr, cm^{-1}): 3330 (OH), 2940, 2915, 2850 (-C-H, stretching), 1712 (C=O, stretching), 1602, 1509 (C=C, stretching), 1428 (-CH₂-, bending) and 1327, 1248, 1169 (C-O, stretching). ¹H-NMR (400 MHz, DMSO-*d*₆, δ , ppm): 8.21 (br, 1H, Ar-CH=), 7.60 (br, 2H, Ar-H), 6.97 (br, 2H, Ar-H), 6.45 (br, 1H, =CH-COOR), 4.66, 4.46 and 4.21 (br, 88H, -OH), 4.1-3.7 (br, 99H, of -CH-OH and -CH-OCOCH₃), 3.35 (br, 3H, OCH₃) and 2.30-0.80 (br, 33H of CH₃-CO and 200H of -CH-CH₂-CH- of PV(OH) backbone). UV-vis (DMSO) λ_{max} , nm (ϵ , M⁻¹cm⁻¹, per monomeric unit): 311 (131).

PB2: white solid. DS: 9.1. T_g : 79.1 °C. FT-IR (KBr, cm^{-1}): 3362 (OH), 2939, 2841 (-C-H, stretching), 1724 (C=O, stretching), 1605, 1513 (C=C, stretching), 1429 (-CH₂-, bending) and 1256, 1173 (C-O, stretching). ¹H-NMR (400 MHz, DMSO-*d*₆, δ , ppm): 7.59 (br, 2H, Ar-H), 6.90 (br, 2H, Ar-H), 6.41 (br, 1H, =CH-COOR), 4.68,

4.47 and 4.22 (br, 9H, -OH), 4.0-3.6 (br, 10H, of -CH-OH and -CH-OCOCH₃), 3.79 (br, 3H, OCH₃) and 2.30-0.80 (br, 4H of CH₃-CO and 22H of -CH-CH₂-CH- of PV(OH) backbone). UV-vis (DMSO) λ_{\max} , nm (ϵ , M⁻¹cm⁻¹, per monomeric unit): 311 (2109).

PB3: light brown solid. DS: 26.5. T_g: 79.6 °C. FT-IR (KBr, cm⁻¹): 3485 (OH), 3072 (=C-H, stretching), 2931, 2835 (-C-H, stretching), 1710 (C=O, stretching), 1632, 1603 (C=C, stretching), 1426 (-CH₂-, bending) and 1253, 1169 (C-O, stretching). ¹H-NMR (400 MHz, DMSO-*d*₆, δ , ppm): 8.15 (br, 1H, Ar-CH=), 7.56 (br, 2H, Ar-H), 6.90 (br, 2H, Ar-H), 6.39 (br, 1H, =CH-COOR), 5.5-4.4 (br, 2H, -OH), 4.3-3.9 (br, 3H, of -CH-OH and -CH-OCOCH₃), 3.74 (br, 3H, OCH₃) and 2.30-1.00 (br, 1H of CH₃-CO and 2H of -CH-CH₂-CH- of PV(OH) backbone). UV-vis (DMSO) λ_{\max} , nm (ϵ , M⁻¹cm⁻¹, per monomeric unit): 309 (4242).

PB4: brown solid. DS: 44.4. T_g: 82.0 °C. FT-IR (KBr, cm⁻¹): 3493 (OH), 3069, 3026 (=C-H, stretching), 2934, 2839 (-C-H, stretching), 1709 (C=O, stretching), 1632, 1604 (C=C, stretching), 1427 (-CH₂-, bending) and 1252, 1166 (C-O, stretching). ¹H-NMR (400 MHz, DMSO-*d*₆, δ , ppm): 8.14 (br, 1H, Ar-CH=), 7.48 (br, 3H, Ar-H), 6.82 (br, 3H, Ar-H), 6.29 (br, 1H, =CH-COOR), 5.6-4.5 (br, 1H, -OH), 4.4-3.9 (br, 2H, of -CH-OH and -CH-OCOCH₃), 3.72 (br, 4H, OCH₃) and 2.30-0.80 (br, 1H of CH₃-CO and 6H of -CH-CH₂-CH- of PV(OH) backbone). UV-vis (DMSO) λ_{\max} , nm (ϵ , M⁻¹cm⁻¹, per monomeric unit): 310 (10072).

P5B: brown solid. DS: 27.6. T_g: 84.5 °C. FT-IR (KBr, cm⁻¹): 3349 (OH), 3072, 3023 (=C-H, stretching), 2934, 2840 (-C-H, stretching), 1707 (C=O, stretching), 1632, 1604 (C=C, stretching), 1427 (-CH₂-, bending) and 1253, 1168 (C-O, stretching). ¹H-NMR (400 MHz, DMSO-*d*₆, δ , ppm): 8.17 (br, 1H, Ar-CH=), 7.57 (br, 2H, Ar-H), 6.89 (br, 2H, Ar-H), 6.37 (br, 1H, =CH-COOR), 5.5-4.4 (br, 2H, -OH), 4.3-4.0 (br, 3H, of -CH-OH and -CH-OCOCH₃), 3.75 (br, 3H, OCH₃) and 2.30-0.80 (br, 1H of CH₃-CO and 7H of -CH-CH₂-CH- of PV(OH) backbone). UV-vis (DMSO) λ_{\max} , nm (ϵ , M⁻¹cm⁻¹, per monomeric unit): 310 (6681).

P₉B: brown solid. DS: 45.6. T_g: 78.7 °C. FT-IR (KBr, cm⁻¹): 3504 (OH), 3063, 3029 (=C-H, stretching), 2936, 2839 (-C-H, stretching), 1710 (C=O, stretching), 1632, 1604 (C=C, stretching), 1428 (-CH₂-, bending) and 1250, 1168 (C-O, stretching). ¹H-NMR (400 MHz, DMSO-*d*₆, δ, ppm): 8.13 (br, 1H, Ar-CH=), 7.54 (br, 3H, Ar-H), 6.87 (br, 3H, Ar-H), 6.33 (br, 1H, =CH-COOR), 5.5-4.5 (br, 1H, -OH), 4.3-3.9 (br, 2H, of -CH-OH and -CH-OCOCH₃), 3.72 (br, 4H, OCH₃) and 2.30-0.80 (br, 2H of CH₃-CO and 6H of -CH-CH₂-CH- of PV(OH) backbone). UV-vis (DMSO) λ_{max}, nm (ε, M⁻¹cm⁻¹, per monomeric unit): 310 (8585).

Poly(vinylalcohol-co-vinyl-2,4-dimethoxycinnamate) product

PC: light yellow solid. DS: 46.2. T_g: 88 °C. FT-IR (KBr, cm⁻¹): 3467 (OH), 3072 (=C-H, stretching), 2940, 2839 (-C-H, stretching), 1706 (C=O, stretching), 1606 (C=C, stretching) and 1262, 1209, 1160 (C-O, stretching). ¹H-NMR (400 MHz, DMSO-*d*₆, δ, ppm): 7.66 (br, 1H, Ar-CH=), 7.42, 6.42 (br, 3H, Ar-H), 6.29 (br, 1H, =CH-COOR), 5.5-4.6 (br, 1H, -OH), 4.5-3.9 (br, 1H, of -CH-OH and -CH-OCOCH₃), 3.74 (br, 6H, 2xOCH₃) and 2.30-1.00 (br, 1H of CH₃-CO and 4H of -CH-CH₂-CH- of PV(OH) backbone). UV-vis (DMSO) λ_{max}, nm (ε, M⁻¹cm⁻¹, per monomeric unit): 295 (6991) and 328 (8900).

Poly(vinylalcohol-co-vinyl-2,4,5-trimethoxycinnamate) product

PD: light yellow solid. DS: 53.4. T_g: 106.7 °C. FT-IR (KBr, cm⁻¹): 3486 (OH), 3082 (=C-H, stretching), 2938, 2837 (-C-H, stretching), 1705 (C=O, stretching), 1611, 1575 (C=C, stretching) and 1256, 1211, 1163 (C-O, stretching). ¹H-NMR (400 MHz, DMSO-*d*₆, δ, ppm): 7.71 (br, 1H, Ar-CH=), 7.05, 6.46 (br, 3H, Ar-H), 6.26 (br, 1H, =CH-COOR), 5.5-4.6 (br, 1H, -OH), 4.5-4.0 (br, 1H, of -CH-OH and -CH-OCOCH₃), 3.76 (br, 4H, 3xOCH₃) and 2.30-1.00 (br, 1H of CH₃-CO and 6H of -CH-CH₂-CH- of PV(OH) backbone). UV-vis (DMSO) λ_{max}, nm (ε, M⁻¹cm⁻¹, per monomeric unit): 292 (5232) and 354 (5679).

2.5 Preparation of the substituted polymeric nanoparticles

The polymeric micro/nanoparticles were prepared by dialysis method [4,40,41]. Twenty four milligrams of the substituted PV(OH) were dissolved in DMF and adjusting the final volume to 40 ml, yielding polymeric solution at concentration of 600 ppm. The resulting solution was subsequently loaded into the dialysis membrane tube and was then dialyzed against deionized water (Milli-Q[®]) for 5 days (15x1,000 ml changes of water). Then, the aqueous suspension of the resulting nanoparticles in the membrane tube was analyzed or freeze-dried.

2.6 General procedure for molar absorptivity measurements [42,43]

The stock solution of each obtained PV(OH) was prepared in a 100 ml volumetric flask using dimethylformamide (DMF) as a solvent. The resulting stock solution was then diluted to five final concentrations. The each final solution was subjected to UV-vis spectroscopic analysis by scanning wavelength between 200 to 600 nm. The molar absorptivity (ϵ) at the wavelength of maximum absorption (λ_{\max}) was calculated by Beer's law:

$$A = \epsilon bc$$

Where A is absorbance

b is the cell path length (1 cm)

c is the concentration of the absorbing species in mole per liter

สถาบันวิทยบริการ
จุฬาลงกรณ์มหาวิทยาลัย

CHAPTER III

RESULT AND DISCUSSION

3.1 Synthesis of *trans*-substituted cinnamic acid derivatives

The *trans*-substituted cinnamic acids, 2,4-dimethoxycinnamic acid and 2,4,5-trimethoxycinnamic acid, were successfully synthesized using Knoevenagel-Doebner condensation between benzaldehyde and malonic acid. The structure of both acids, see chapter II, Figure 2.1) were characterized using ¹H-NMR, UV and IR (Appendix A1 and A2). The *trans*-configuration of C=C double bond of all cinnamic acids were confirmed by ¹H-NMR; two signals at approximately 6.6 and 8.3 ppm with $J = 16$ Hz.

3.2 Synthesis of poly(vinylalcohol-co-vinylcinnamate)

Grafting of cinnamoyl moieties (CA) onto PV(OH) (Mw 124,000-186,000), (PV(OH) (124,000 Daltons) could be done successfully using classical esterification reaction between hydroxyl functionalities of the PV(OH) and the cinnamoyl chloride, which was prepared *in-situ* from the synthesized cinnamic acids and thionyl chloride (see chapter II, Scheme 2.2). Since PV(OH) is hydrophilic polymer, introducing cinnamoyl onto the chain means putting on some hydrophobicity onto the polymer. The obtained products, poly(vinylalcohol-co-vinylcinnamate), are, therefore, amphiphilic. The ratio of hydrophobicity/hydrophilicity of the polymer varies with the degree of cinnamoyl substitution.

PV(OH) (124,000 Daltons) was reacted with various mole ratios of cinnamic acid (Table 3.1). Structures of the products were elucidated using ¹H-NMR, IR and UV absorption.

¹H-NMR spectrum of PV(OH) in DMSO shows resonances of the backbone methylene protons at 0.8-1.8 ppm and the methine protons attached to -OH and -OCOCH₃, at 3.83 and 3.88 ppm, respectively (Appendix A3). The -CH₃ protons of the acetate group resonance at 1.94 ppm while the hydroxyl protons are separated into triads at 4.25, 4.49 and 4.68 ppm due to their hydrogen bonding with DMSO [12,13]. The ¹H spectra of the synthesized poly(vinylalcohol-co-vinylcinnamate) in DMSO

show all the above described peaks with additional resonances at 6-8 ppm from cinnamoyl protons. Degree of substitution (n, m and p; see Table 3.1, Appendix A6-A8) was obtained from the ^1H -NMR spectrum of each product using the integration of peaks at 0.8-2.3 ppm (-CH-CH₂-CH- of PV(OH) backbone) and CH₃-CO-, and 6.2-8.4 ppm (-COCH=CH-Ar and Ar-H). It should be noted here that the ^1H NMR spectra obtained using the long delay times between pulses (25 s for 45 ° pulses) were similar to the spectra obtained using normal delay times (1 s for 45 ° pulses). Structures, degree of substitution, UV absorption, molar absorption coefficient per monomer unit and glass transition temperature (T_g) of the obtained poly(vinylalcohol-co-vinylcinnamate) derivatives are shown in Table 3.1.



สถาบันวิทยบริการ
จุฬาลงกรณ์มหาวิทยาลัย

Table 3.1 Structure and physicochemical properties of the poly(vinylalcohol-co-vinylcinnamate) derivatives.

$\left[\text{CH}_2 - \underset{\text{O}-\text{C}(=\text{O})-\text{CH}_3}{\text{CH}} \right]_n \left[\text{CH}_2 - \underset{\text{OH}}{\text{CH}} \right]_m \left[\text{CH}_2 - \underset{\text{O}-\text{C}(=\text{O})-\text{CH}=\text{CH}-\text{C}_6\text{H}_5}{\text{CH}} \right]_p$								
Compound	mole ratio ^a PV(OH):CA	Product characterization						
		n	m	p (DS)	λ_{max}	ϵ ^b	T_g ^c (°C)	T_m ^d (°C)
PV(OH) ^e	-	0.11	0.89	-	-	-	-	191.5
PA1	1:0.1	0.11	0.85	0.04	279	1364	71.6	142.1
PA2	1:1	0.11	0.75	0.14	282	2544	72.8	-
PA3	1:3	0.11	0.64	0.25	280	4814	73.1	-

^a Used in the reaction (mole OH:mole CA)

^b Molar absorption coefficient values ($\text{M}^{-1}\text{cm}^{-1}$ per the monomeric unit)

^c glass transition temperature

^d melting temperature

^e Mw 124,000-186,000

In this work, the highest substitution degree of cinnamoyl moiety in the prepared poly(vinylalcohol-co-vinylcinnamate) was $\sim 25\%$ (DS = 0.25). The structures of the obtained poly(vinylalcohol-co-vinylcinnamate) polymers (**PA1**, **PA2** and **PA3**) were also confirmed by UV-vis spectroscopy (Figure 3.1). Normally, PV(OH) shows no absorption around 280-320 nm (Figure 3.1 (a)). In contrast, **PA1**, **PA2** and **PA3** showed obvious absorption in the UVB region ($\lambda_{\text{max}} \sim 280$ nm). In addition, IR spectra of the products show obvious C=O stretching at $\sim 1710 \text{ cm}^{-1}$. Thus, it can be concluded that cinnamoyl was successfully grafted

onto PV(OH). Molar absorption coefficient values (Table 3.1) indicated that **PA3** ($\epsilon_{280\text{nm}} = 4814 \text{ M}^{-1} \text{ cm}^{-1}$ per monomeric unit) was more efficient in absorbing the UVB radiation than **PA2** ($\epsilon_{282\text{nm}} = 2544 \text{ M}^{-1} \text{ cm}^{-1}$ per monomeric unit) and **PA2** was more efficient in absorbing the UVB radiation than **PA1** ($\epsilon_{279\text{nm}} = 1364 \text{ M}^{-1} \text{ cm}^{-1}$ per monomeric unit). The increases in UV absorbance of the three products agree well with their degree of substitution obtained from ^1H NMR data.

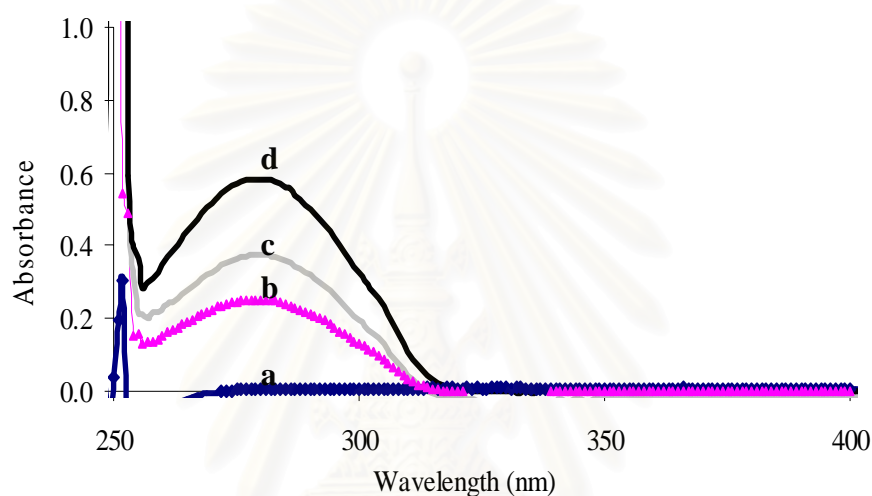


Figure 3.1 UV absorption spectra of 200 ppm (in DMSO) of **PV(OH)** (**124,000 Dalton**) (a) and 10 ppm (in DMSO) of poly(vinylalcohol-co-vinylcinnamate) **PA1** (b), **PA2** (c) and **PA3** (d).

The thermogram of **PV(OH)** (**124,000 Daltons**) showed melting temperature (T_m) at $191.5 \text{ }^\circ\text{C}$ (Table 3.1, Appendix A17). The **PA1**, **PA2** and **PA3** polymer, however, possess glass transition temperature at 71.6 , 72.8 and $73.1 \text{ }^\circ\text{C}$, respectively with no melting characteristic (Appendix A18-A20). This indicates that the thermal property of PV(OH) changed with grafting of cinnamic acid onto its backbone.

Then, the obtained polymers (**PA1-PA3**) (600 ppm) were induced into nanoparticles by dialysis method using DMF as a solvent and water as an anti-solvent. When DMF was displaced by water the hydrophobic groups (cinnamoyl) are probably directed inwards while the hydrophilic domains of the PV(OH) backbone will probably arrange themselves to give maximum interaction with the hydrophilic water leading to spontaneous particle formation. This results in aqueous colloidal

suspension of the polymeric particles. The aqueous suspension of the resulting nanoparticles was subjected to SEM, TEM and dynamic light scattering analyses.

The shape, size, and surface characteristics of **PA1**-, **PA2**- and **PA3**-nanoparticles are shown in Figure 3.2. The underivatized PV(OH) (80% hydrolysis 124,000-186,000 Daltons) (**PV(OH)124K**) could not self-assemble into particles via dialysis method. However, PV(OH) with grafted cinnamoyl on the chain can self-assemble into particles (Figure 3.2). All poly(vinylalcohol-co-vinylcinnamate) nanoparticles (**PA1**, **PA2** and **PA3**) are spherical with smooth surfaces. It should be noted here that particles from **PA1** (DS 0.04) could not be analyzed with scanning electron microscopy (the particles melted during the operation) but the particles could be visualized by transmission electron microscopy.

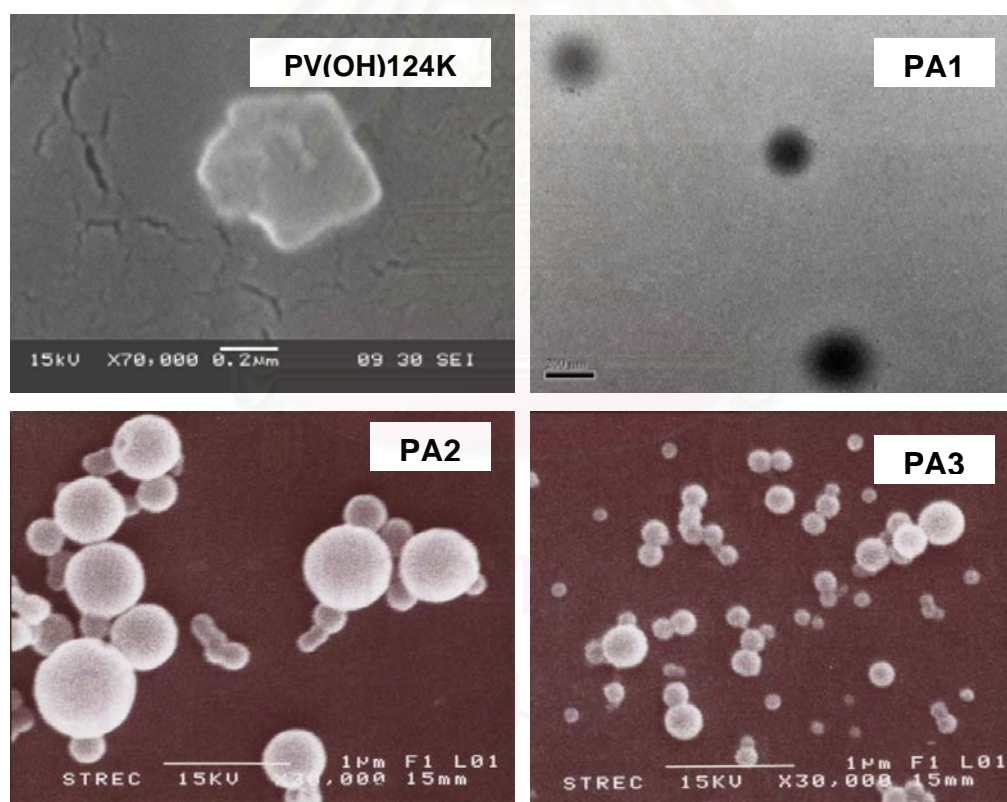


Figure 3.2 Morphology of poly(vinyl alcohol) (Mw 124,000-186,000), (**PV(OH)124K**), **PA1** particles, **PA2** particles and **PA3** particles. All images were obtained by SEM except that of **PA1** particles which was obtained by TEM.

The hydrodynamic diameter was determined by dynamic light scattering (DLS) method. The averages of hydrodynamic diameter of **PA1**, **PA2** and **PA3** were 344 ± 12 nm (PDI = 0.23), 323 ± 2 nm (PDI = 0.12) and 177 ± 0.2 nm (PDI = 0.09), respectively. The particle sizes of poly(vinylalcohol-co-vinylcinnamate) decreased with the increasing substitution degree of cinnamic acid onto PV(OH) backbone. Size distribution of particles obtained from polymer with higher degree of substitution is narrower than from those with lower degree of substitution (Figure 3.3 (a)). It is possible that polymers with more hydrophobicity can tightly packed at their cores, thus forming smaller particles. This speculation has been proposed earlier by Minsu Lee and coworker. They prepared amphiphilic polymer by grafting hydrophobic fluorescein isothiocyanate (FITC) onto hydrophilic glycol chitosan (GC) at various degrees of substitution (DS). The obtained amphiphilic polymers were induced into nanoparticles using dialysis method. The size of self-assembled nanoparticles was dependent on DS. As DS increased from 1.9 to 2.5, the hydrodynamic diameters were decreased from 380 to 280 nm [44]. Jong-Duk Kim and coworker prepared amphiphilic grafted copolymer of poly(asparagine) as the hydrophilic backbone and poly (capolactone) (PCL) as the hydrophobic part. Then, the obtained polymers were induced into nanoparticles using dialysis method. They found that size of the particles decreased with increasing DS of the hydrophobic PCL. They explained the result through the strong hydrophobic interaction of PCL [45].

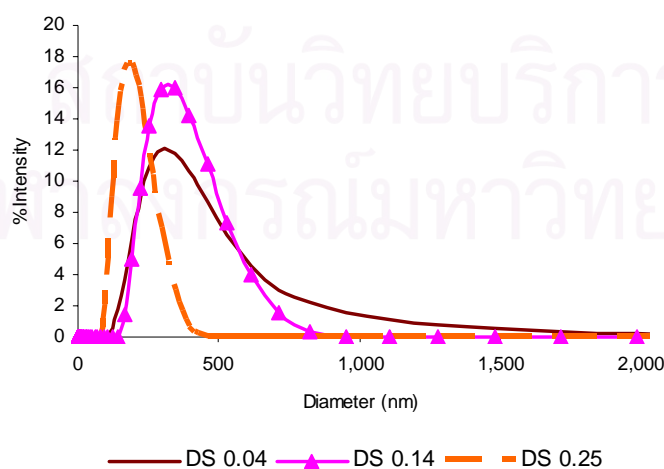
Zeta-potential is a useful indicator of surface charge property and can be employed as an index to the stability of the nanoparticles. In most circumstances, the higher the absolute value of the zeta-potential of the particles, the larger the amount of charge on their surface. These might result in stronger repellent interactions among the particles, and hence, higher stability of the particles is achieved. It should be noted here that the values of < -30 mV or $> +30$ mV were usually used as an indicator of particle stability [46]. Zeta-potential of poly(vinyl alcohol-co-vinylcinnamate) nanoparticles were negative values. Therefore, the nanoparticles had negative charge on the surface and may be attributed to the presence of the oxygen atoms (high electronegative oxygen atom) at the hydroxyl groups. Among particles from the three products, the **PA3** particles are the most stable aqueous colloid. This is because **PA3** particles show the most negative zeta-

potential value (-32.9 mV). **PA2** particles also possess the zeta-potential value of -30.3 mV which indicates that they are quite stable colloid. % Substitution of cinnamoly also affected the surface charge of the obtained particles. Increasing % substitution increased surface charge (Zeta-potential) value of the resulted particles (Table 3.2, Figure 3.3(c)). This is probably related to the size of the particles. The smaller size of particles from higher substituted polymer probably helped increasing the charge density on their surfaces.

Table 3.2 The hydrodynamic diameters determined from dynamic light scattering technique and Zeta-potential of nanoparticulate suspensions prepared from poly(vinylalcohol-co-vinylcinnamate) with DS 0.04 (**PA1**), DS 0.14 (**PA2**) and DS 0.25 (**PA3**), respectively.

Compound	DS	Hydrodynamic diameters (nm) (Average size \pm SD)	Polydisperse Index (PDI)	Zeta-Potential (mV)
PA1	0.04	344 \pm 12	0.23	- 22.7
PA2	0.14	323 \pm 2	0.12	- 30.3
PA3	0.25	177 \pm 0.2	0.09	- 32.9

Size distribution



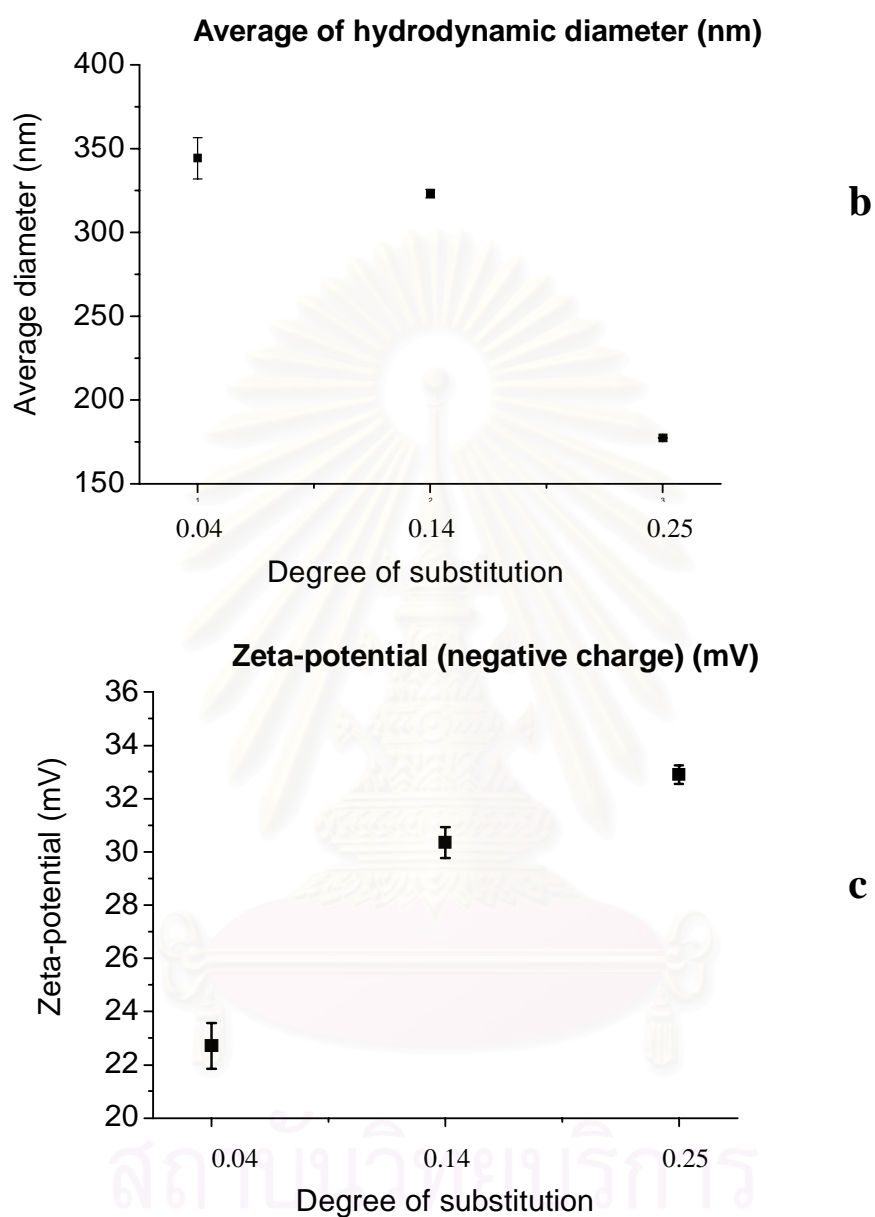


Figure 3.3 Size distribution (a), Average of hydrodynamic diameter (b) and Zeta-potential (c) of nanoparticles prepared from poly(vinylalcohol-co-vinylcinnamate) of various degrees of cinnamate substitution.

Since **PA3** particles are the smallest and most stable particles, **PA3** polymer was prepared into **PA3** particles at various concentrations during particle formation: 6, 60, 600, 6,000, and 12,000 ppm. The obtained nanoparticulate suspensions were subjected to SEM analyses (Figure 3.4).

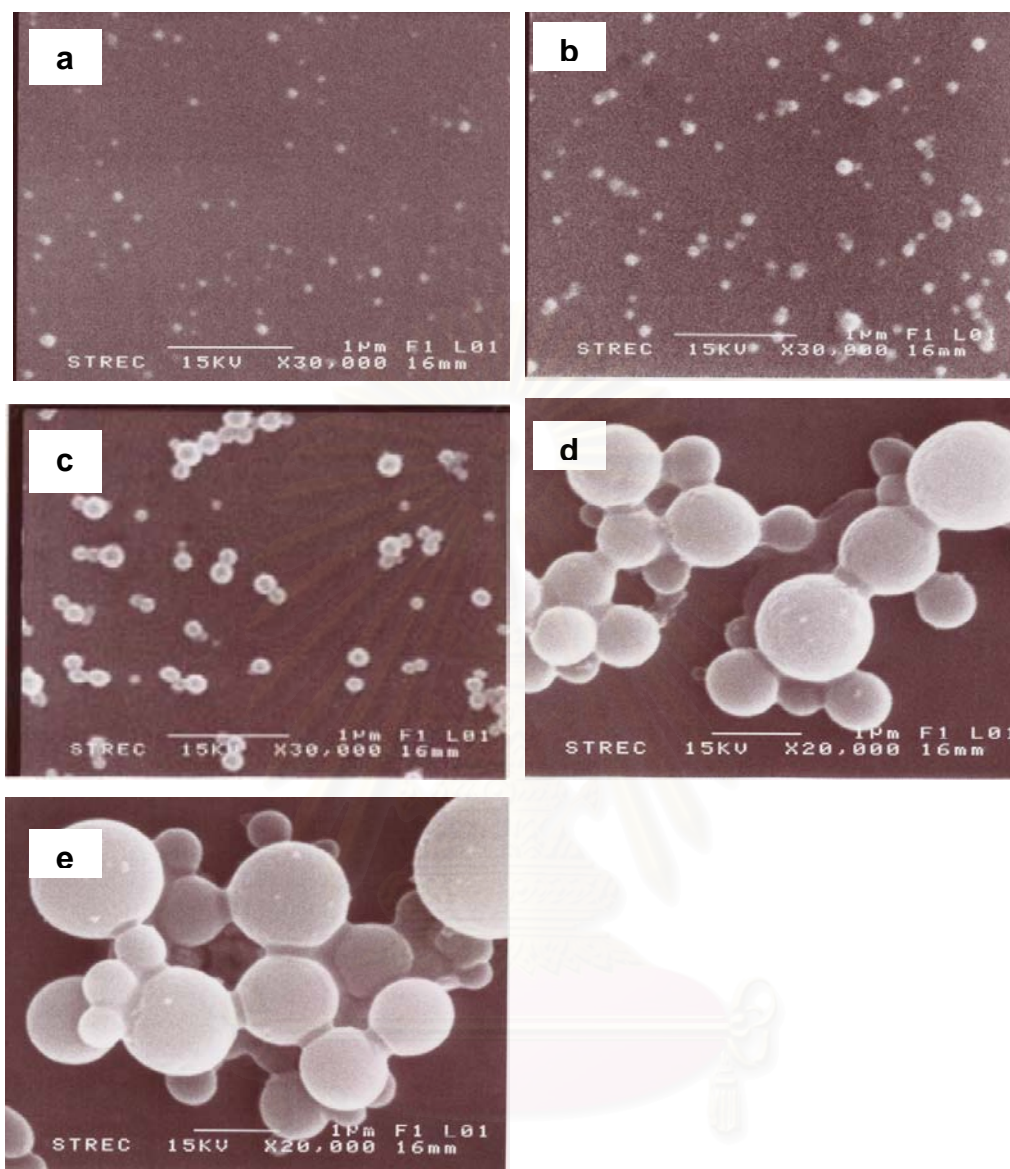


Figure 3.4 Scanning electron micrographs of **PA3** nanoparticles prepared at the concentrations of 6 ppm (a), 60 ppm (b), 600 ppm (c), 6,000 ppm (d), 12,000 ppm (e).

The shape of **PA3** particles obtained at every concentration during the particle formation, is spherical. The particle sizes vary with polymer concentration used during the particle formation. The results revealed that nanoparticles (diameter < 400 nm) can be prepared using low concentration of the poly(vinylalcohol-co-vinyl cinnamate) while microparticles (diameter > 1000 nm) can be prepared using high concentration of the material during the dialysis method. The possible explanation on this, is that at low concentrations, the polymer chains are far away from each other so

it can self-assemble by intramolecular interaction while at high concentration, the polymer chains start to associate to one another by intermolecular interaction between neighboring hydrophobic side chains (Figure 3.5). Therefore, particles formed from associated polymeric chains should be resulted from solution with higher concentration. This, of course, should yield particles with bigger sizes than particles formed from less associated polymeric chains. In addition, the large particles could be a result of interparticle-interaction between neighboring particle's surfaces which resulted in combining of smaller particles into bigger particles (Figure 3.4 (d,e)). This result agrees well with previous work done by Wei Wu and coworkers. They prepared nanoparticles from poly (methoxypolyethleneglycol-co-alkylcyanoacrylate) copolymers with various polymer concentrations via nanoprecipitation/solvent diffusion method. As polymer concentration increased from 2.5 to 15 mg/ml, the particle diameters increased from 170 to 303 nm [47].

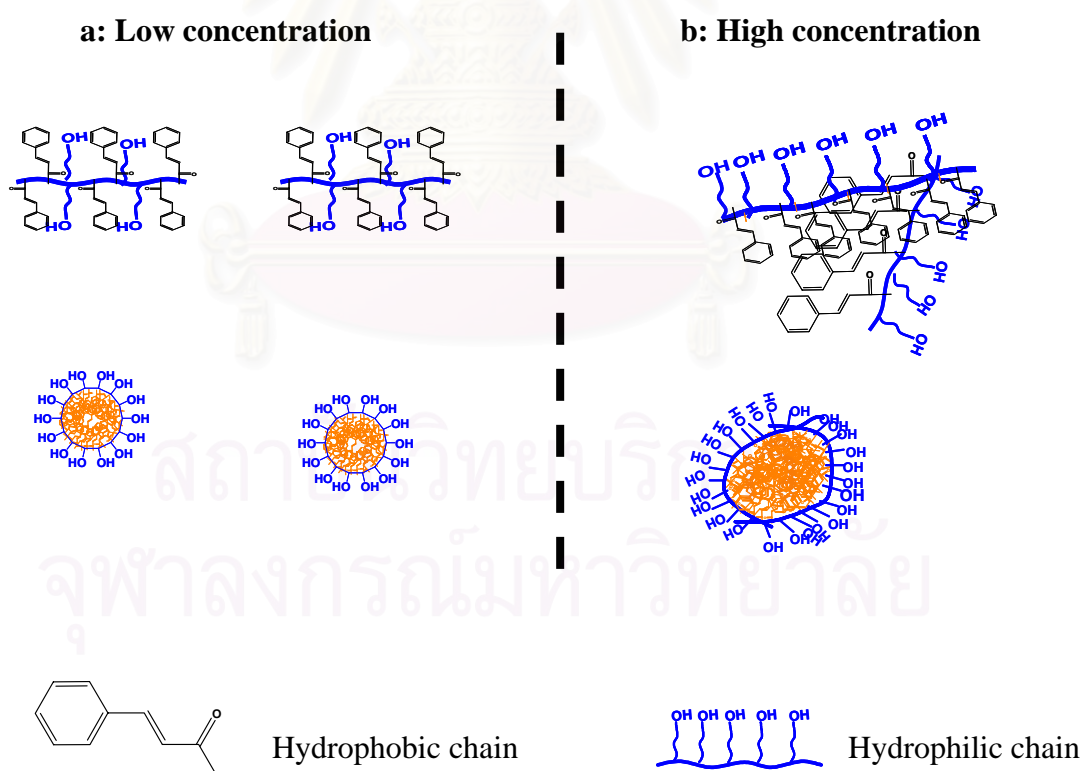


Figure 3.5 Schematic representation of particles at lower polymers concentration (a) and higher polymers concentration (b).

3.3 Synthesis of poly(vinylalcohol-co-vinyl-4-methoxycinnamate)

PV(OH) (Mw 124,000-186,000), (PV(OH) (124,000 Daltons) was reacted with various mole ratios of 4-methoxycinnamic acid (4-MCA) (Table 3.3) to produce poly(vinylalcohol-co-vinyl-4-methoxycinnamate) with various degrees of 4-methoxy cinnamate substitution. Structures of the products were elucidated using $^1\text{H-NMR}$, IR and UV absorption spectroscopy (Appendix A9-A12). The ^1H spectra of the synthesized poly(vinylalcohol-co-vinyl-4-methoxycinnamate) in DMSO are similar to that of poly(vinylalcohol-co-vinylcinnamate) except that the formers have resonances at 3.7 ppm from methoxy protons. Degree of substitution (n, m and p; see Table 3.3) was obtained from the $^1\text{H-NMR}$ spectrum of each product using the integration of peaks at 0.8-2.3 ppm (-CH-CH₂-CH- of PV(OH) backbone and CH₃-CO-), and 6.0-8.4 ppm (-COCH=CH-Ar and Ar-H). Structures, substitution degrees, UV absorption, molar absorption coefficient per monomer unit and glass transition temperature (T_g) of the obtained poly(vinylalcohol-co-vinyl-4-methoxycinnamate) derivatives are shown in Table 3.3.

Table 3.3 Structure and physicochemical properties of the poly(vinylalcohol-co-vinyl-4-methoxycinnamate) derivatives

Compound	mole ratio ^a PV(OH):MCA	Product characterization						
		n	m	p (DS)	λ_{\max}	ϵ ^b	T_g ^c (°C)	T_m ^d (°C)
PV(OH) ^e	-	0.11	0.89	-	-	-	-	191.5
PB1	1:0.1	0.11	0.88	0.01	311	131	63.8	163.8
PB2	1:0.3	0.11	0.80	0.09	311	2109	79.1	-
PB3	1:1	0.11	0.62	0.27	309	4242	79.6	-
PB4	1:3	0.11	0.45	0.44	310	10072	82.0	-

^a Used in the reaction (mole OH:mole MCA)

^b Molar absorption coefficient values ($M^{-1}cm^{-1}$ per the monomeric unit)

^c glass transition temperature

^d melting temperature

^e Mw 124,000-186,000

The highest substitution degree of 4-methoxycinnamoyl moiety on PV(OH) backbone of the poly(vinylalcohol-co-vinyl-4-methoxycinnamate) was ~ 44% (DS = 0.44). The structure of the obtained poly(vinylalcohol-co-vinyl-4-methoxycinnamate) polymers (**PB1**, **PB2**, **PB3** and **PB4**) were also confirmed by IR (Appendix **A9-A12**) and UV-vis absorption spectra (Figure 3.6). IR spectra of the products show obvious

C=O stretching at $\sim 1710\text{ cm}^{-1}$. **PB1**, **PB2**, **PB3** and **PB4** polymer showed obvious absorption in the UVB region ($\lambda_{\text{max}} \sim 310\text{ nm}$). Molar absorption coefficient values (Table 3.3) indicated that **PB4** ($\epsilon_{311\text{nm}} = 10072\text{ M}^{-1}\text{cm}^{-1}$ per monomeric unit) was more efficient in absorbing the UVB radiation than **PB3** ($\epsilon_{311\text{nm}} = 4242\text{ M}^{-1}\text{cm}^{-1}$ per monomeric unit) and **PB3** was more efficient in absorbing the UVB radiation than **PB2** ($\epsilon_{309\text{nm}} = 2109\text{ M}^{-1}\text{cm}^{-1}$ per monomeric unit) and **PB2** was more efficient in absorbing the UVB radiation than **PB1** ($\epsilon_{310\text{nm}} = 131\text{ M}^{-1}\text{cm}^{-1}$ per monomeric unit). The increases in UV absorbance of the four products agree well with their degree of substitution obtained from ^1H NMR data.

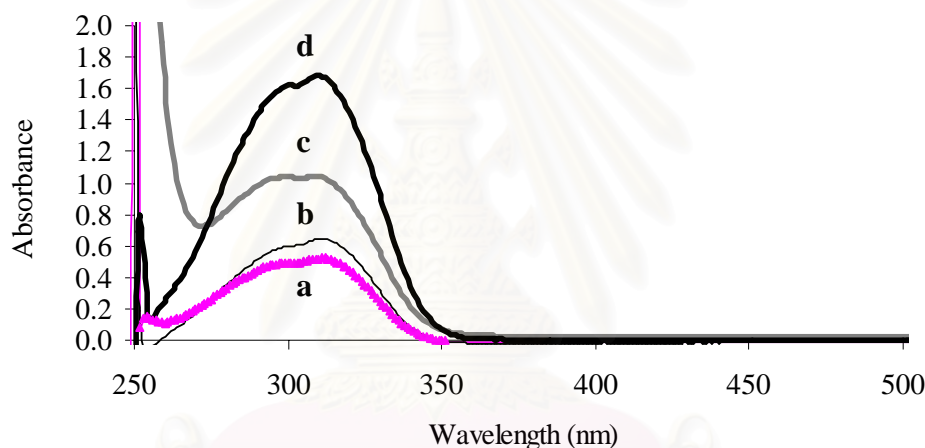


Figure 3.6 UV absorption spectra of poly(vinylalcohol-co-vinyl-4-methoxy cinnamate): 200 ppm (in DMSO) of **PB1** (a) and 20 ppm (in DMSO) of **PB2** (b), **PB3** (c) and **PB4** (d).

The thermogram of **PV(OH)** (**124,000 Daltons**) showed melting temperature (T_m) at $191.5\text{ }^\circ\text{C}$. The **PB1**, **PB2**, **PB3** and **PB4** polymer, however, possess glass transition temperature (T_g) at 63.8 , 79.1 , 79.6 and $82.0\text{ }^\circ\text{C}$, respectively with no melting characteristic (Table 3.3, Appendix **A21-A24**). This indicates that the thermal property of **PV(OH)** changed with grafting of 4-methoxycinnamic acid onto its backbone.

Then, the obtained polymers (**PB1-PB4**) (600 ppm) were induced into nanoparticles by dialysis method using DMF as a solvent and water as an anti-solvent. Then, the aqueous suspension of the resulting nanoparticles was subjected to SEM, TEM and dynamic light scattering analyses.

The shape, size, and surface characteristics of poly(vinylalcohol-co-vinyl-4-methoxycinnamate) nanoparticles are shown in Figure 3.7. Similar to PV(OH), the compound **PB1** (DS 0.01) could not self-assemble into particles via dialysis method. However, PV(OH) with higher 4-methoxycinnamoyl substitution on the chain can self-assemble into particles (Figure 3.7). All poly(vinylalcohol-co-vinyl-4-methoxycinnamate) nanoparticles (**PB2**, **PB3** and **PB4**) are spherical with smooth surfaces. Consequently, it can be concluded that the hydrophobicity from 4-methoxycinnamoyl moieties are crucial for particle formation. It should be noted that particles from **PB1** (DS 0.01) and **PB2** (DS 0.09) could not be analyzed with SEM (the particles melted during the operation) but the particle could be visualized by TEM.

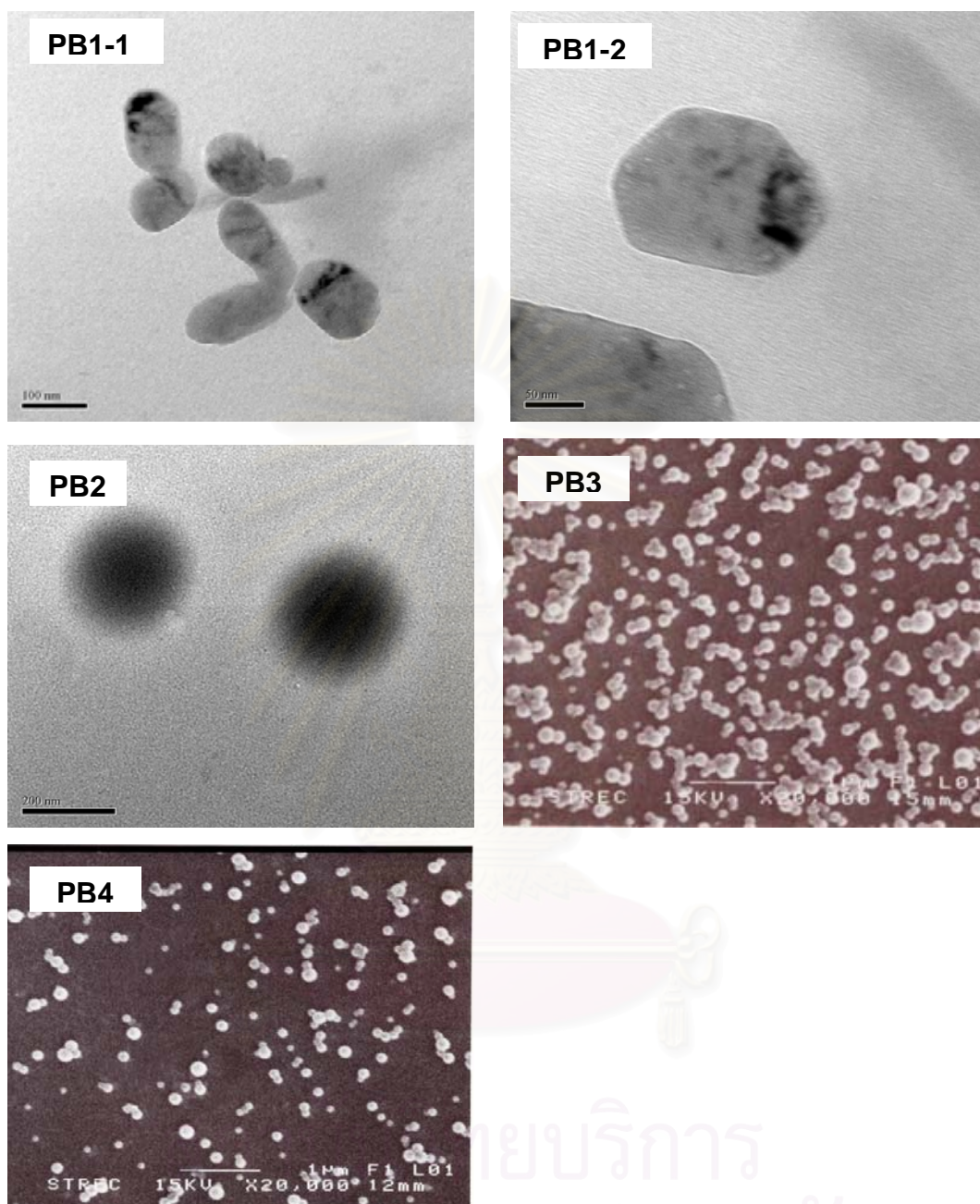


Figure 3.7 Morphology of **PB1** particles, **PB2** particles, **PB3** particles and **PB4** particles. **PB1** and **PB2** images were obtained by SEM except that of **PB1** particles and **PB2** particles which were obtained by TEM.

The hydrodynamic diameter was determined by dynamic light scattering (DLS) method. The averages of hydrodynamic diameter of **PB1**, **PB2**, **PB3** and **PB4** were 251 ± 7 nm (PDI = 0.25), 259 ± 7 nm (PDI = 0.22), 151 ± 0.9 nm (PDI = 0.03) and 142 ± 3 nm (PDI = 0.05), respectively. The particle sizes of poly(vinylalcohol-co-vinyl-4-

methoxycinnamate) decreased with the increasing substitution degree of 4-methoxy cinnamoly onto PV(OH) backbone. In addition, the size distribution of particles obtained from polymer with higher degree of substitution is narrower than from those with lower degree of substitution (Figure 3.9 (a)). This result agrees with previous results (Section 3.2) on **PA1-PA3** polymer. The hypothesis that polymers with more hydrophobicity can tightly packed at the cores of the particles, is supported by the fact that some big particles are dented. The dent of the particle indicates loosely packed at the core, which interestingly - is similar to the morphology of red blood cell. An average red blood cell is typically 7-8 microns in diameter. **PB4** particles prepared at very high concentration gave particles with diameter of ~ 1000 nm. These big particles are mostly dented (Figure 3.8).

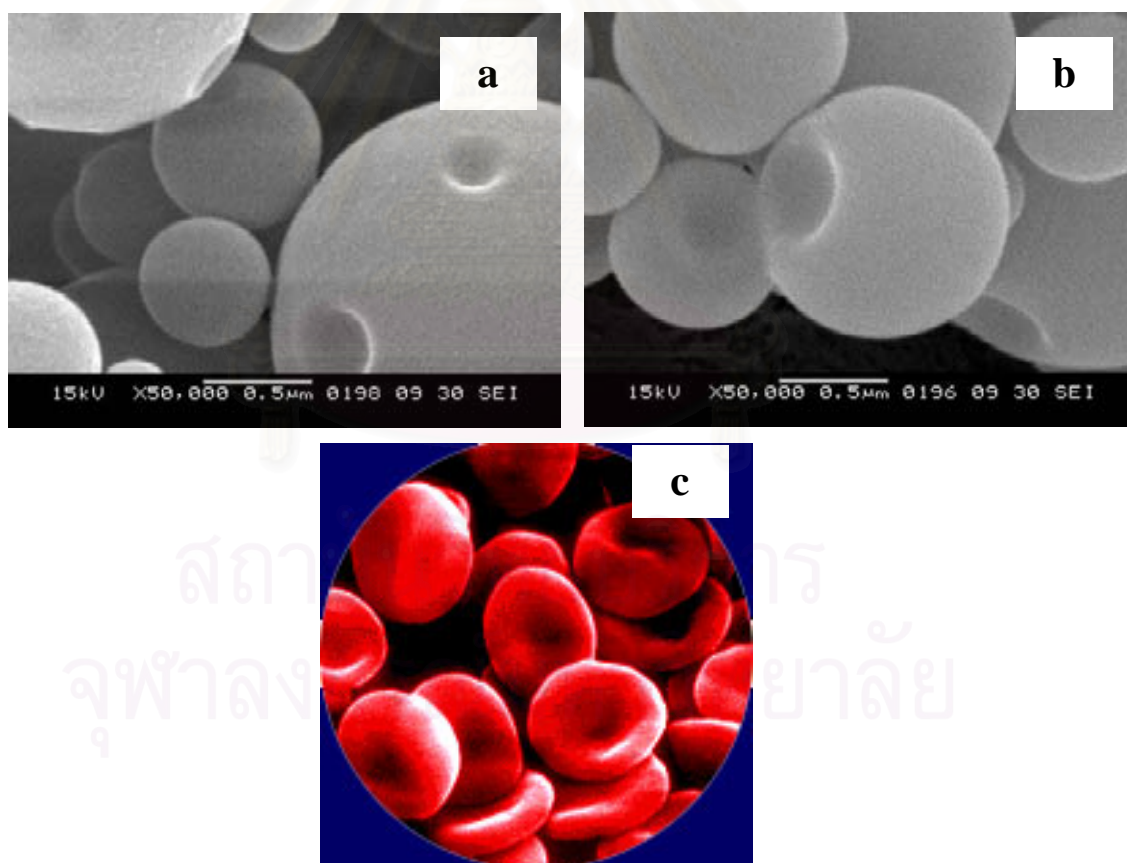
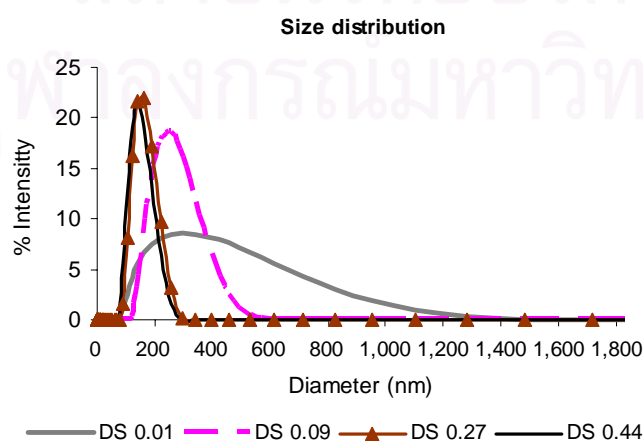


Figure 3.8 Morphology of loosely packed particles of poly(vinylalcohol-co-vinyl-4-methoxycinnamate) (a,b) and red blood cell (c).

Substitution percentage of 4-methoxycinnamoyl also affected the surface charge of the obtained particles. Increasing % substitution increased surface charge (Zeta-potential) value of the resulted particles (Table 3.4, Figure 3.9 (c)). Zeta-potential of poly(vinylalcohol-co-vinyl-4-methoxycinnamate) nanoparticles were negative values. Among particles from the four products, the **PB3** and **PB4** particles are the most stable aqueous colloid. This is because **PB3** and **PB4** particles show the most negative zeta-potential value (~ -29 mV). In contrast, **PB1** shows the lowest negative zeta-potential value (-1.9 mV).

Table 3.4 The hydrodynamic diameters determined from dynamic light scattering technique and Zeta-potential of nanoparticulate suspensions prepared from poly(vinylalcohol-co-vinyl-4-methoxycinnamate) with DS 0.01 (**PB1**), DS 0.09 (**PB2**), DS 0.27 (**PB3**) and DS 0.44 (**PB4**), respectively.

Compound	DS	Hydrodynamic diameters (nm) (Average size \pm SD)	Polydisperse Index (PDI)	Zeta-Potential (mV)
PB1	0.01	251 \pm 7	0.25	- 1.9
PB2	0.09	259 \pm 7	0.22	- 20.5
PB3	0.27	151 \pm 0.9	0.03	- 29.2
PB4	0.44	142 \pm 3	0.05	- 29.1



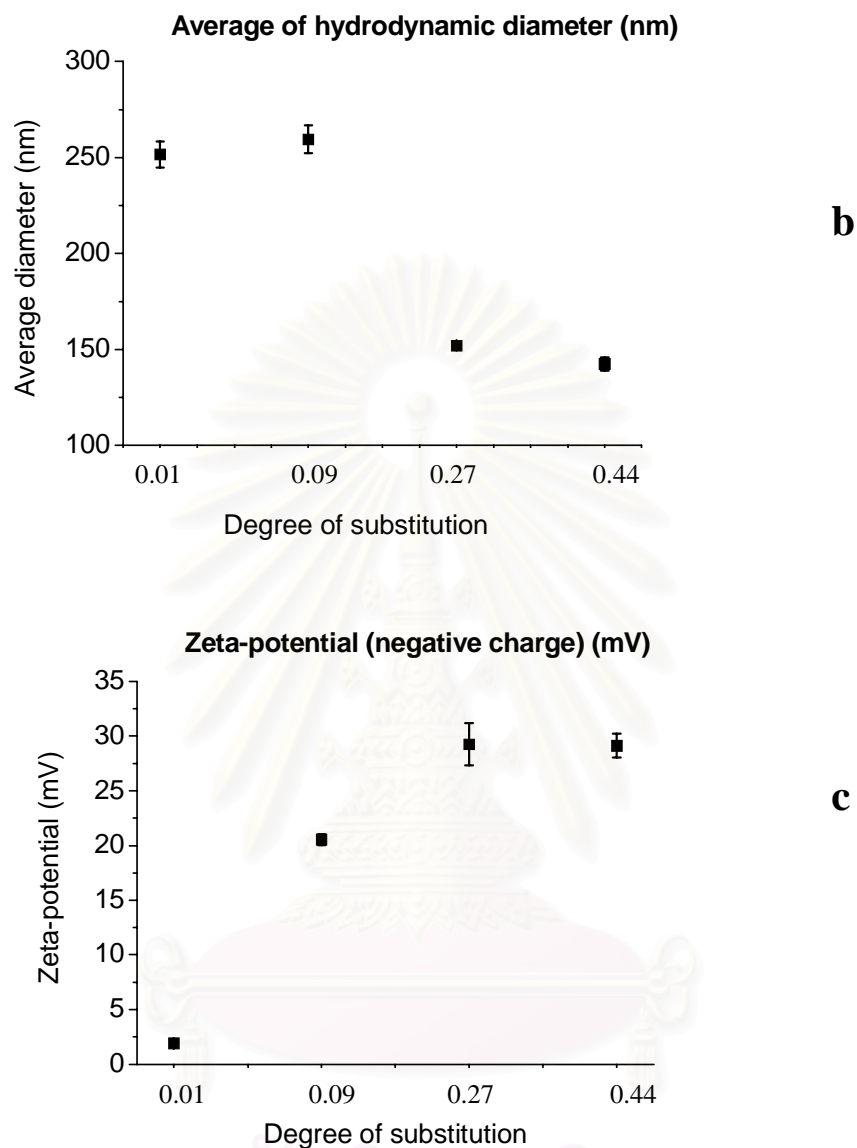


Figure 3.9 Size distribution (a), Average of hydrodynamic diameter (b) and Zeta-potential (c) of nanoparticles prepared from poly(vinylalcohol-co-vinyl-4-methoxy cinnamate) of various degrees of 4-methoxycinnamate substitution.

The compound **PB3** and **PB4** were prepared into particles at various concentrations during particle formation: 6, 60, 600, 6,000, and 12,000 ppm. The obtained nanoparticulate suspensions were subjected to SEM analyses (Figure 3.10 and 3.11).

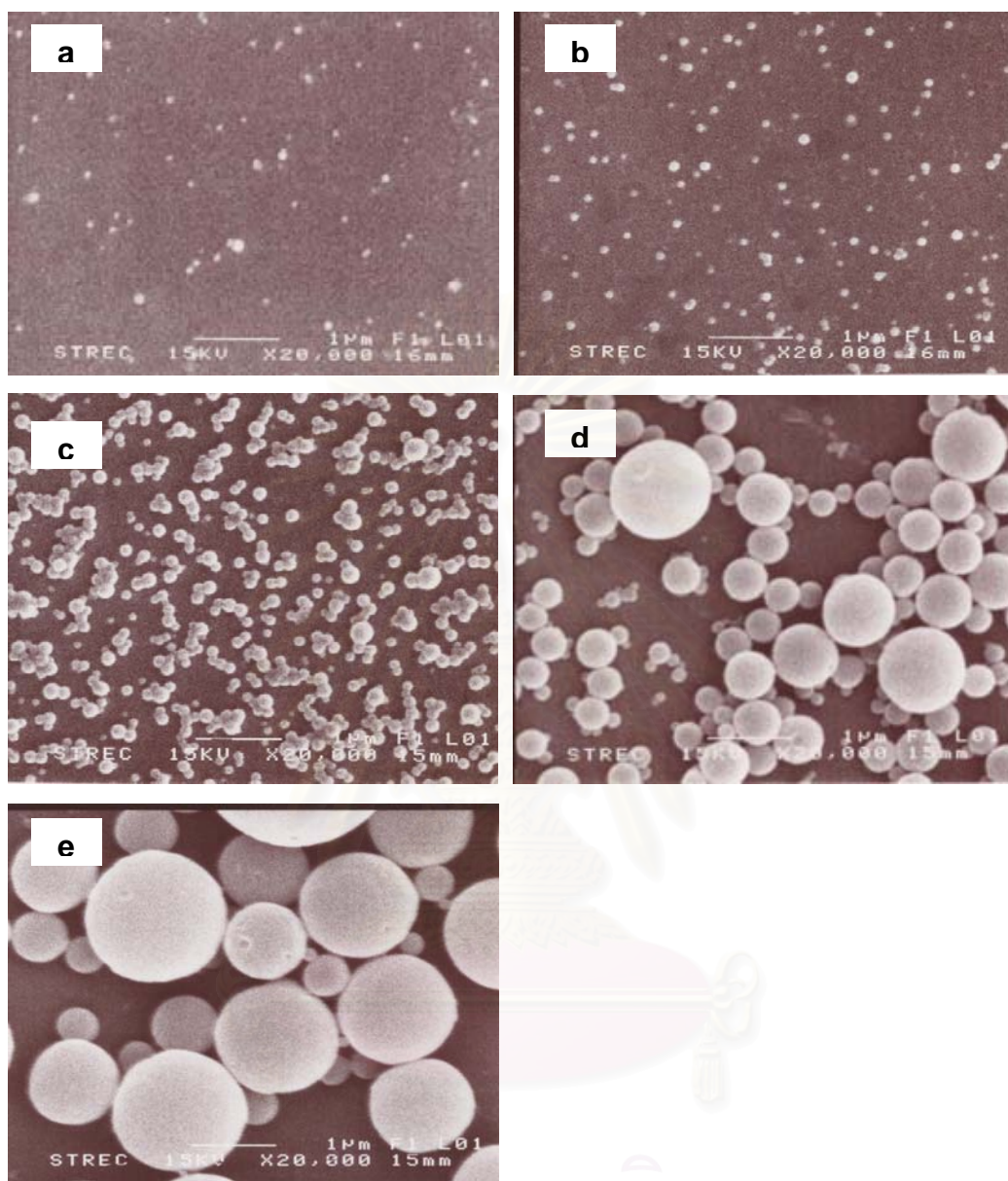


Figure 3.10 Scanning electron micrographs of **PB3** nanoparticles prepared from concentrations of 6 ppm (a), 60 ppm (b), 600 ppm (c), 6,000 ppm (d), 12,000 ppm (e).

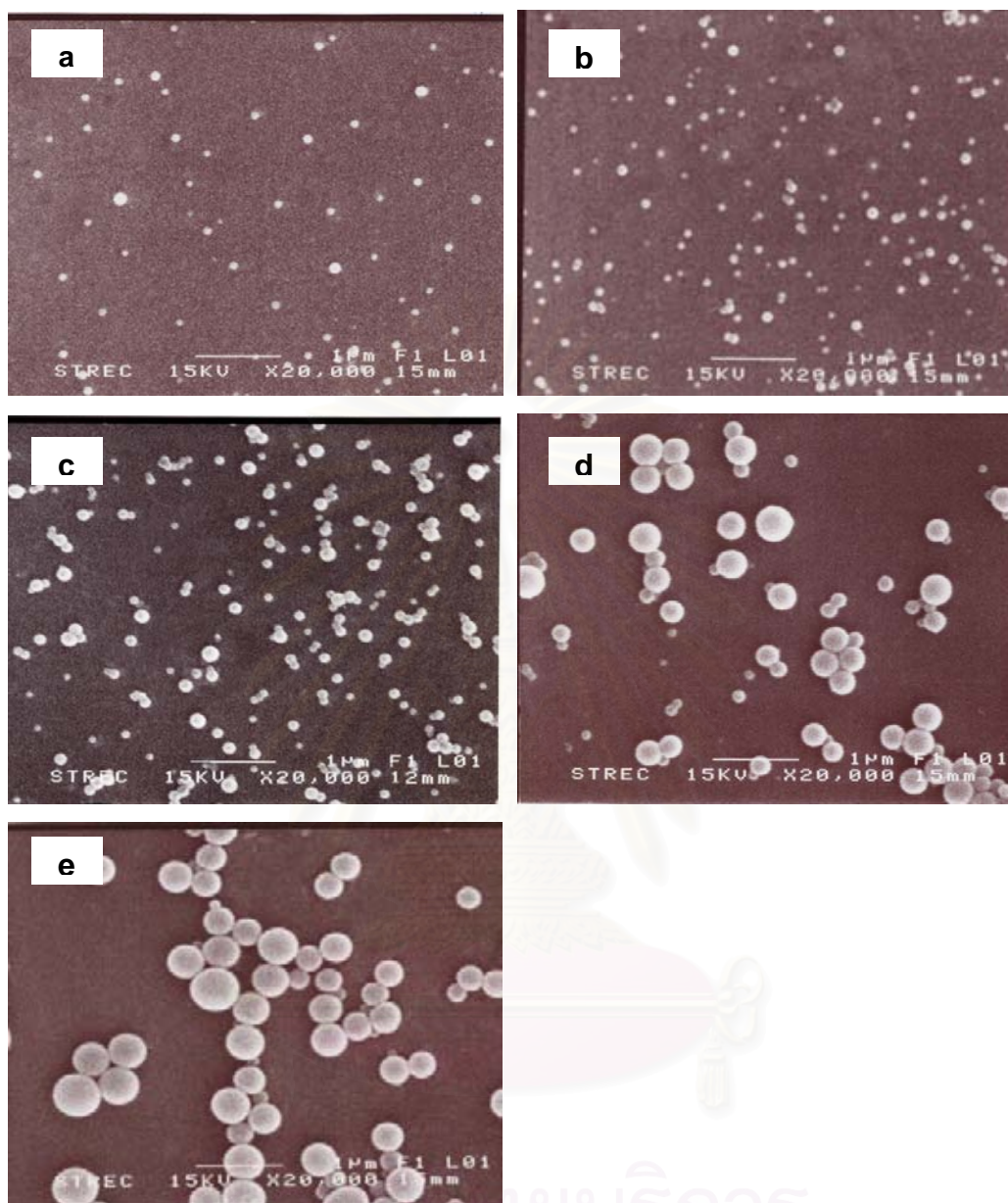


Figure 3.11 Scanning electron micrographs of **PB4** nanoparticles prepared from concentrations of 6 ppm (a), 60 ppm (b), 600 ppm (c), 6,000 ppm (d), 12,000 ppm (e).

The shape of **PB3** and **PB4** particles obtained at every concentration during the particle formation, is spherical. The particle sizes vary with polymer concentration used during the particle formation. The particle size increased with increasing polymer concentration. This result agrees well with previous experiment carried out using poly(vinylalcohol-co-vinylcinnamate) (section 3.2).

3.4 Synthesis of poly(vinylalcohol-co-vinyl-2,4-dimethoxycinnamate)

PV(OH) Mw 124,000-186,000 (**PV(OH)124,000 Daltons**) was reacted with 2,4-dimethoxycinnamic acid to give poly(vinylalcohol-co-vinyl-2,4-dimethoxycinnamate) (**PC**). Structure of the product was elucidated using $^1\text{H-NMR}$, IR and UV absorption (Appendix **A13**). The degree of substitution calculated from the ^1H spectrum of poly(vinylalcohol-co-vinyl-2,4-dimethoxycinnamate) was 46.2% (DS 0.46). Structures, degree of substitution (n, m and p), UV absorption, molar absorption coefficient per monomer unit and glass transition temperature (T_g) of the obtained polymer are shown in Table 3.5.

Table 3.5 Structure and physicochemical properties of the poly(vinylalcohol-co-vinyl-2,4-dimethoxycinnamate) compound.

Compound	Product characterization					
	n	m	p (DS)	λ_{max}	ϵ ($\text{M}^{-1}\text{cm}^{-1}$ per the monomeric units)	T_g ($^{\circ}\text{C}$)
PC	0.11	0.43	0.46	295, 328	6991, 8900	88

The structure of poly(vinylalcohol-co-vinyl-2,4-dimethoxycinnamate) polymer (**PC**) was also confirmed by IR and UV-vis spectroscopy (Figure 3.12). IR spectrum of the products show obvious C=O stretching at $\sim 1706\text{ cm}^{-1}$. **PC** polymer shows obvious absorption in the UVB region ($\lambda_{\text{max}} \sim 295$ and 328 nm). Molar

absorption coefficient values of **PC** compound is 6991 (λ_{\max} 295) and 8900 (λ_{\max} 328) $M^{-1}cm^{-1}$ per monomeric unit). Thus, it can be concluded that 2,4-dimethoxy cinnamoyl was successfully grafted onto PV(OH).

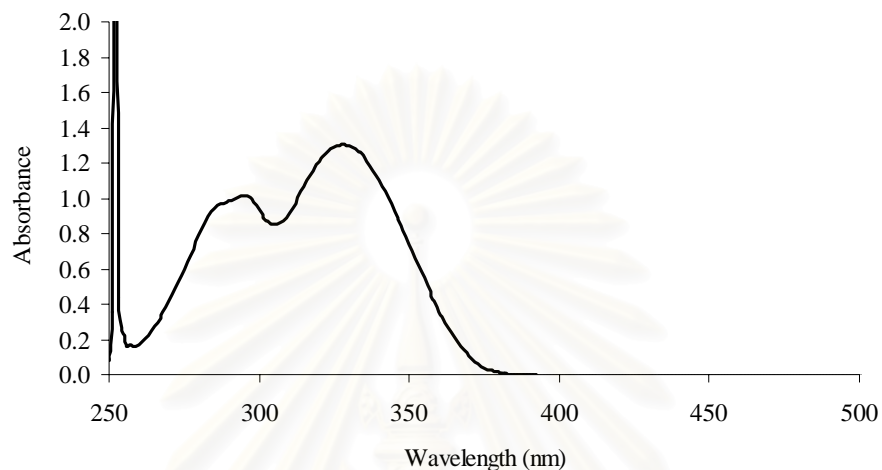


Figure 3.12 UV absorption spectrum of 20 ppm (in DMSO) of poly(vinylalcohol-co-vinyl-2,4-dimethoxycinnamate) polymer.

Then, the obtained **PC** polymer (600 ppm) was induced into nanoparticles by dialysis method using DMF as a solvent and water as an anti-solvent. The shape of poly(vinylalcohol-co-vinyl-2,4-dimethoxycinnamate) nanoparticles was spherical (Figure 3.13).

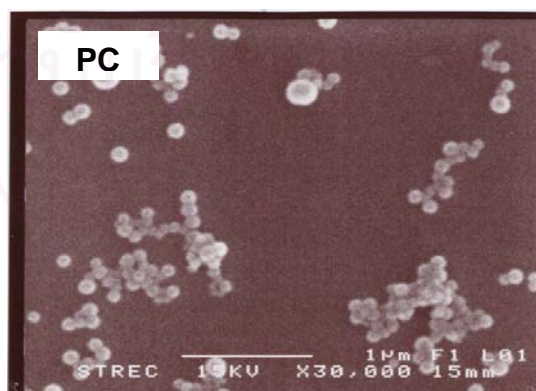


Figure 3.13 Scanning electron micrograph of poly(vinylalcohol-co-vinyl-2,4-dimethoxycinnamate) nanoparticles (**PC**).

3.5 Synthesis of poly(vinylalcohol-co-vinyl-2,4,5-trimethoxycinnamate)

PV(OH) Mw 124,000-186,000 (**PV(OH)124,000 Daltons**) was reacted with 2,4,5-trimethoxycinnamic acid to give poly(vinylalcohol-co-vinyl-2,4,5-trimethoxycinnamate) (**PD**). The structure of the product was elucidated using $^1\text{H-NMR}$, IR and UV absorption (Appendix **A14**). The degree of substitution calculated from the ^1H spectrum of poly(vinylalcohol-co-vinyl-2,4-dimethoxycinnamate) was 53.4% (DS 0.53). Structures, degree of substitution (n, m and p), UV absorption, molar absorption coefficient per monomer unit and glass transition temperature (T_g) of the obtained polymer are shown in Table 3.6.

Table 3.6 Structure and physicochemical properties of the poly(vinylalcohol-co-vinyl-2,4,5-trimethoxycinnamate) compound.

Compound	Product characterization					
	n	m	p (DS)	λ_{max}	ϵ ($\text{M}^{-1}\text{cm}^{-1}$ per the monomeric units)	T_g ($^{\circ}\text{C}$)
PD	0.11	0.36	0.53	292, 354	5232, 5679	106.7

The structure of poly(vinylalcohol-co-vinyl-2,4,5-trimethoxycinnamate) polymer (**PD**) was also confirmed by IR and UV-vis spectroscopy (Figure 3.14). IR spectrum of the products show obvious C=O stretching at $\sim 1705\text{ cm}^{-1}$. **PD** polymer shows obvious absorption in the UVA and UVB region ($\lambda_{\text{max}} \sim 292$ and 354 nm)

(Figure 3.14). Molar absorption coefficient values of **PD** compound is 5232 (λ_{\max} 292) and 5679 (λ_{\max} 354) $M^{-1}cm^{-1}$ per monomeric unit). Thus, it can be concluded that 2,4,5-trimethoxycinnamoyl was successfully grafted onto PV(OH).

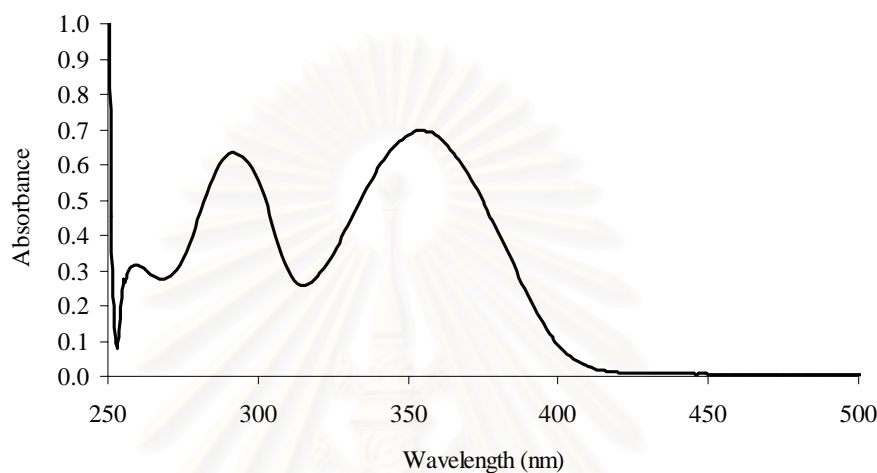


Figure 3.14 UV absorption spectrum of 20 ppm (in DMSO) of poly(vinylalcohol-co-vinyl-2,4,5-trimethoxycinnamate) polymer.

Then, the obtained **PD** polymer (600 ppm) was induced into nanoparticles by dialysis method using DMF as a solvent and water as an anti-solvent. The shape of poly(vinylalcohol-co-vinyl-2,4,5-trimethoxycinnamate) nanoparticles was spherical (Figure 3.15).

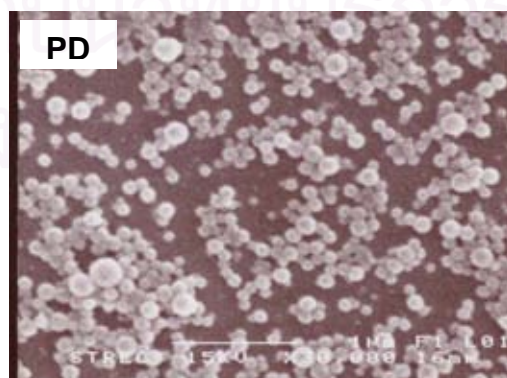
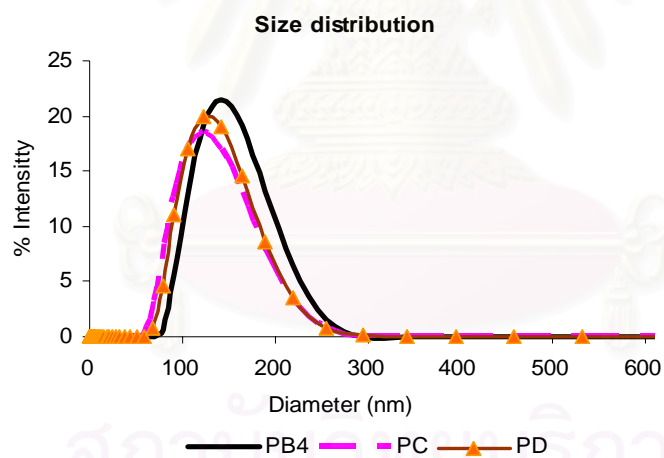


Figure 3.15 Scanning electron micrographs of poly(vinylalcohol-co-vinyl-2,4,5-trimethoxycinnamate) nanoparticles (**PD**).

To investigate the effect of the grafted cinnamoyl structure on the morphology of the obtained particles, particle diameters and surface charges (Zeta-potential), particles obtained from PV(OH) grafted with 4-methoxycinnamoyl (**PB4**), 2,4-dimethoxycinnamoyl (**PC**) and 2,4,5-trimethoxycinnamoyl (**PD**), were compared (Figure 3.7, 3.13, 3.15). All **PB4**, **PC** and **PD** particles were spherical. The averages of hydrodynamic diameter of **PB4**, **PC** and **PD** were 142 ± 3 nm (0.05), 120 ± 1 nm (0.07) and 124 ± 1 nm (0.07), respectively. Particles from **PB4**, **PC** and **PD** have similar size and surface charge (Figure 3.16). It should be noted here that degrees of substitution of cinnamoyl moiety on PV(OH) backbone of **PB4**, **PC** and **PD** are quite similar; DS of 0.44 for **PB4**, DS of 0.46 for **PC** and DS of 0.53 for **PD**. Thus, it can be concluded that at about 50% substitution, structure of the grafted cinnamoyl groups does not affect particles's morphology.



a

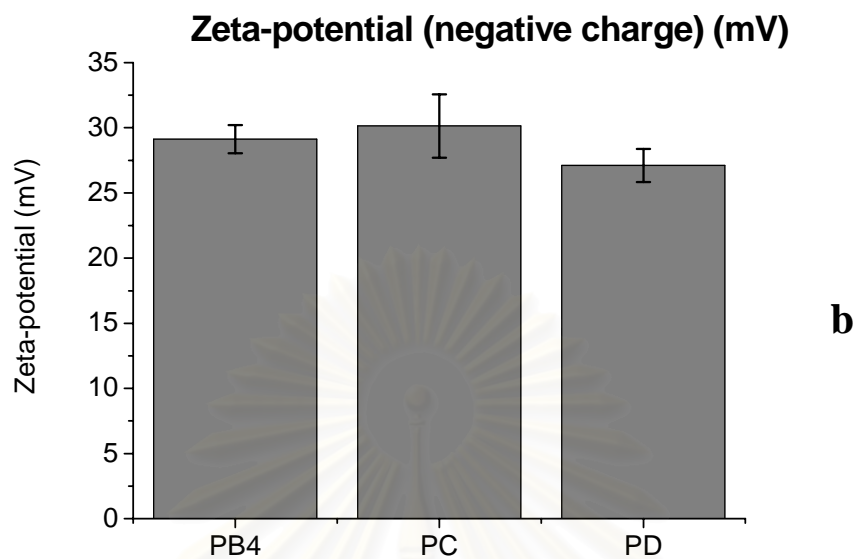


Figure 3.16 Size distribution (a) and Zeta-potential (b) of nanoparticles prepared from poly(vinylalcohol-co-vinylcinnamate) of various *trans*-substituted cinnamic acid derivatives.

To investigate the effect of chain length of PV(OH) backbone on the obtained particle, grafting 4-methoxycinnamic acid onto PV(OH) Mw 35,000-50,000 (**PV(OH)50,000 Daltons**) and PV(OH) Mw 9,000-10,000 (**PV(OH)10,000 Daltons**) backbone were carried out. Structures of the products were elucidated using $^1\text{H-NMR}$, IR and UV absorption (Appendix **A15** and **A16**). Structures, substitution degrees, UV absorption, molar absorption coefficient per monomer unit and glass transition temperature (T_g) of the obtained polymers are shown in Table 3.7.

Table 3.7 Structure and physicochemical properties of the poly(vinylalcohol-co-vinyl-4-methoxycinnamate) prepared from PV(OH)50,000 Daltons (**P₅B**), PV(OH)10,000 Daltons (**P₉B**) and PV(OH)124,000 Daltons (**PB3**, **PB4**).

Compound	Mw of PV(OH) used	Product characterization					
		n	m	p (DS)	λ_{\max}	ϵ^a	T_g^b (°C)
P₅B	50,000	0.10	0.62	0.28	310	6681	84.5
P₉B	10,000	0.20	0.34	0.46	310	8585	78.7
PB3	124,000	0.11	0.62	0.27	309	4242	79.6
PB4	124,000	0.11	0.45	0.44	310	10072	82.0

^a Molar absorption coefficient values ($M^{-1}cm^{-1}$ per the monomeric unit)

^b glass transition temperature

Then, the obtained polymers (600 ppm) were induced into nanoparticles by dialysis method using DMF as a solvent and water as an anti-solvent. It can be seen (Figure 3.17 and Table 3.8) that changing the starting PV(OH) for that of Mw 124,000 to 10,000 and 50,000, does not affect sizes, shape and surface charge of the obtained particles much. Size, shape and surface charge are comparable for all four particles (**P₅B**, **P₉B**, **PB3** and **PB4**).

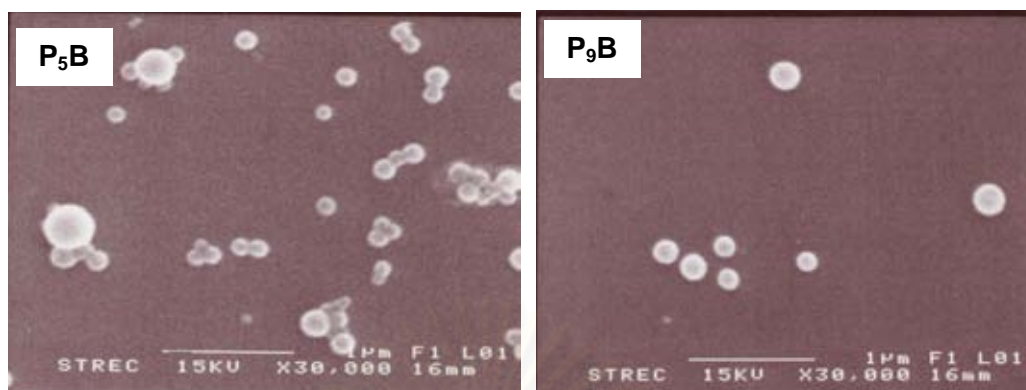


Figure 3.17 Scanning electron micrographs of poly(vinylalcohol-co-vinylcinnamate) prepared from PV(OH)50,000 Daltons (**P₅B**) and PV(OH)10,000 Daltons (**P₉B**).

Table 3.8 The hydrodynamic diameters determined from dynamic light scattering technique and Zeta-potential of the poly(vinylalcohol-co-vinyl-4-methoxycinnamate) nanoparticulate suspensions prepared from PV(OH)50,000 Daltons (**P₅B**), PV(OH)10,000 Daltons (**P₉B**) and PV(OH)124,000 Daltons (**PB3**, **PB4**).

Product	Mw of PV(OH) used	DS	Hydrodynamic diameters (nm) (Average size \pm SD)	Polydisperse Index (PDI)	Zeta-Potential (mV)
P₅B	50,000	0.28	160 \pm 3	0.06	- 30.5
P₉B	10,000	0.46	157 \pm 1	0.06	- 28.6
PB3	124,000	0.27	151 \pm 0.9	0.03	-29.2
PB4	124,000	0.44	142 \pm 3	0.05	-29.1

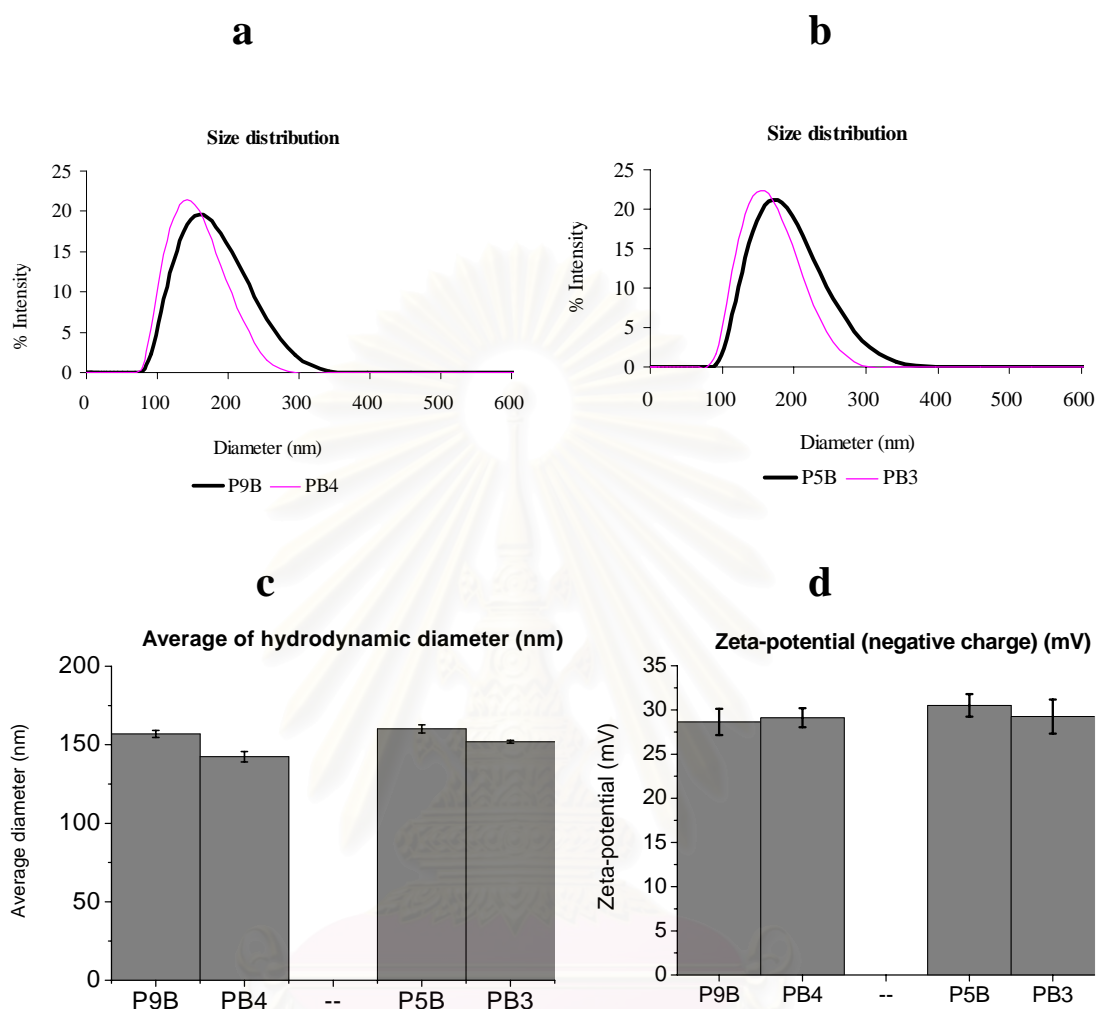


Figure 3.18 Comparing size distribution (a, b), Average of hydrodynamic diameter (c) and Zeta-potential values (d) between particles from poly(vinylalcohol-co-vinyl-4-methoxycinnamate) of different molecular weight.

3.6 Effects of solvent used in the self-assembly process

Six hundreds ppm **PB4** solutions in dimethyl formamide (DMF) and dimethyl-sulfoxide (DMSO) were prepared. The solutions were dialyzed against water to obtained **PB4** particles. SEM photographs revealed that **PB4** particles obtained using DMF as a solvent are similar to **PB4** particles obtained using DMSO as a solvent (Figure 3.19). This may be explained by the fact that the polarities of DMF and DMSO are similar. Although the two solvents possess different viscosity (0.80 cP for DMF and 2.00 cP for DMSO), during self-assembly in which water is more abundant,

the two processes can occur at comparable rate. This result agree well with previous works done by Mitsuru Akashi and coworker in which amphiphilic polymer from grafting of poly(γ -glutamic acid) onto L-phenyllalanine ethylester were prepared. The obtained polymer was induced into nanoparticles with various solvent: DMF, DMSO and dimethyl acetamide (DMAc). They found that the hydrodynamic diameter of obtained polymeric nanoparticles did not differ much [47].

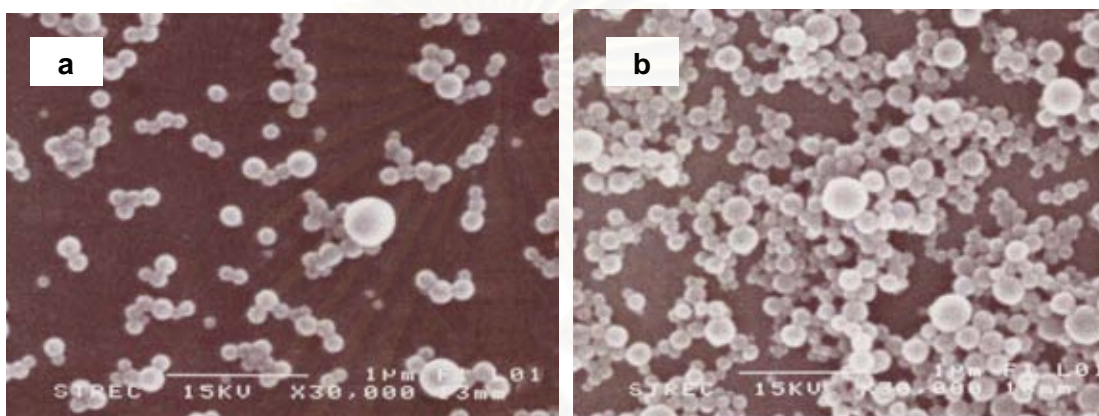


Figure 3.19 Scanning electron micrographs of poly(vinylalcohol-co-vinyl-4-methoxycinnamate) nanoparticles (**PB4**) prepared from DMF (a) and DMSO (b) using as the solvent.

3.7 Effects of anti-solvent used in the self-assembly process

Six hundreds ppm **PB4** solution was prepared in DMF. The resulting solution was dialyzed against deionized water (polar solvent) or hexane (non-polar solvent) to induce the self-assembly of **PB4** into nanoparticles. SEM photographs revealed that when water and hexane were used as an anti-solvent, **PB4** can self-assembly into particles. However, hexane gave particles' diameter of > 1000 nm while water gave particles' diameter of ~ 142 nm (Figure 3.20). This indicated that the obtained polymer although, can self-assembly into particle by dialysis method using non-polar solvent as anti-solvent, the process gave much bigger particles. The difference in size might be a result of different viscosity between water (0.89 cP) and hexane (0.30 cP). Lower viscosity of hexane means quicker self assembly process, comparing to the process in water which has higher viscosity. When DMF was displaced by hexane the

hydrophilic groups (PV(OH) backbone) are probably directed inwards while the hydrophobic (cinnamoyl) will probably arrange themselves to give interaction with the hydrophobic hexane leading to spontaneous particle formation.

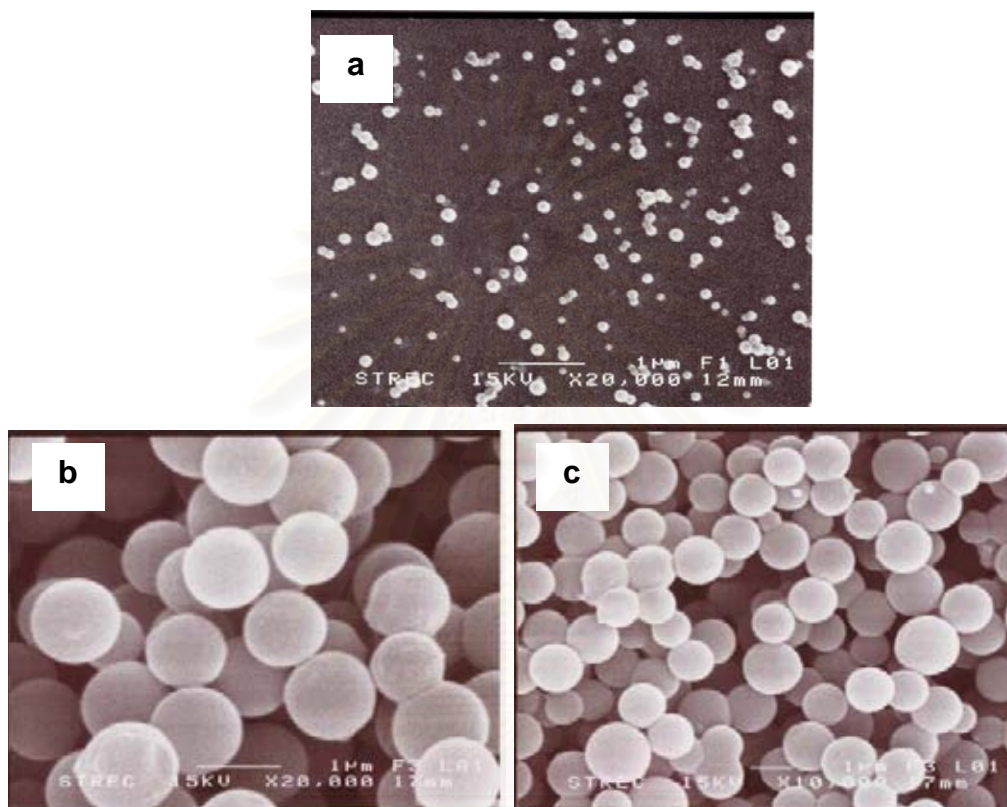


Figure 3.20 Scanning electron micrographs of **PB4** prepared from water (Milli-Q®) (a) and Hexane (b,c) using as the anti-solvent.

3.8 Nanoparticles Stability in various pH of phosphate buffer solution

Two hundred ppm and 600 ppm **PB4** solutions in DMF were prepared and the obtained solutions were dialyzed against water in order to obtain aqueous suspension of nanoparticles. The two nanoparticle suspensions were subjected to dispersibility evaluation under pH 4, 7 and 10, using 0.01 M phosphate buffer. The colloidal stability and aggregation behavior of the aqueous suspensions were observed by vision at room temperature. It was found that the 200 ppm nanoparticle suspensions gave detectable precipitates after 2 weeks at pH 4 and 7 but at pH 10, the nanoparticle suspension gave no detectable precipitate (Figure 3.21). However, the 600 ppm suspensions gave detectable precipitates after 1 hour when kept at all three

pH values. SEM analyses revealed that all precipitates were aggregates of spherical nanoparticles of the 600 ppm suspension (Figure 3.22).

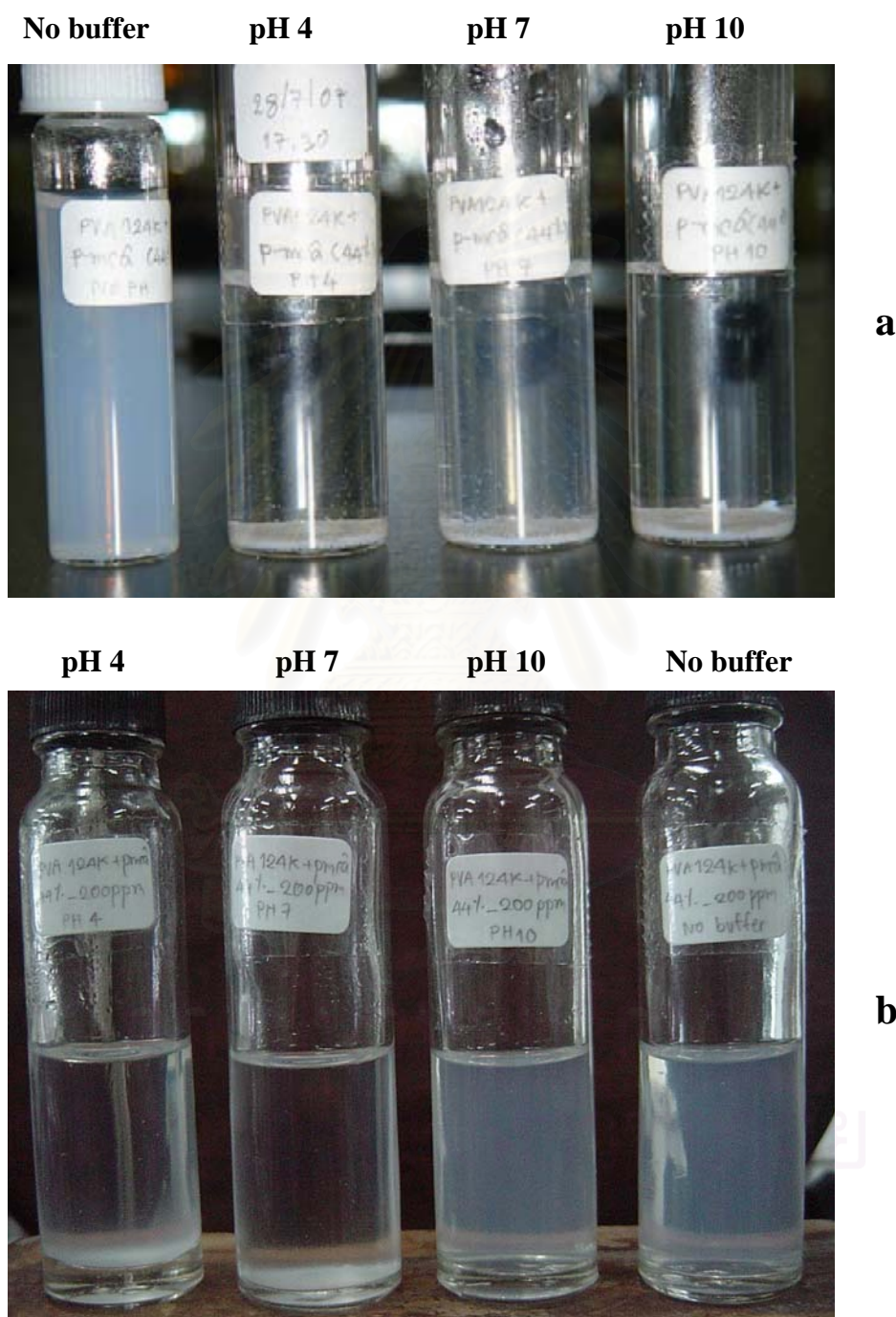


Figure 3.21 Pictures of the colloidal stability and aggregation behavior in various pH of phosphate buffer solution (no buffer, pH 4, pH 7 and pH 10) of 600 ppm (a) and 200 ppm (b) of **PB4** nanoparticle suspensions.

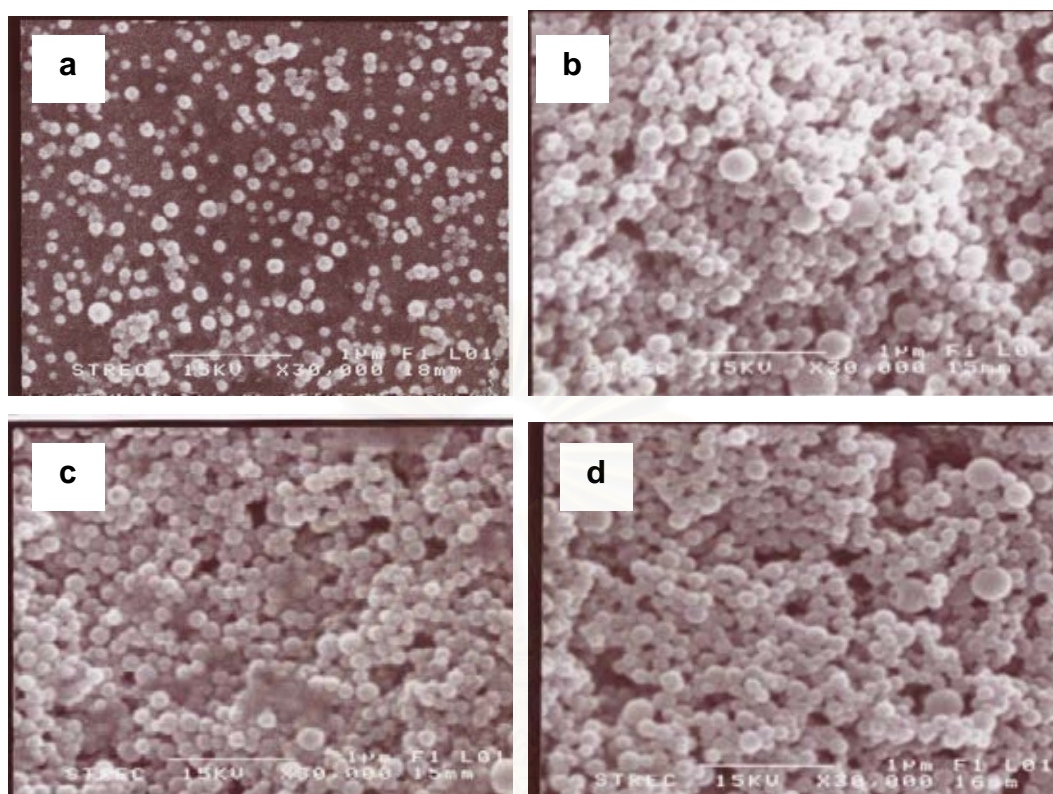


Figure 3.22 Scanning electron micrographs of aggregated nanoparticles of 600 ppm of **PB4** in various pH of phosphate buffer solution. (a) No buffer (b) pH 4 (c) pH 7 and (d) pH 10.

The exact nature of this aggregation phenomenon is not clear. While at 200 ppm unbuffered nanoparticles could be well dispersed some addition of acidic and neutral phosphate buffers lead to aggregation of the particles which resulted in obvious precipitation. Interestingly, the pH 10 dispersion did not precipitate. Explanation on this may lie on the possible deprotonation of the hydroxyl groups around the surface of the particles. Deprotonation of the hydroxyl functionality should create enough negative charges on the particles' surfaces which then will protect particles from aggregation to one another due to charge-repulsion. This repulsion together with Brownian motion of the small particles, thus, overrides the aggregation and setting of the particles from gravitational force. At 600 ppm, however, particles are in much closer proximity to one another, aggregation and gravitational settling, thus, override the charge-repulsion and Brownian motion.

CHAPTER IV

CONCLUSION

During the course of this research, polymeric micro/nanoparticle could be done successfully using amphiphilic polymer, poly(vinylalcohol-co-vinylcinnamate) derivatives, were induced into particle by dialysis method. In this work UV absorbers (cinnamic acid, 4-methoxy cinnamic acid, 2,4-dimethoxycinnamic acid and 2,4,5-trimethoxycinnamic acid) were chosen as hydrophobic substitute to be grafted onto hydrophilic PV(OH) chain. The amphiphilic polymer was successfully synthesized using the classical esterification reaction between hydroxyl functionalities of the PV(OH) and the *trans*-substituted cinnamoyl chloride. This was prepared *in-situ* from the synthesized cinnamic acids and thionyl chloride (see chapter II, Scheme 2.2). Therefore, nanoparticles should also possess some UV screening properties.

Relationships between sizes/shapes of particles and chemical structures of the PV(OH) derivatives were investigated. In addition, influence of polymer's concentration and the type of solvent used during dialysis method, and size/shape of the particles were also studied. From the result, it was found that the degree of substitution (DS) of cinnamoyl moieties on the PV(OH) backbone affected the particle size. The size of the particles and size distribution, decreased with increased DS. The obtained nanoparticles from grafted polymer with higher DS gave more negative zeta potential value than those with lower DS. In addition, poly(vinylalcohol-co-vinyl-cinnamate) (DS = 0.25) and poly(vinylalcohol-co-vinyl-4-methoxycinnamate) (DS = 0.27 and 0.44) polymer were chosen as a model to study how polymer concentration affected particle size during the dialysis method. It was found that the obtained nanoparticles can be prepared using a low concentration of grafted polymer, while microparticles can be prepared using high concentration of the material (Figure 3.4, 3.9, 3.10). However, molecular weight of the PV(OH) backbone (**PV(OH)124000 Daltons**, **PV(OH)50000 Daltons** and **PV(OH)10000 Daltons**), cinnamic acid structure (**CA**, **4-MCA**, **2,4-DMC** and **2,4,5-TMC**), grafted onto the PV(OH) backbone and the solvent (DMF and DMSO) selected to prepare the obtained particles by dialysis method had no effect on the particle size and zeta potential value in this work.

This work demonstrated that poly(vinyl-co-vinylcinnamate) derivatives can be induced into nanoparticles. Future work will be studied about drug or cosmetic active encapsulation, control release, formulation and safety assessment of the materials.



สถาบันวิทยบริการ
จุฬาลงกรณ์มหาวิทยาลัย

REFERENCES

- [1] Matsumoto, J.; Nakada, Y.; Sakurai, K.; Nakamura, T.; and Takahashi, Y. Preparation of nanoparticles consisted of poly(L-lactide)-poly(ethylene glycol)-poly(L-lactide) and their evaluation in vitro. *Int. J. Pharm.* **1999**, *185*, 93-101.
- [2] Williams, J.; Lansdown, R.; Sweitzer, R.; Romanowski, M.; LaBell, R.; Ramaswami, R.; and Unger, E. Nanoparticle drug delivery system for intravenous delivery of topoisomerase inhibitors. *J. Control. Rel.* **2003**, *91*, 167-172.
- [3] Leroux, J. C.; Allemann, E.; Jaeghere, F. D.; Doelker, E.; and Gurny, R. Biodegradable nanoparticles-From sustained release formulations to improved site specific drug delivery. *J. Control. Rel.* **1996**, *39*, 339-350.
- [4] Lee, J. H.; Jung, S. W.; Kim, I. S.; Jeong, YII.; Kim, Y. H.; and Kim, S. H. Polymeric nanoparticle composed of fatty acids and poly(ethylene glycol) as a drug carrier. *Int. J. Pharm.* **2003**, *251*, 23-32.
- [5] Trimaille, T.; Pichot, C.; Elaissari, A.; Fessi, H.; Briancon, S.; and Delair, T. Poly(D,L lactic acid) nanoparticle preparation and colloidal characterization. *Coll. Polym. Sci.* **2003**, *281*, 1184-1190.
- [6] Zambaux, M. F.; Bonneaux, F.; Gref, R.; Dellacherie, E.; and Vigneron, C. MPEO-PLA nanoparticles: Effect of MPEO content on some of their surface properties. *J. Biomed. Mater. Res.* **1999**, *44*, 109-115.
- [7] Akagi, T.; Kaneko, T.; Kida, T.; and Akashi, M. Multifunctional conjugation of proteins on/into bio-nanoparticles prepared by amphiphilic poly(γ -glutamic acid). *J. Biom. Sci., Polym. Ed.* **2006**, *17*, 875-892.
- [8] Li, J. L.; Wang, N.; and Wu, X. S. Poly(vinyl alcohol) nanoparticles prepared by freezing-thawing process for protein/peptide drug delivery. *J. Control. Rel.* **1998**, *56*, 117-126.
- [9] Kimura, T.; Okuno, A.; Miyazaki, K.; Furuzono, T.; Ohya, Y.; Ouchi, T.; Mutsuo, S.; Yoshizawa, H.; Kitamura, Y.; Fujisato, T.; and Kishida, A.

- Novel PVA-DNA nanoparticles prepared by ultra high pressure technology for gene delivery. *Mater. Sci. Eng.* **2004**, *24*, 797-801.
- [10] Jeon, H. J.; Jeong, Y.H.; Jang, M. K.; Park, Y. H.; and Nah, J. W. Effect of solvent on the preparation of surfactant-free poly(DL-lactide-co-glycolide) nanoparticles and norfloxacin release characteristics. *Int. J. Pharm.* **2000**, *207*, 99-108.
- [11] JEONG, Y. I.; CHO, C. H.; KIM, S. H.; KO, K. S.; KIM, S. I.; SHIM, Y. H.; and NAH, J. W. Preparation of Poly(DL-lactide-co-glycolide) Nano particles Without Surfactant. *J. Appl. Polymer. Sci.* **2001**, *80*, 2228-2236.
- [12] Dong, Y.; and Feng, S. S. Poly(D,L-lactide-co-glycolide)/montmorillonite nanoparticles for oral delivery of anticancer drugs. *Biomaterials.* **2005**, *26*, 6068-6076.
- [13] Westedt, U.; Kalinowski, M.; Wittmar, M.; Merdan, T.; Unger, F.; Fuchs, J.; Schaller, S.; Bakowsky, U.; and Kissel, T. Poly(vinyl alcohol)-graft-poly(lactide-co-glycolide) nanoparticles for local delivery of paclitaxel for restenosis treatment. *J. Control. Rel.* **2007**, (in press).
- [14] Christiane, D.; Henri, V.; Peter, B.; and Patrick C. Poly(alkyl cyanoacrylate) Nanospheres for Oral Administration of Insulin. *J. Pharm. Sci.* **1997**, *86*, 1403-1409.
- [15] Soppimath, K. S.; Aminabhavi, T. M.; Kulkarni, A. R.; and Rudzinski, W. E. Biodegradable polymeric nanoparticles as drug delivery devices. *J. Control. Rel.* **2001**, *70*, 1-20.
- [16] Florence, D.; and Maria, J. B. Polymeric Particulates to Improve Oral Bioavailability of Peptide Drugs. *Molecules* **2005**, *10*, 65-80.
- [17] Florence, A. T.; and Hussain, N. Transcytosis of nanoparticle and dendrimer deliver systems: evolving vistas. *Adv. Drug. Deliv. Rev.* **2001**, *50*, 69-89.
- [18] Torche, A. M.; Jouan, H.; Le Corre, P.; Albina, E.; Primault, R.; Jestin, A.; and Le Verge, R. Ex vivo and in situ PLGA microspheres uptake by pig ileal Peyer's patch segment. *Int. J. Pharm.* **2000**, *201*, 15-27.
- [19] Lemoine, D.; and Preat, V. Polymeric nanoparticles as delivery system for influenza virus glycoproteins. *J. Control. Rel.* **1998**, *54*, 15-27.

- [20] Blanco, M. D.; and Alonso, M. J. Development and characterization of protein-loaded poly(lactide-co-glycolide) nanospheres. *Eur. J. Pharm. Biopharm.* **1997**, *43*, 287-294.
- [21] Wade, A.; and Weller, P. J. (Eds.). 1994. Handbook of Pharmaceutical Excipients. American Pharmaceutical Association, Washington, DC.
- [22] Zuccari, G.; Carosio, R.; Fini, A.; Montaldo, P. G.; and Orienti, I. Modified polyvinylalcohol for encapsulation of all-trans-retinoic acid in polymeric micelles. *J. Control Rel.* **2005**, *103*, 369-380.
- [23] Jingwei, X.; and Chi-Hwa, W. Self-assembled biodegradable nanoparticles developed by direct dialysis for the delivery of paclitaxel. *Pharm. Res.* **2005**, *22(12)*, 2079-2090.
- [24] Olenik, I. D.; Kim, M. W.; Rastegar, A.; and Rasing, T. Probing photo-induced alignment in poly(vinyl cinnamate) films by surface second-harmonic generation. *Appl. Phys. B: Lasers and Optics.* **1999**, *68*, 599-603.
- [25] Assaid, I.; Bosc, D.; and Hardy, I. Improvements of the Poly(vinyl cinnamate) Photoresponse in Order to Induce High Refractive Index Variations. *J. Phys. Chem.* **2004**, *108*, 2801-2806.
- [26] Sung, S. J.; Cho, K. Y.; Hah, H.; Lee, S.; and Park, J. Effect of Plasticization of Poly(Vinyl Cinnamate) on Liquid Crystal Orientation Stability. *Jpn. J. Appl. Phys.* **2005**, *44*, L412-L415.
- [27] Lee, E. J.; Kim, S. R.; Kim, J.; and Kim, Y. C. Hepatoprotective Phenyl propanoids from *Scrophularia buergeriana* Roots against CCl₄-Induced Toxicity: Action Mechanism and Structure-Activity Relationship. *Planta Med.* **2002**, *68*, 407-411.
- [28] Shi, Y.; Chen, Q. X.; Wang, Q.; Song, K. K.; and Qiu, L. Inhibitory effects of cinnamic acid and its derivatives on the diphenolase activity of mushroom (*Agaricus bisporus*) tyrosinase. *Food Chemistry.* **2005**, *92*, 707-712.
- [29] Adisakwattana, S.; Sookkongwaree, K.; Roengsumran, S.; Petsom, A.; Ngamrojnavanich, N.; Chavasiri, W.; Deesamerc, S.; and Yibchok-anuna, S. Structure-activity relationships of trans-cinnamic acid derivatives on α -glucosidase inhibition. *Bioorganic & Medicinal Chemistry Letters.* **2004**, *14*, 2893-2896.

- [30] Thitinum Monhaphol. *Synthesis of cinnamate derivatives and related compounds as novel UV filters*. Master's Thesis, Graduate School, Chulalongkorn University, 2002.
- [31] Monhaphol, T.; Albinsson, B; and Wanichwecharungruang, S. P. 2-Ethylhexyl-2,4,5-trimethoxycinnamate and di-(2-ethylhexyl)-2,4,5-trimethoxybenzal malonate as novel broadband UV filters. *J. Pharm. Pharmacol.* **2007**, *59*, 279-288.
- [32] Breitenbach, A.; and Kissel, T. Biodegradable comb polyesters: Part 1 Synthesis, characterization and structural analysis of poly(lactide) and poly(lactide-coglycolide) grafted onto water-soluble poly(vinyl alcohol) as backbone. *Polymer.* **1998**, *39*, 3261-3271.
- [33] Wang, N.; Wu, X. S.; and Li, J. K. A heterogeneously structured composite based on poly(lactic-co-glycolic acid) microspheres and poly(vinyl alcohol) hydrogel nanoparticles for long term protein drug delivery. *Pharm. Res.* **1999**, *16*, 1430-1435.
- [34] Jung, T.; Breitenbach, A.; and Kissel, T. Sulfobutylated poly(vinyl alcohol)-graft-poly(lactide-coglycolide)s facilitate the preparation of small negatively charged biodegradable nanospheres. *J. Control. Rel.* **2000**, *67*, 157-169.
- [35] Jung, T.; Kamm, W.; Breitenbach, A.; Hungerer, K. D.; Hundt, E.; and Kissel, T. Tetanus toxoid loaded nanoparticles from sulfobutylated poly(vinyl alcohol)-graft-poly (lactide-co-glycolide): Evaluation of antibody response after oral and nasal application in mice. *J. Pharm. Res.* **2002**, *18*, 352-360.
- [36] Luppi, B.; Orienti, I.; Bigucci, F.; Cerchiara, T.; Zuccari, G.; Fazzi, S.; and Zecchi, V. Poly(vinylalcohol-co-vinyloleate) for the preparation of micelles enhancing retinyl palmitate transcutaneous permeation. *Drug Delivery.* **2002**, *9*, 147-152.
- [37] Cascone, M. G. Release of dexamethasone from PLGA nanoparticles entrapped into dextran/poly(vinyl alcohol) hydrogel. *J. Materials in Medicine.* **2002**, *13*, 265-269.

- [38] Koo, J.; Fish, M. S.; Walker, G. N.; and Blake, J. 2,3-Dimethoxycinnamic Acid. *Org. Syn. Coll.* **1944**, *4*, 327-328.
- [39] Hartman, R. F.; and Rose, S. D. Kinetics and Mechanism of the Addition of Nucleophiles to Unsaturated Thiol Esters. *J. Org. Chem.* **2006**, *71*, 6342-6350.
- [40] Yokoyama, K.; Satoh, A.; Sakurai, Y.; Okano, T.; Matsumara, Y.; Kakizoe, T.; and Kataoka, K. Incorporation of water-insoluble anticancer drug into polymeric micelles and control of their particle size. *J. Control. Rel.* **1998**, *55*, 219-229.
- [41] Xie, J.; and Wang, C. H. Self-assembled biodegradable nanoparticles developed by direct dialysis for the delivery of paclitaxel. *Pharm. Res.* **2005**, *22(12)*, 2079-2090.
- [42] Agrapidis-Paloympis, L. E.; and Nash R. A. The effect of solvents on the ultraviolet absorbance of sunscreen. *J. Soc. Cosmet. Chem.* **1987**, *38*, 209-227.
- [43] Skoog, D. A.; West, D.; and Holler, F. J. *Fundamentals of analytical chemistry*. 7th ed. New York: Saunders College, 1997, pp 510-511.
- [44] Lee, M.; Cho, Y. W.; Park, J. H.; Chung, H.; Jeong, S. Y.; Choi, K.; Moon, D. H.; Kim, S. Y.; Kim, I. S.; and Kwon, I. C. Size control of self-assembled nanoparticles by an emulsion/solvent evaporation method. *Colloid Polym. Sci.* **2006**, *284*, 506-512
- [45] Jeong, J. H.; Kang, H. S.; Yang, S. R.; Park, K.; and Kim, J. D. Biodegradable poly(asparagine) grafted with poly(caprolactone) and the effect of substitution on self-aggregation, *Colloids and Surfaces A: Physicochem. Eng. Aspects.* **2005**, *264*, 187-194.
- [46] Muller, R. H.; Jacobs, C.; and Kayser, O. Nanosuspensions as particulate drug formulations in therapy Rationale for development and what we can expect for the Future. *Advanced Drug Delivery Reviews.* **2001**, *47*, 3-19.
- [47] Wei, X.; Yan, H.; Xu, H.; and Wu, W. Methoxypolyethylene Glycol Cyanoacrylate-Docosyl Cyanoacrylate Graft Copolymer: Synthesis, Characterization, and Preparation of Nanoparticles. *International Journal of Polymer Anal. Charact.* **2006**, *11*, 353-367.

- [48] Akagi, T.; Kaneko, T.; Kida, T.; and Akashi, M. Preparation and characterization of biodegradable nanoparticles based on poly(γ -glutamic acid) with L-phenylalanine as a protein carrier. *J. Control. Rel.* **2005**, *108*, 226-236.



สถาบันวิทยบริการ
จุฬาลงกรณ์มหาวิทยาลัย



APPENDICES

สถาบันวิทยบริการ
จุฬาลงกรณ์มหาวิทยาลัย

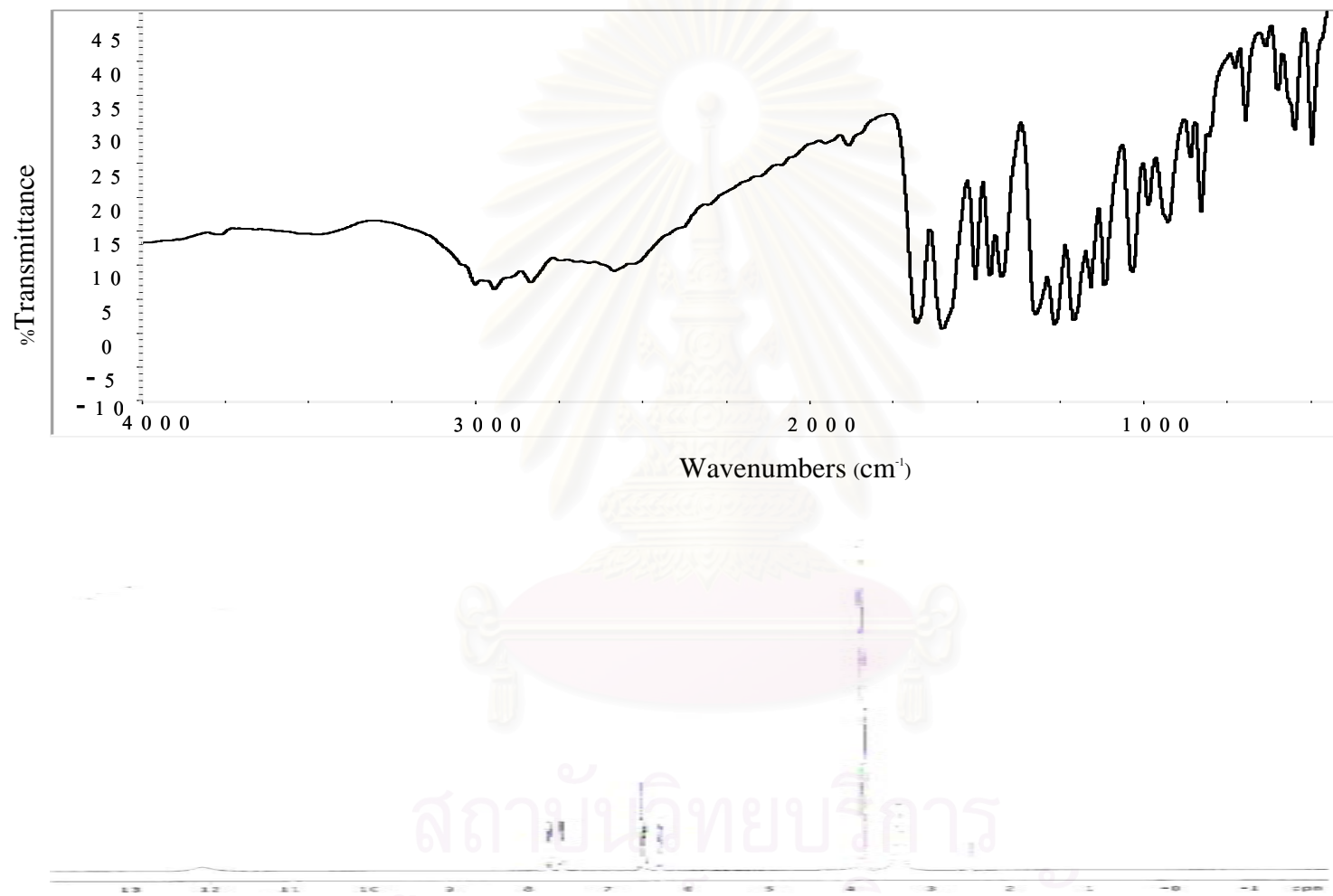


Figure A1 IR (a) and ¹H-NMR spectrum (b) of 2,4-dimethoxycinnamic acid (**2,4-DMC**) in DMSO-*d*₆

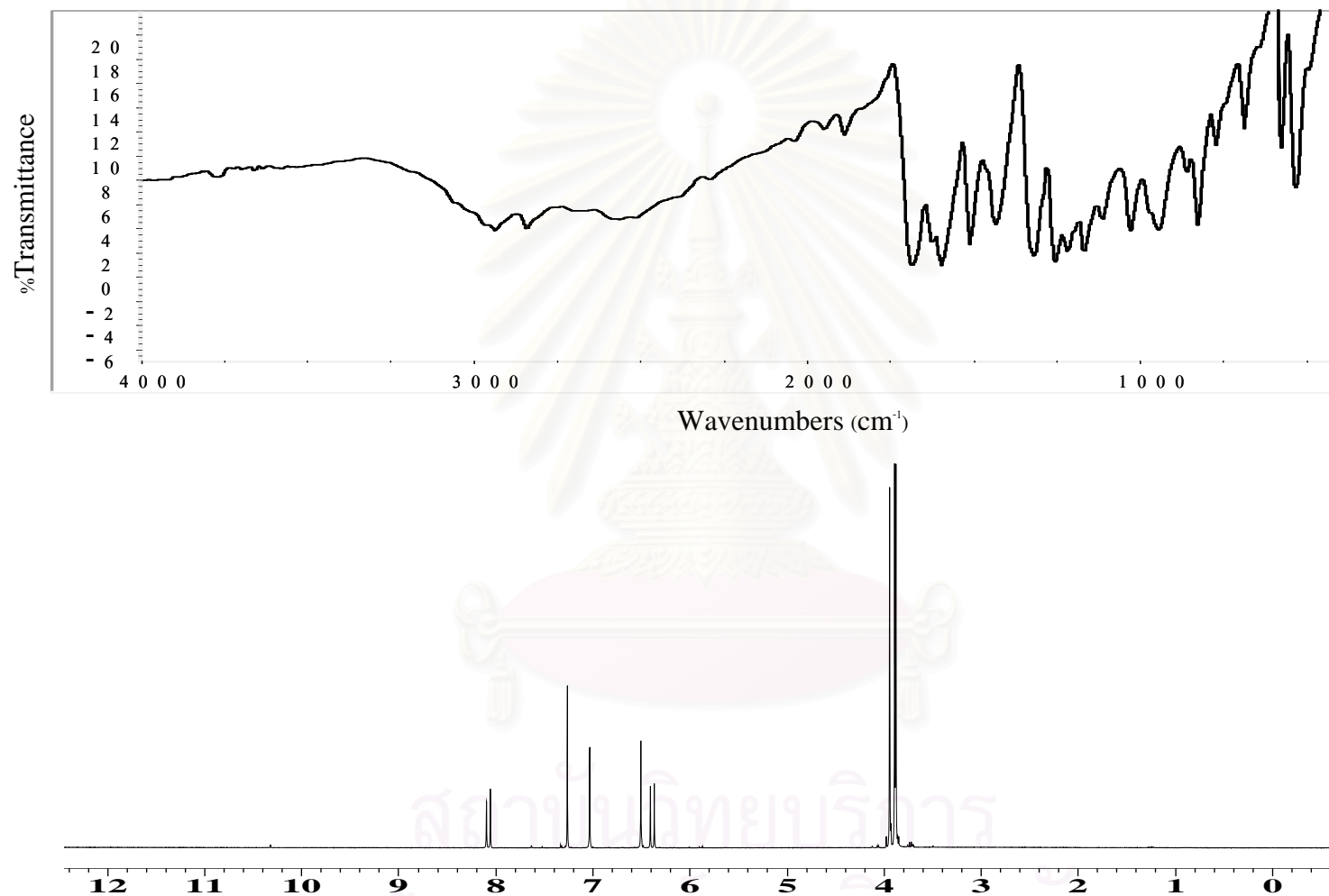


Figure A2 IR (a) and ¹H-NMR spectrum (b) of 2,4,5-trimethoxycinnamic acid (**2,4,5-TMC**) in CDCl₃

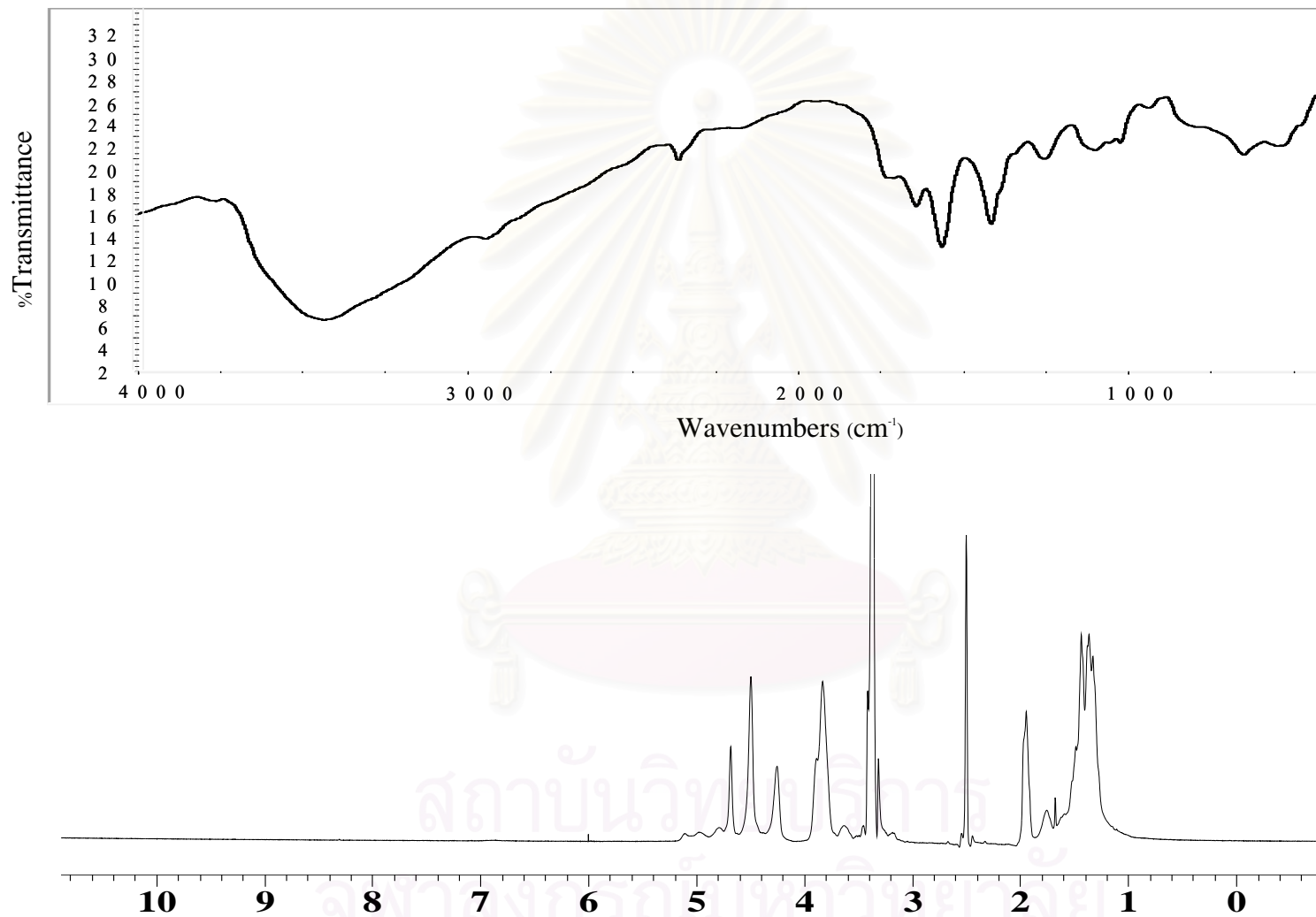


Figure A3 IR (a) and ¹H-NMR spectrum (b) of poly(vinyl alcohol) (PV(OH)124,000 Daltons) in DMSO-*d*₆

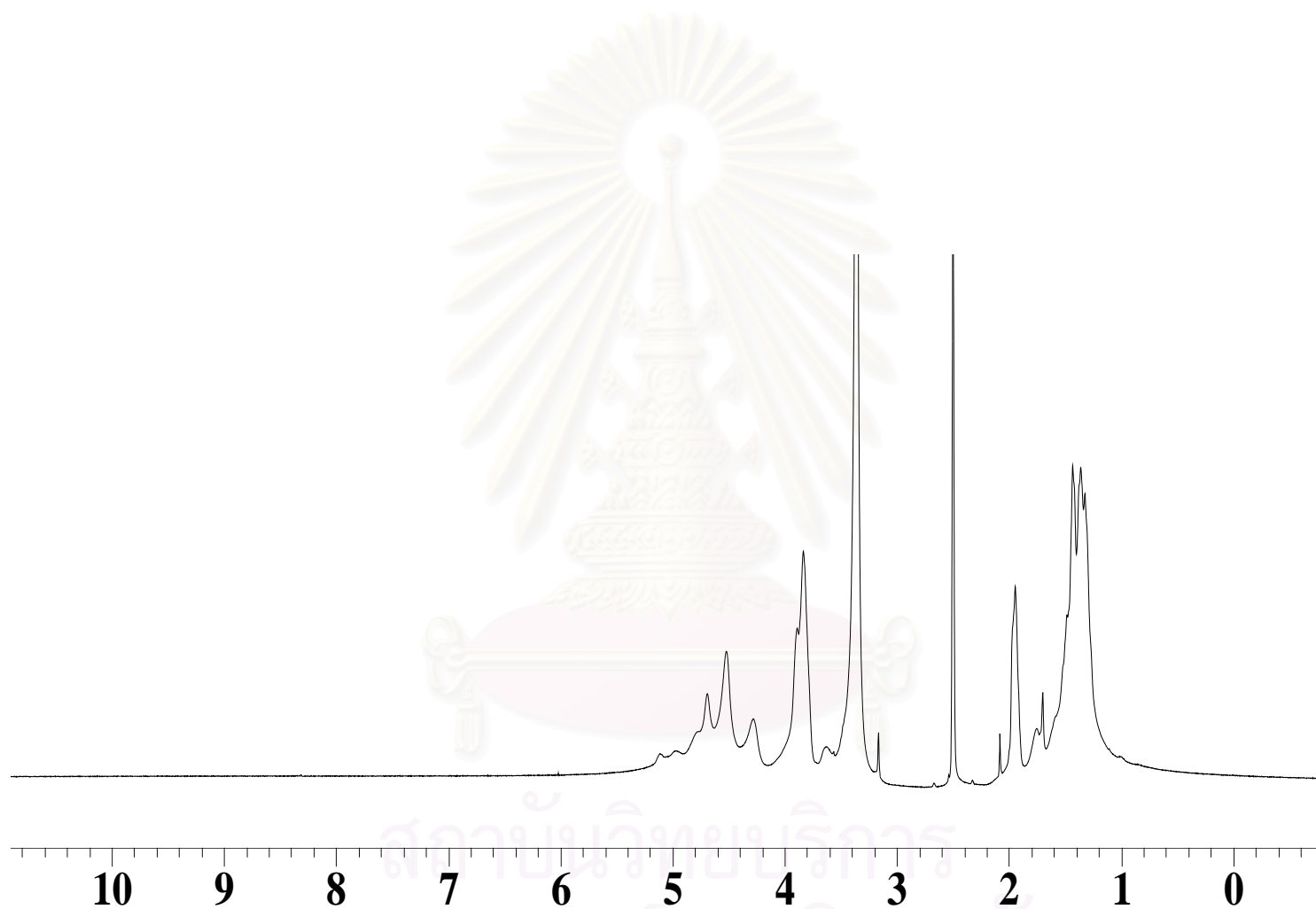


Figure A4 $^1\text{H-NMR}$ spectrum of poly(vinyl alcohol) (PV(OH)50,000 Daltons) in $\text{DMSO-}d_6$

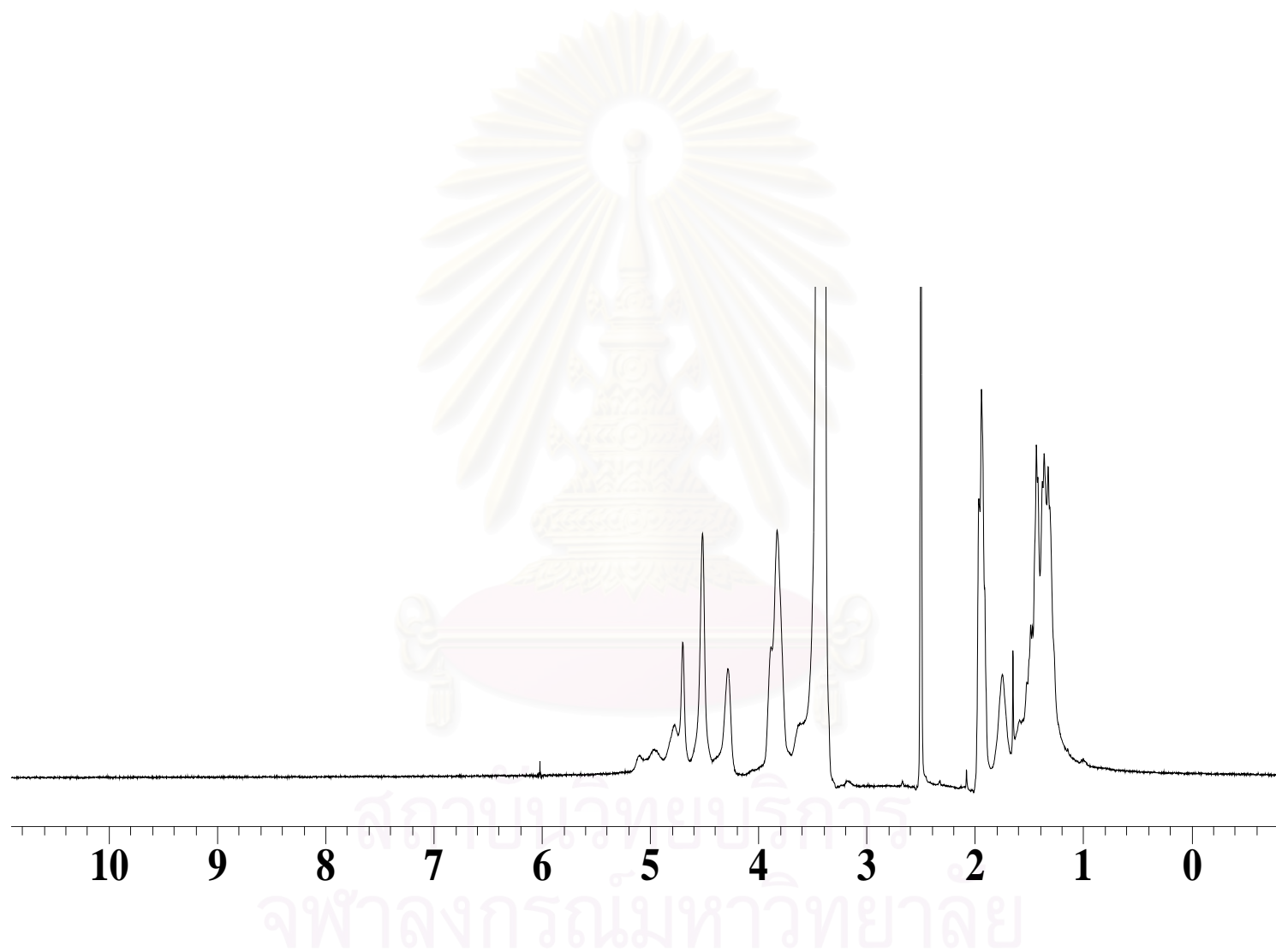


Figure A5 $^1\text{H-NMR}$ spectrum (b) of poly(vinyl alcohol) (PV(OH)10,000 Daltons) in $\text{DMSO-}d_6$

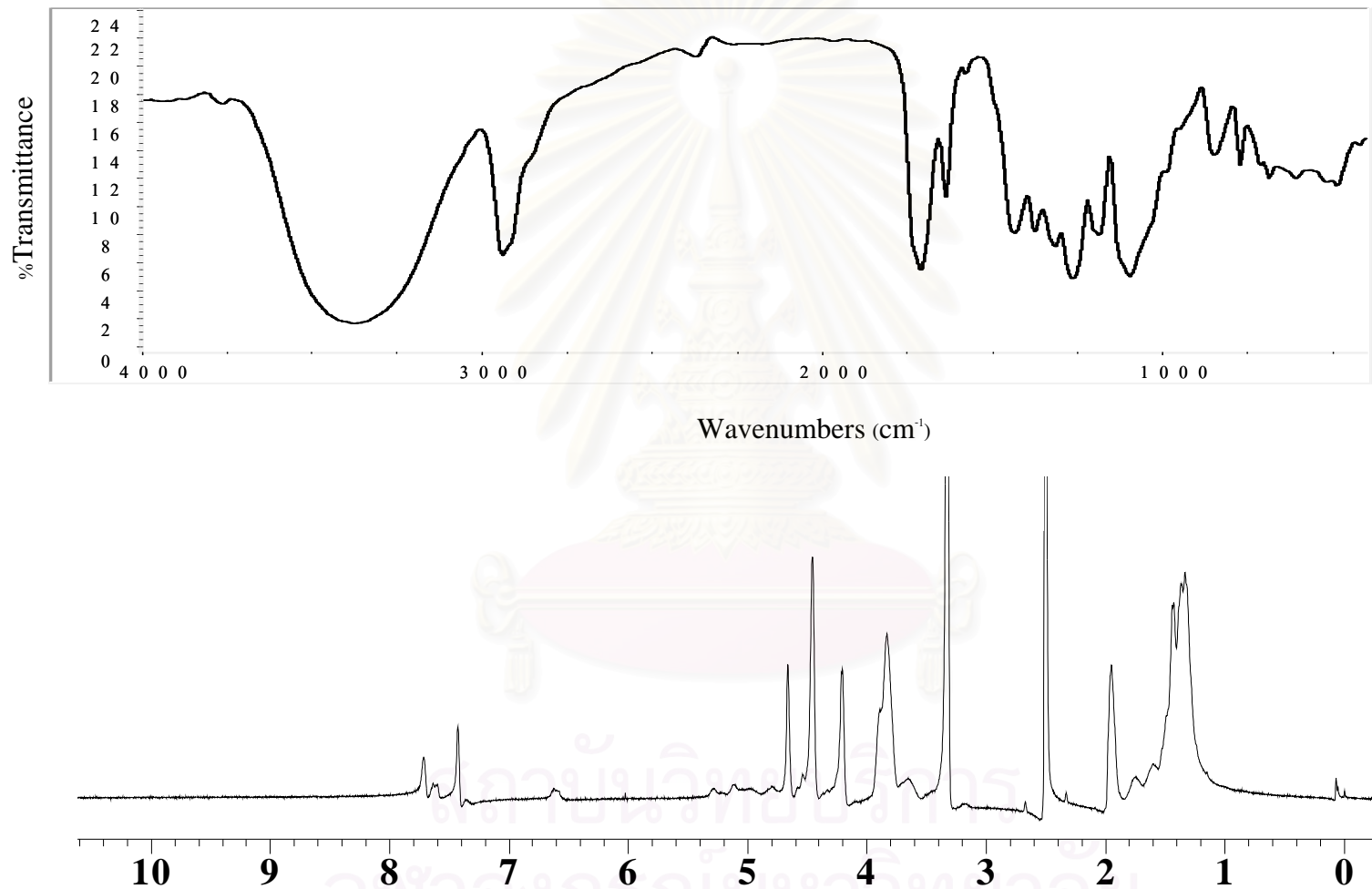


Figure A6 IR (a) and $^1\text{H-NMR}$ spectrum (b) of Poly(vinylalcohol-co-vinylcinnamate), DS 0.04 (**PA1**) in DMSO- d_6

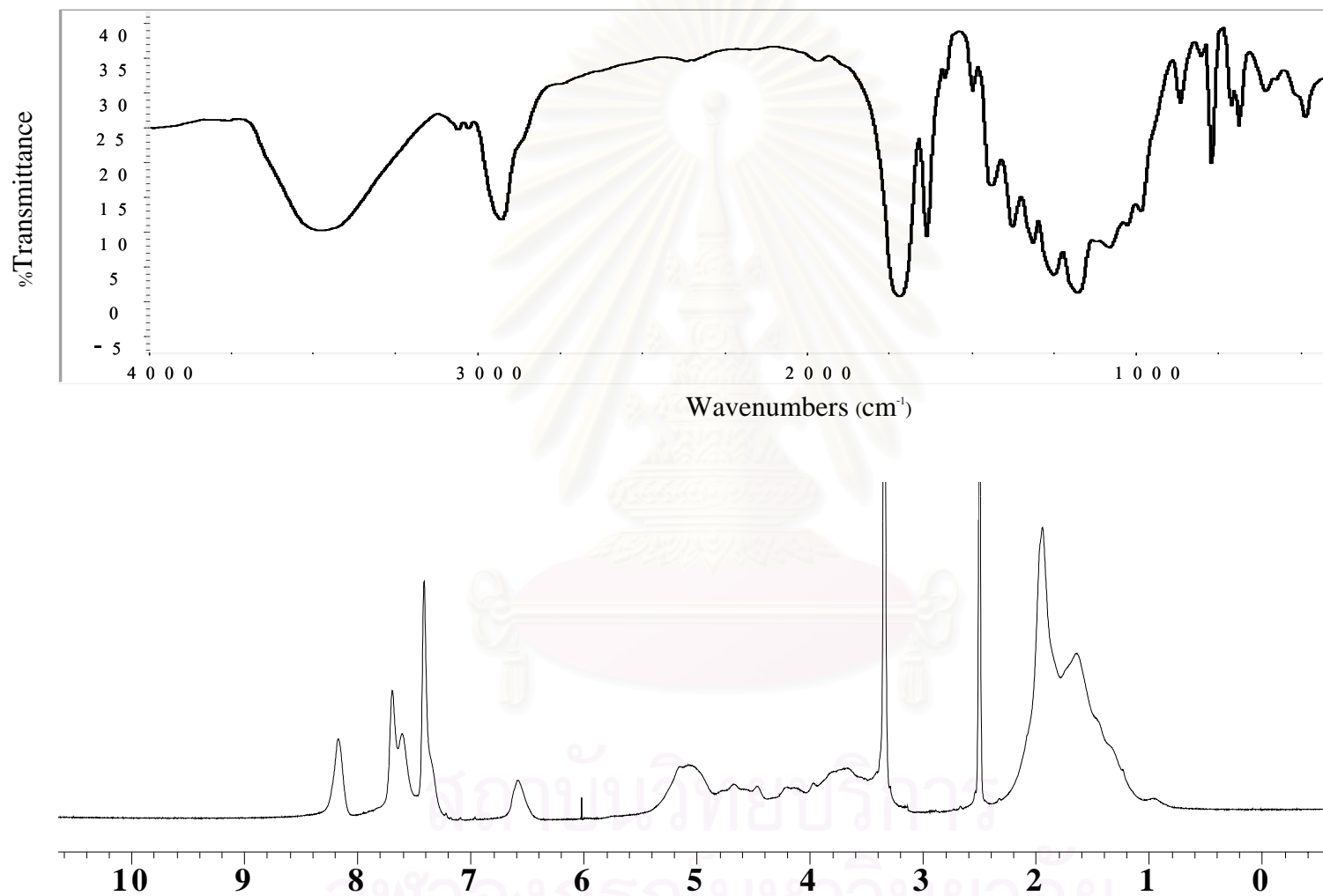


Figure A7 IR (a) and $^1\text{H-NMR}$ spectrum (b) of Poly(vinylalcohol-co-vinylcinnamate), DS 0.14 (**PA2**) in DMSO- d_6

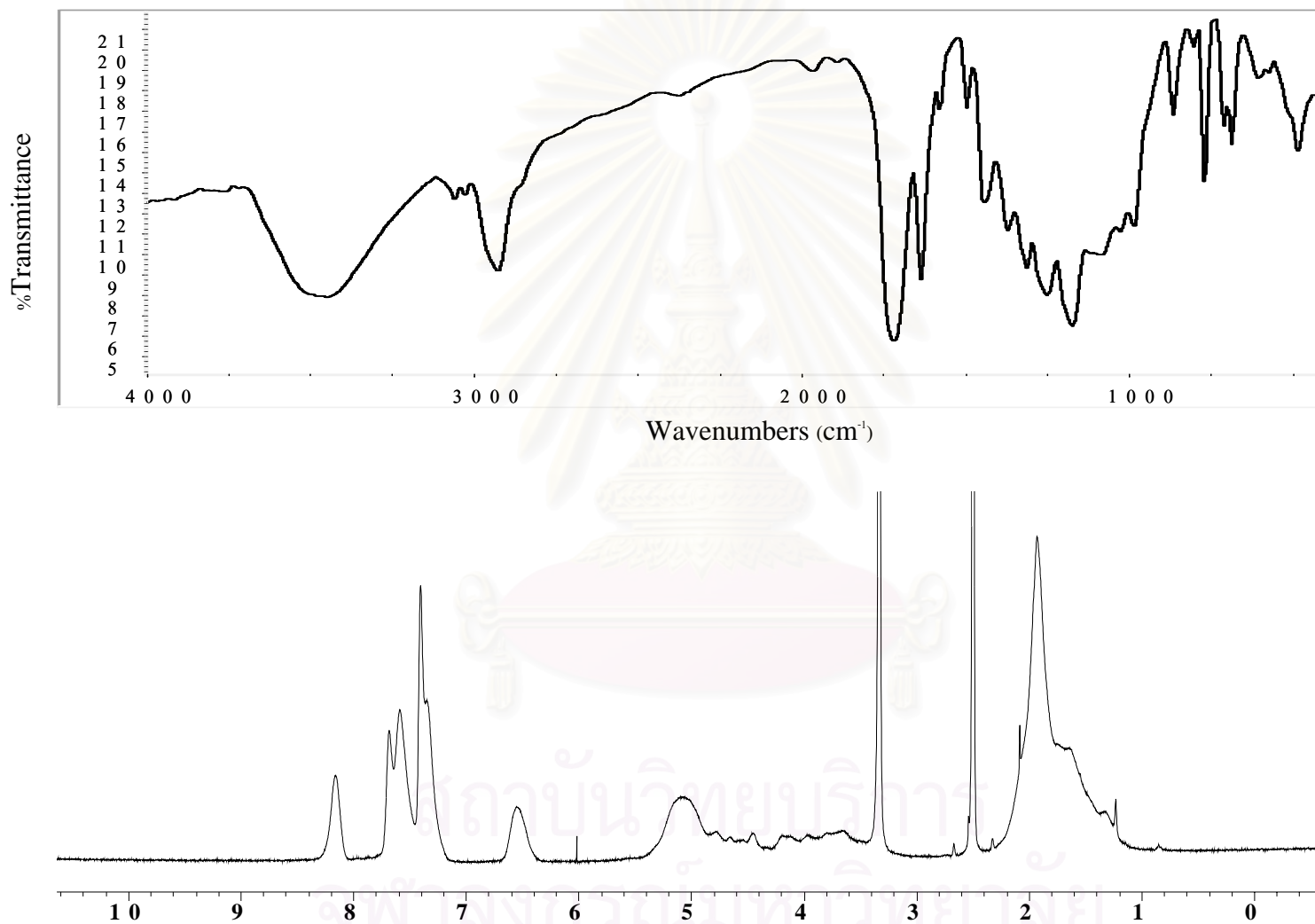


Figure A8 IR (a) and $^1\text{H-NMR}$ spectrum (b) of Poly(vinylalcohol-co-vinylcinnamate), DS 0.25 (**PA3**) in $\text{DMSO-}d_6$

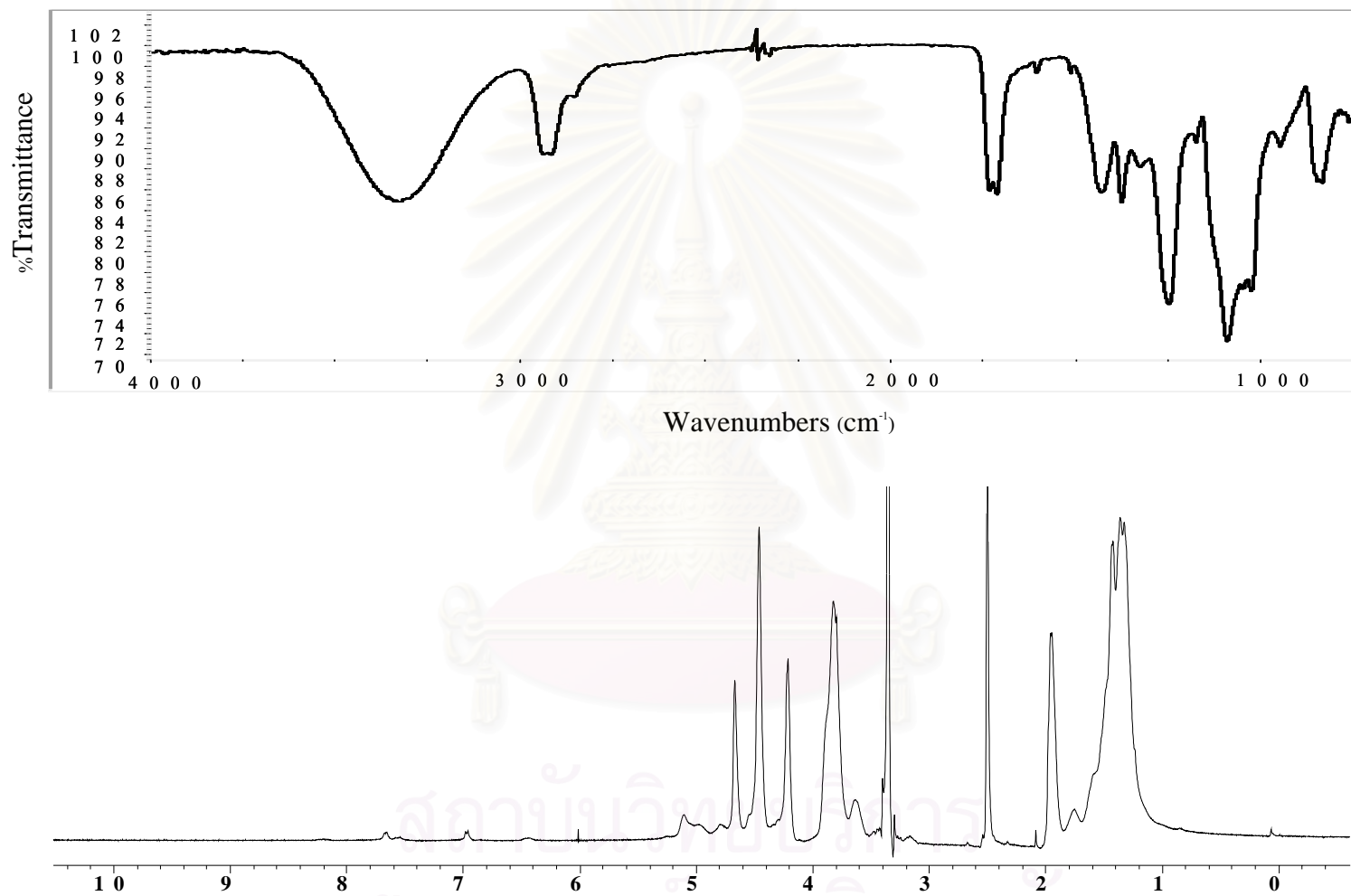


Figure A9 IR (a) and ¹H-NMR spectrum (b) of Poly(vinylalcohol-co-vinyl-4-methoxycinnamate), DS 0.01 (**PB1**) in DMSO-*d*₆

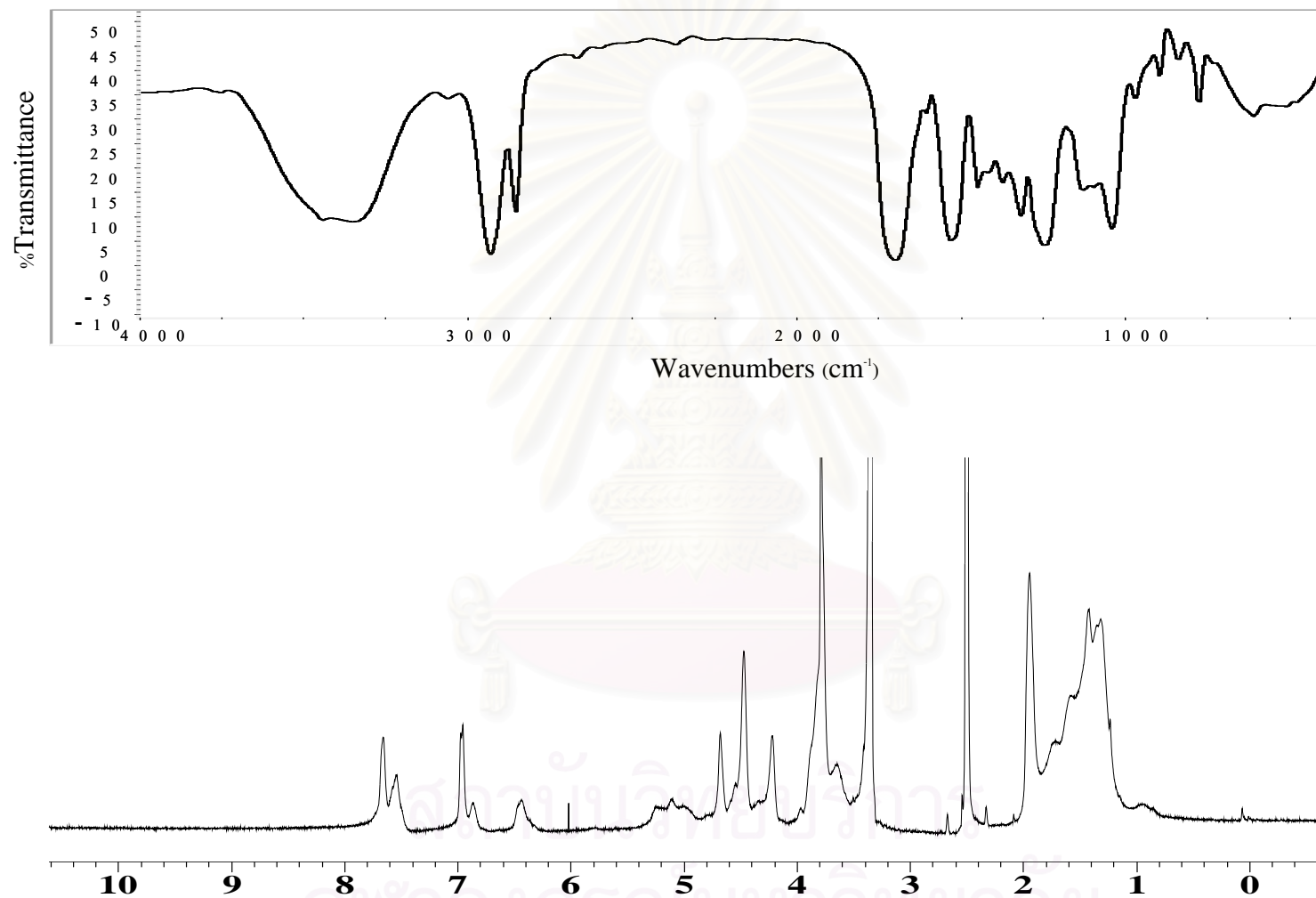


Figure A10 IR (a) and ¹H-NMR spectrum (b) of Poly(vinylalcohol-co-vinyl-4-methoxycinnamate), DS 0.09 (**PB2**) in DMSO-*d*₆

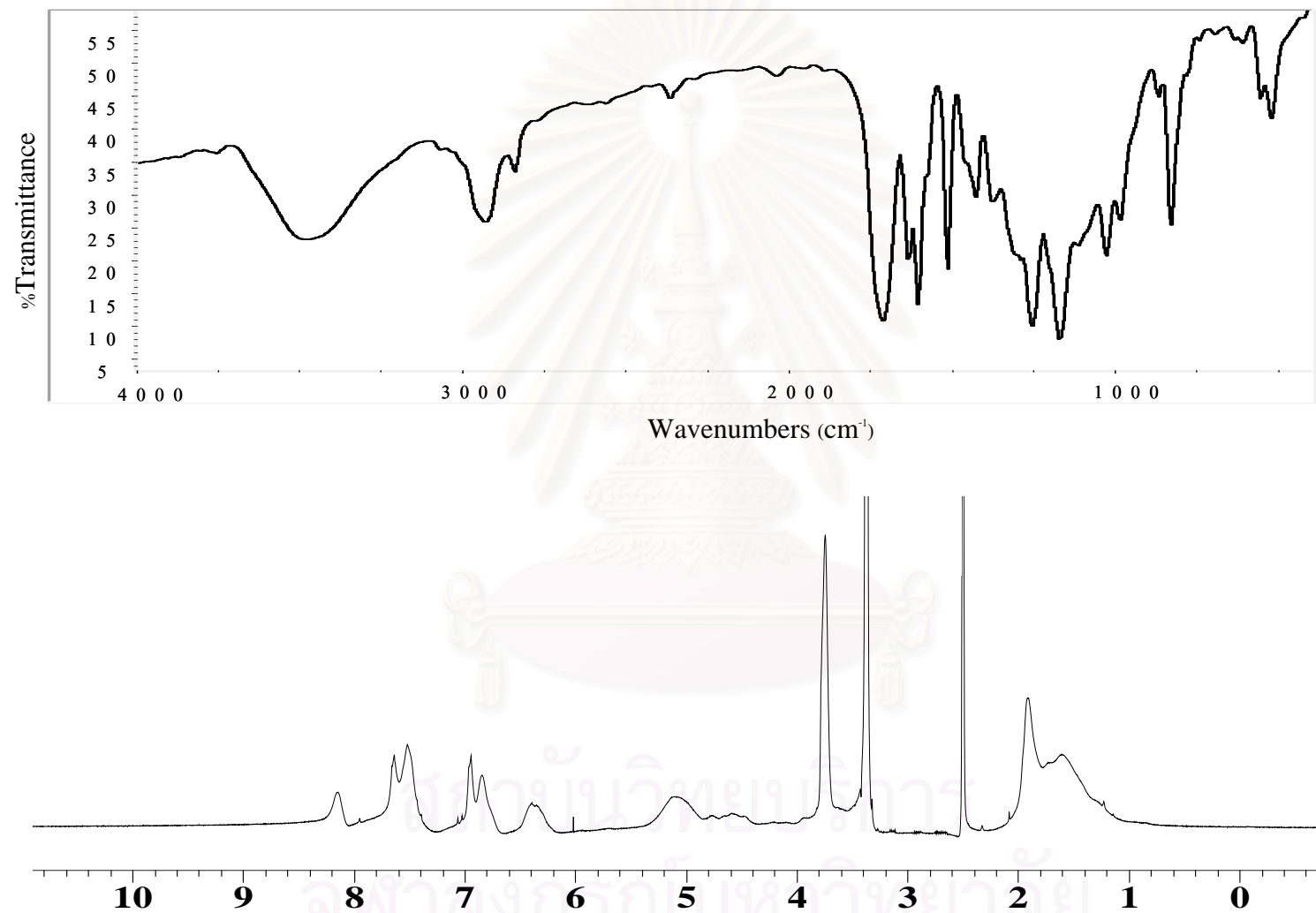


Figure A11 IR (a) and $^1\text{H-NMR}$ spectrum (b) of Poly(vinylalcohol-co-vinyl-4-methoxycinnamate), DS 0.27 (**PB3**) in DMSO- d_6

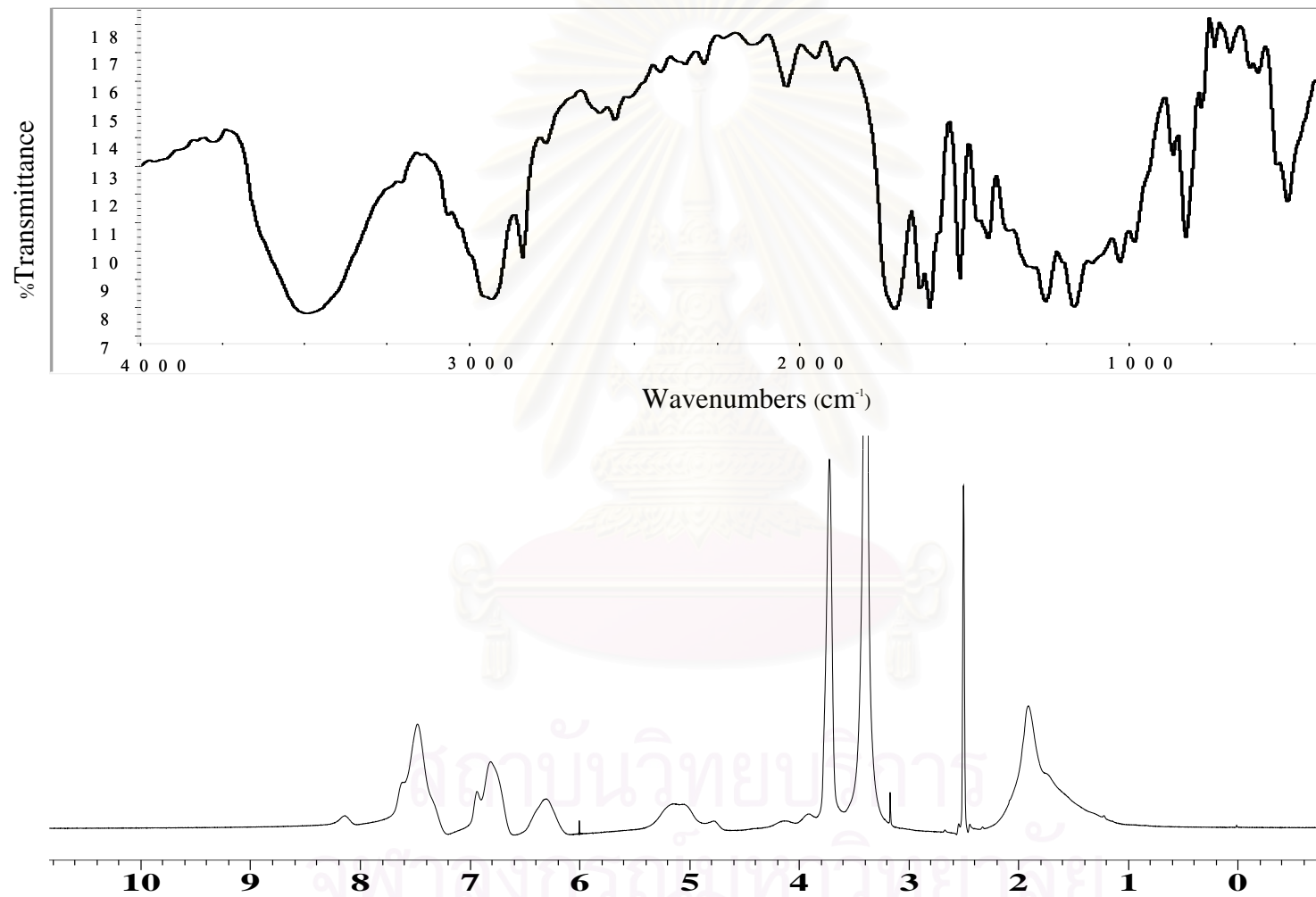


Figure A12 IR (a) and $^1\text{H-NMR}$ spectrum (b) of Poly(vinylalcohol-co-vinyl-4-methoxycinnamate), DS 0.44 (**PB4**) in $\text{DMSO-}d_6$

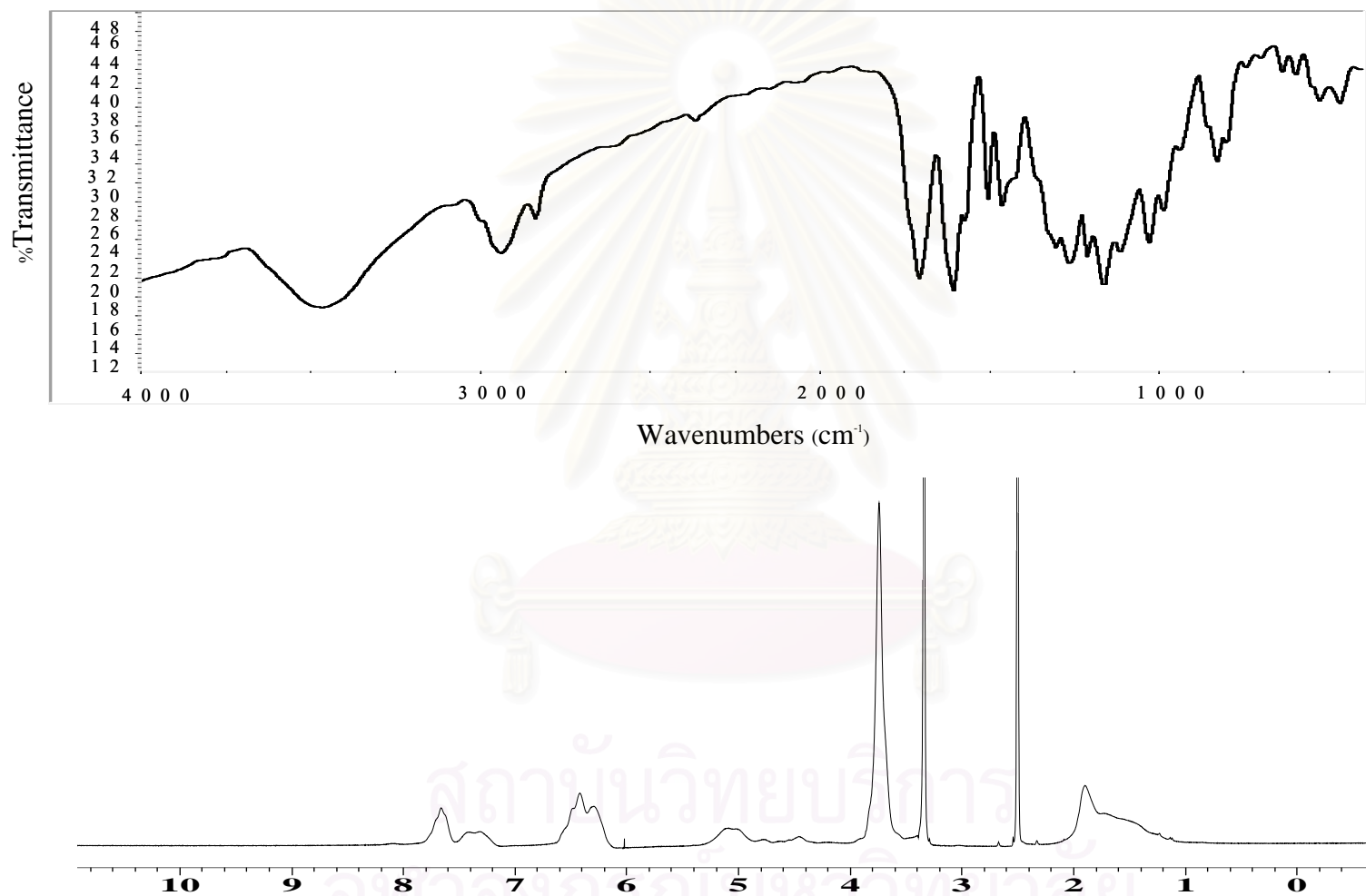


Figure A13 IR (a) and ¹H-NMR spectrum (b) of Poly(vinylalcohol-co-vinyl-2,4-dimethoxycinnamate), DS 0.46 (PC) in DMSO-*d*₆

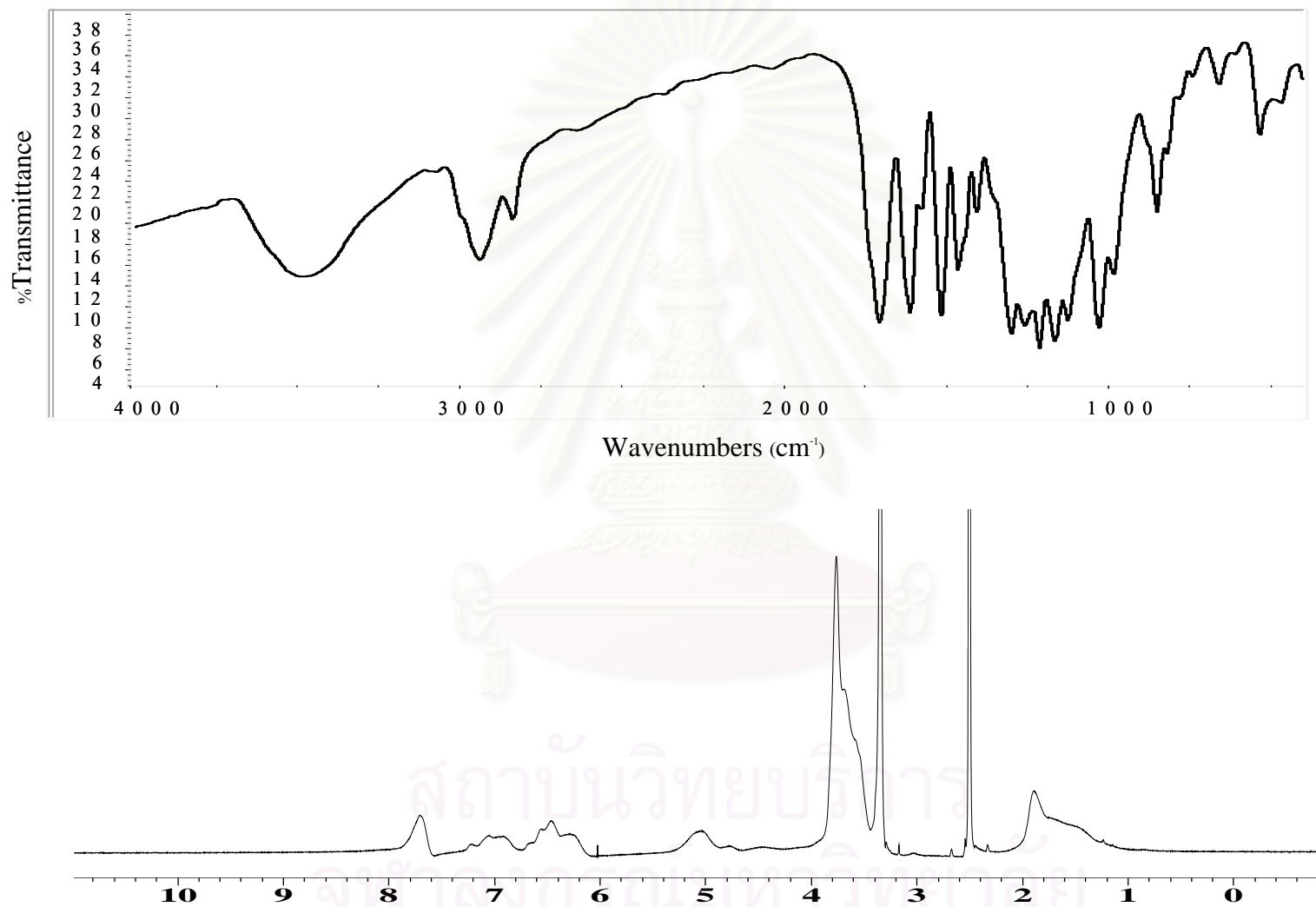


Figure A14 IR (a) and ¹H-NMR spectrum (b) of Poly(vinylalcohol-co-vinyl-2,4,5-trimethoxycinnamate), DS 0.53 (PD) in DMSO-*d*₆

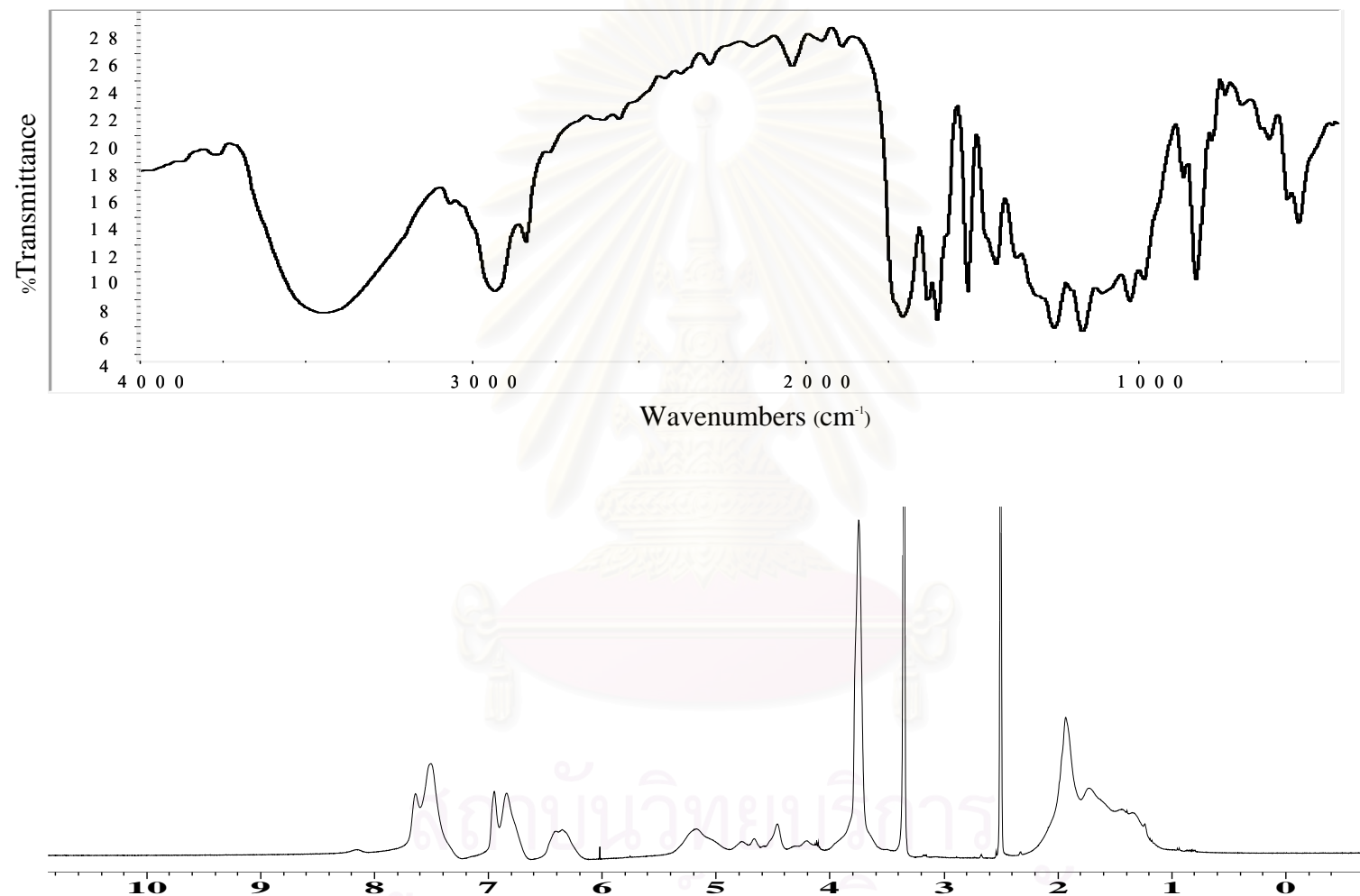


Figure A15 IR (a) and ¹H-NMR spectrum (b) of Poly(vinylalcohol-co-vinyl-4-methoxycinnamate) (Mw 50,000 Daltons, DS 0.28) (**P₅B**) in DMSO-*d*₆

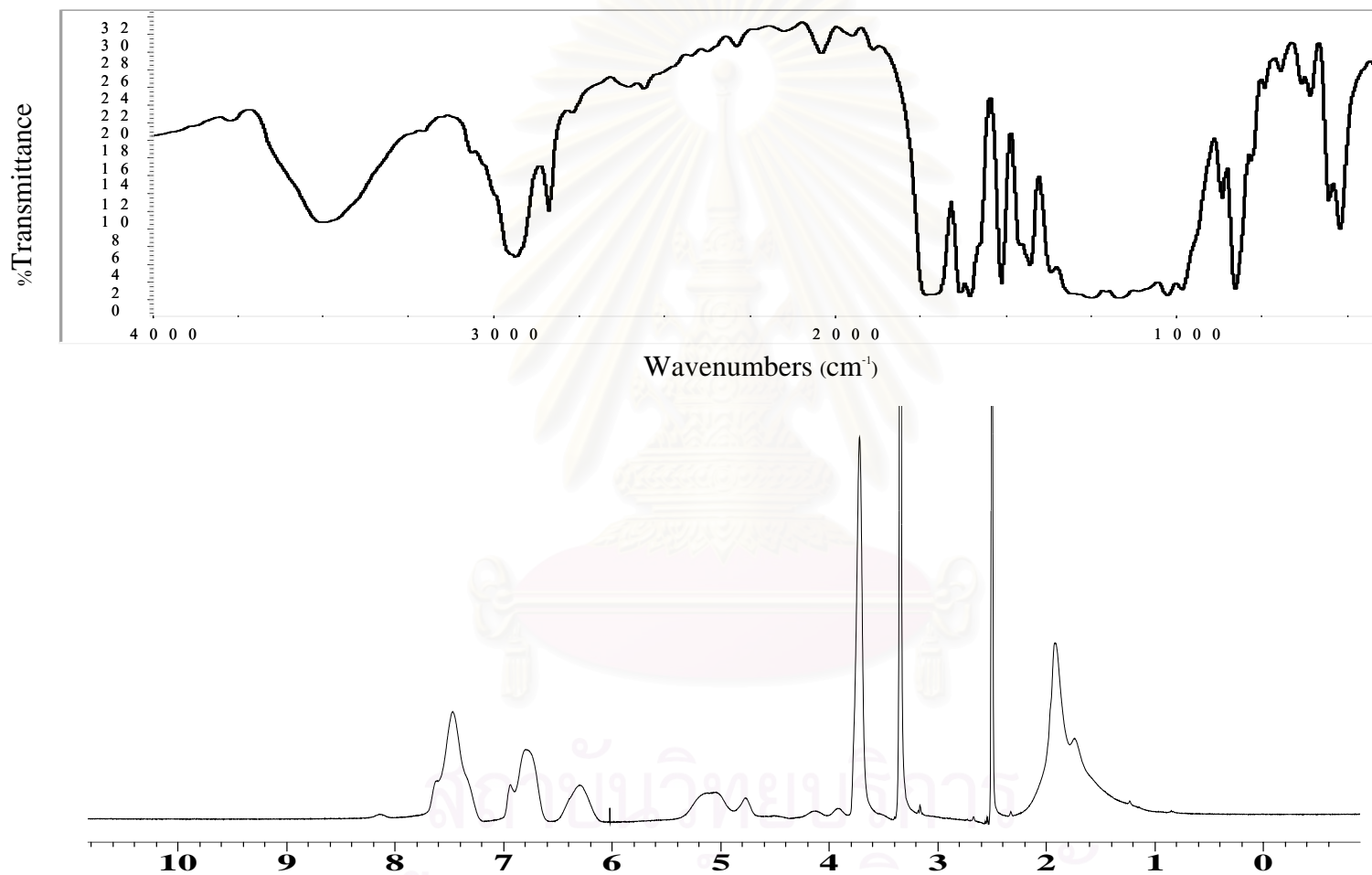


Figure A16 IR (a) and ¹H-NMR spectrum (b) of Poly(vinylalcohol-co-vinyl-4-methoxycinnamate) (Mw 10,000 Daltons, DS 0.46) (**P₉B**) in DMSO-*d*₆

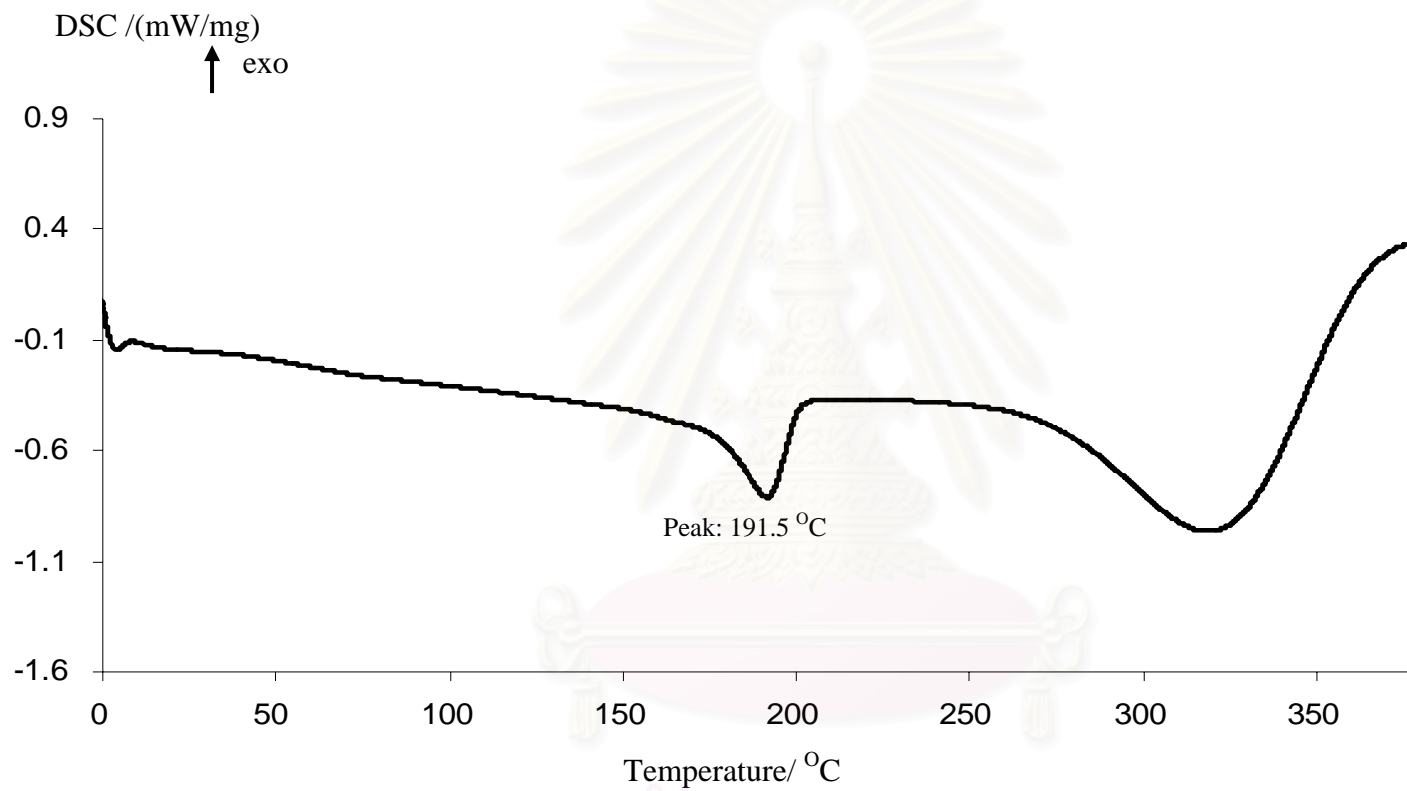


Figure A17 Thermogram of Poly(vinylalcohol-co-vinylcinnamate) Mw 124,000-186,000 (PV(OH) 124,000 Daltons)

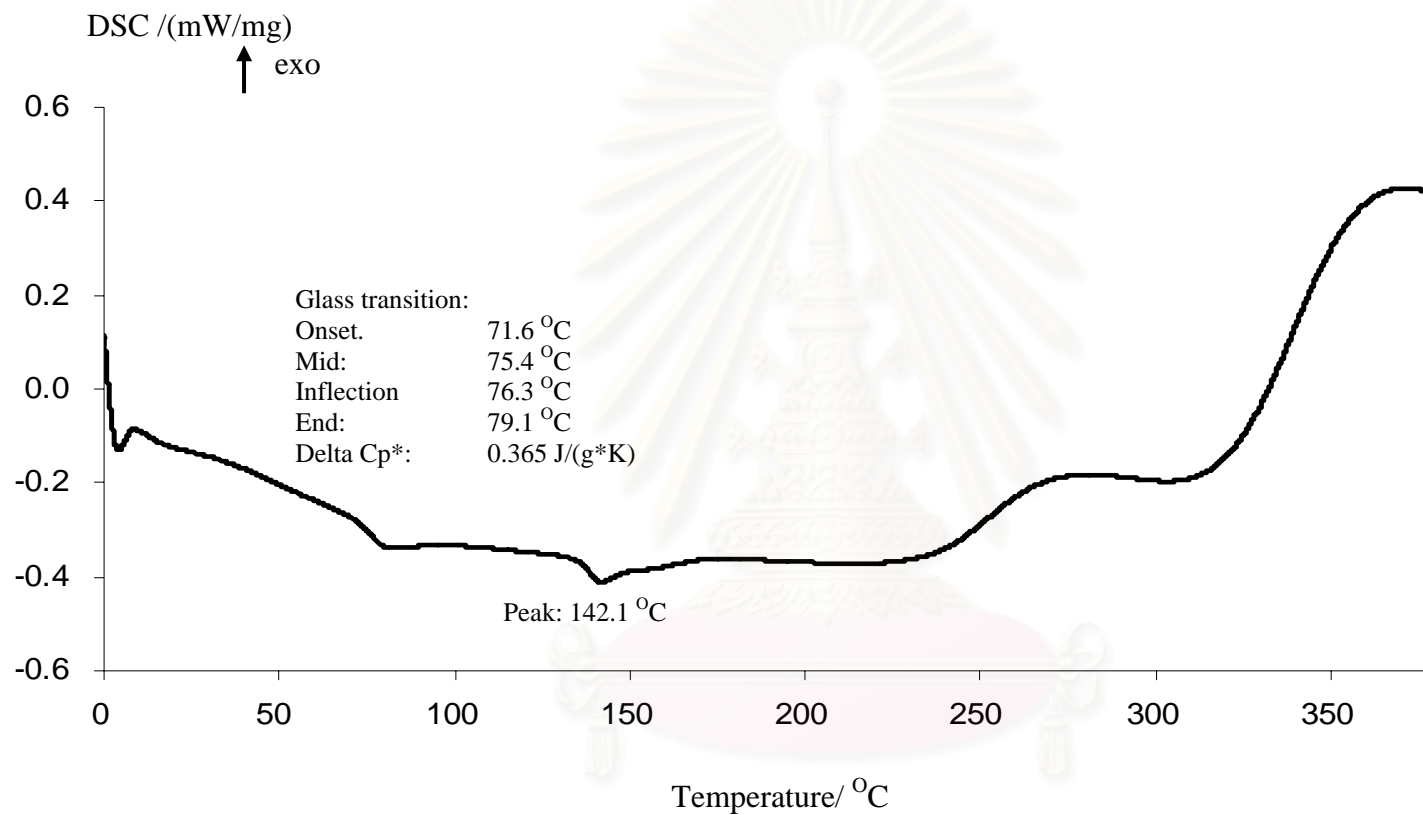


Figure A18 Thermogram of Poly(vinylalcohol-co-vinylcinnamate), DS 0.04 (PA1)

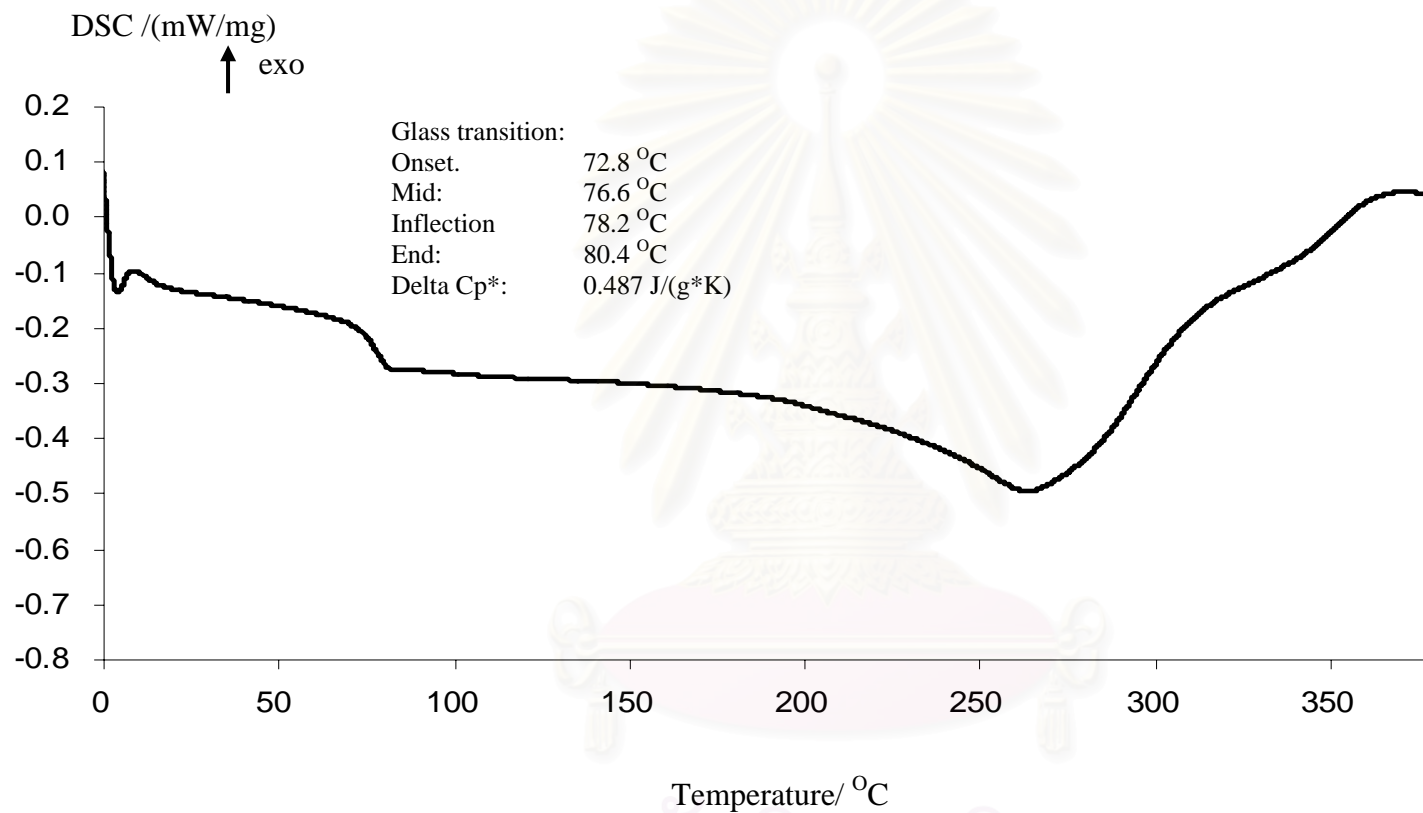


Figure A19 Thermogram of Poly(vinylalcohol-co-vinylcinnamate), DS 0.14 (PA2)

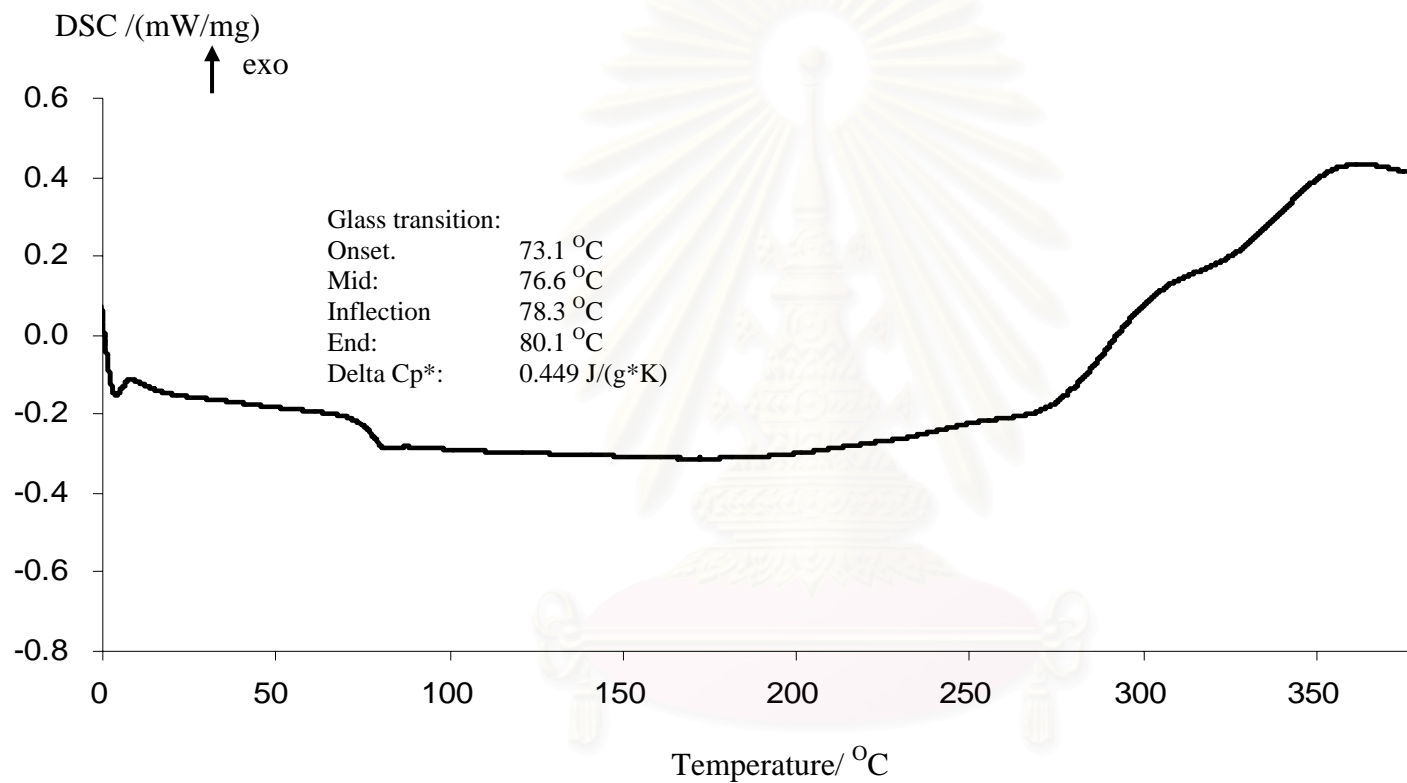


Figure A20 Thermogram of Poly(vinylalcohol-co-vinylcinnamate), DS 0.25 (PA3)

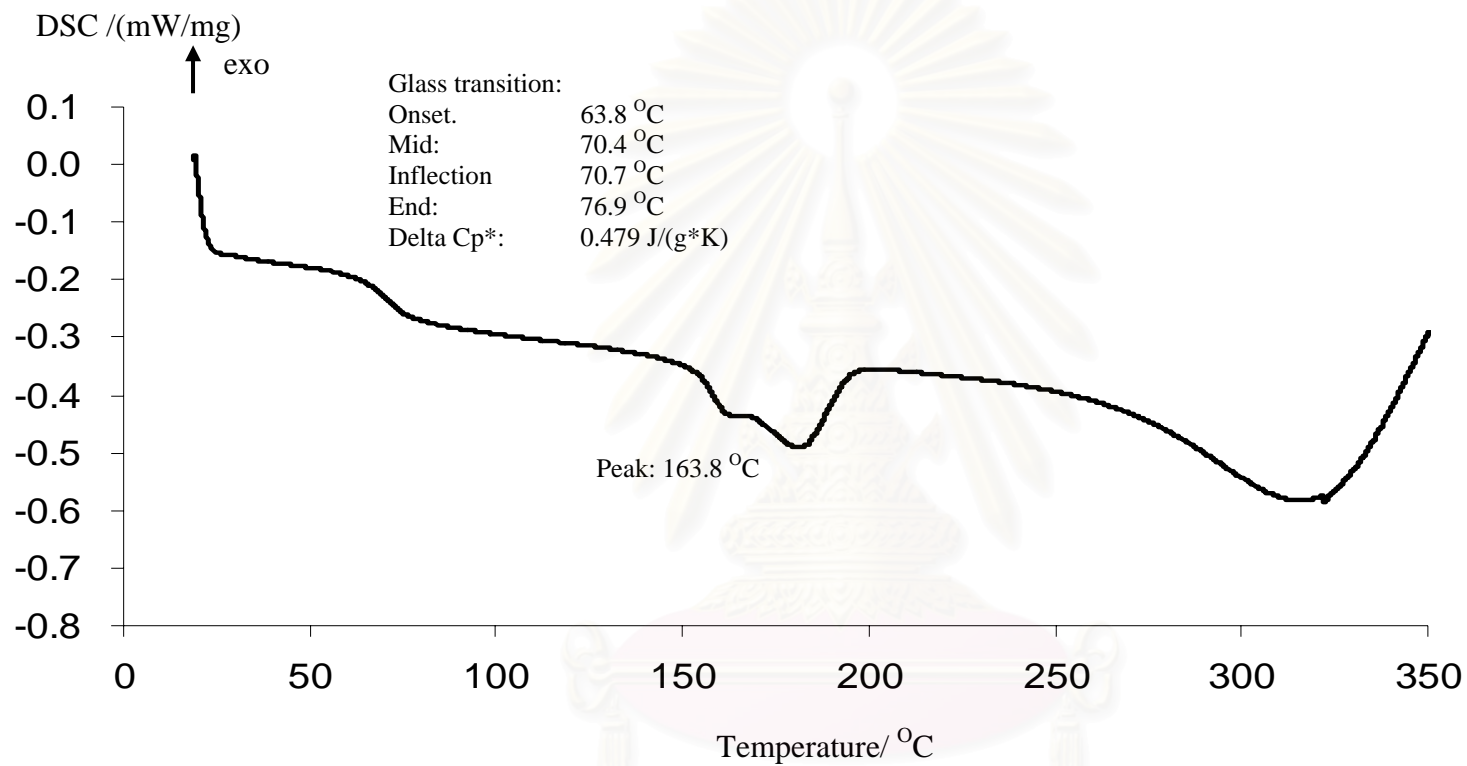


Figure A21 Thermogram of Poly(vinylalcohol-co-vinyl-4-methoxycinnamate), DS 0.01 (**PB1**)

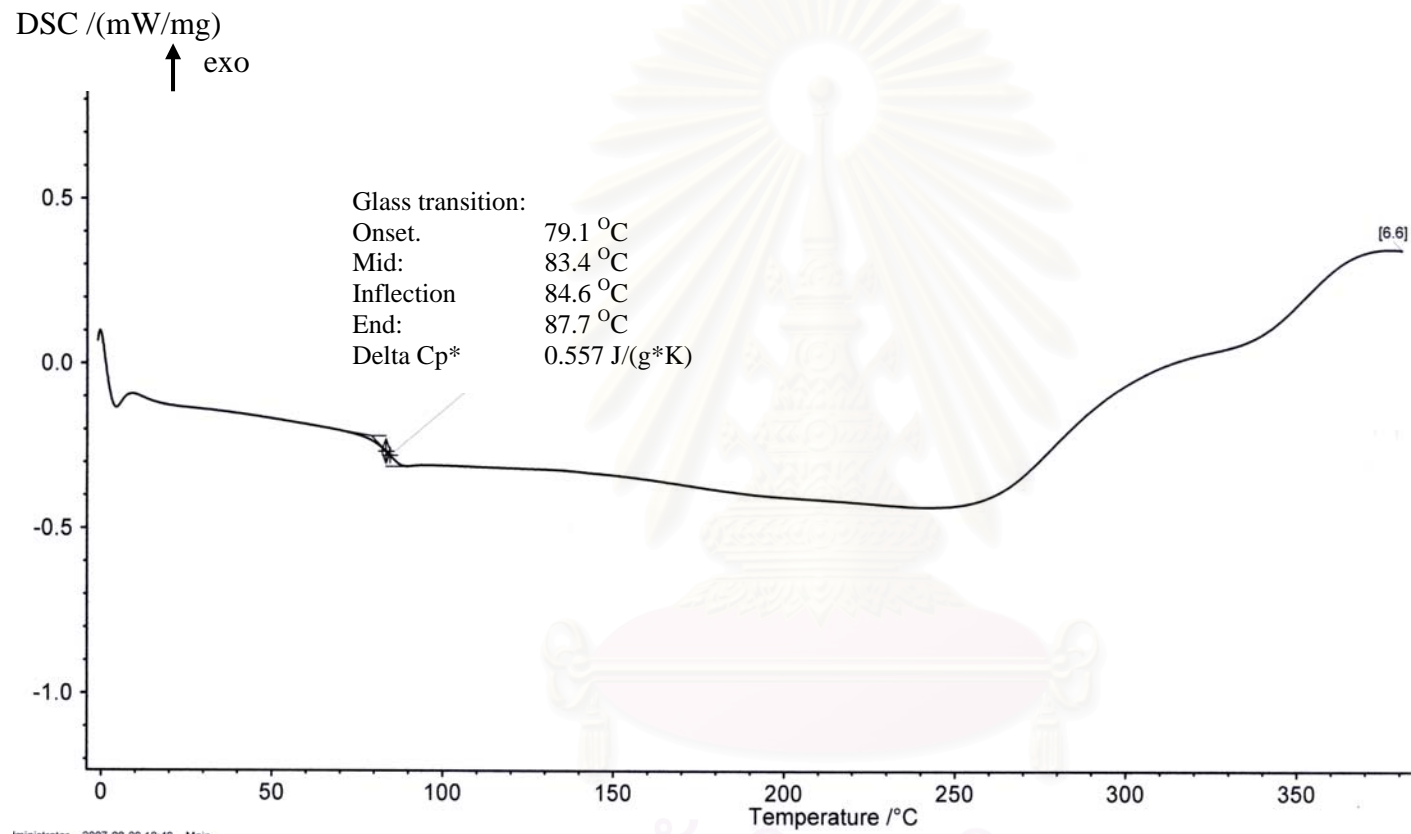


Figure A22 Thermogram of Poly(vinylalcohol-co-vinyl-4-methoxycinnamate), DS 0.09 (**PB2**)

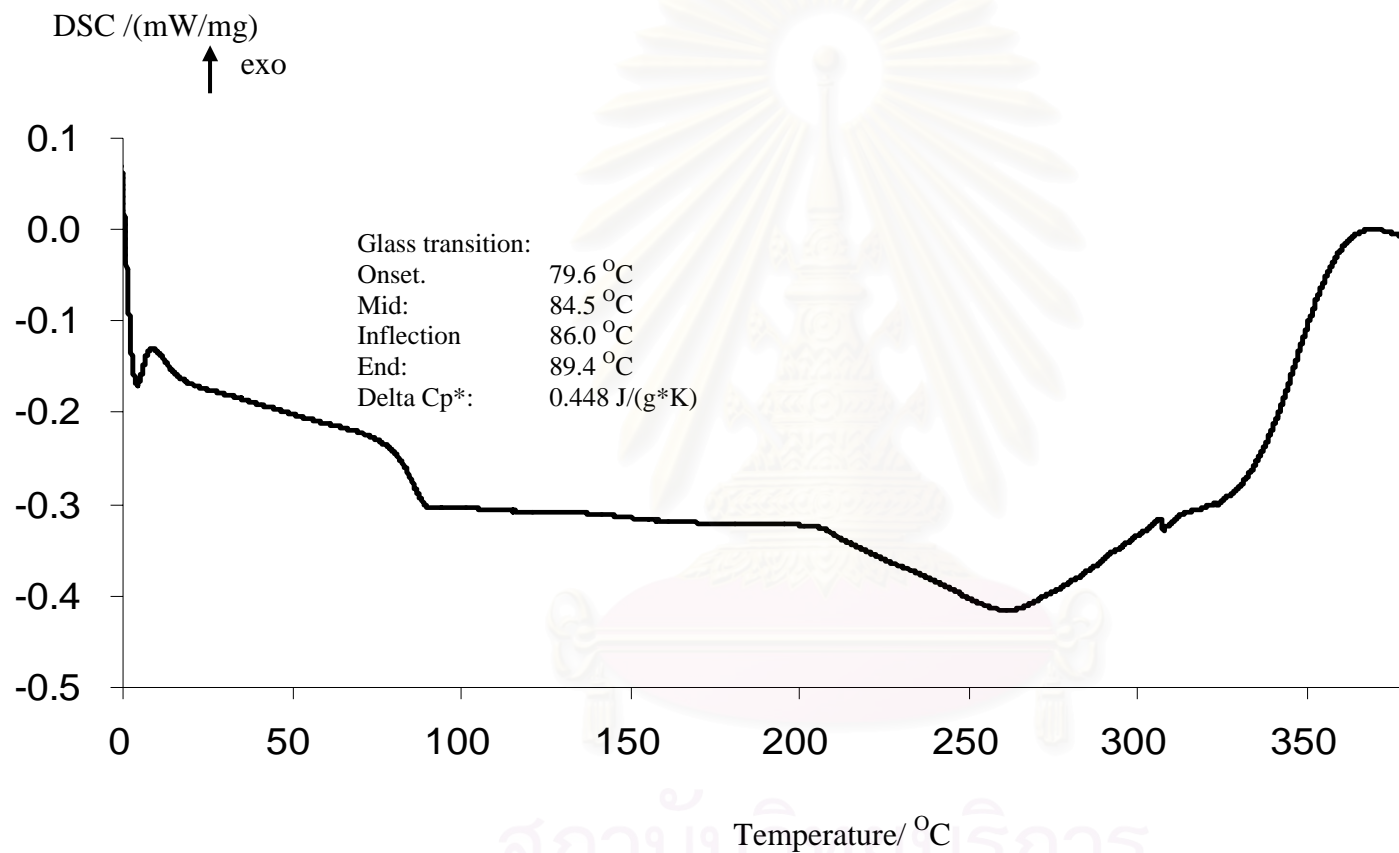


Figure A23 Thermogram of Poly(vinylalcohol-co-vinyl-4-methoxycinnamate), DS 0.27 (**PB3**)

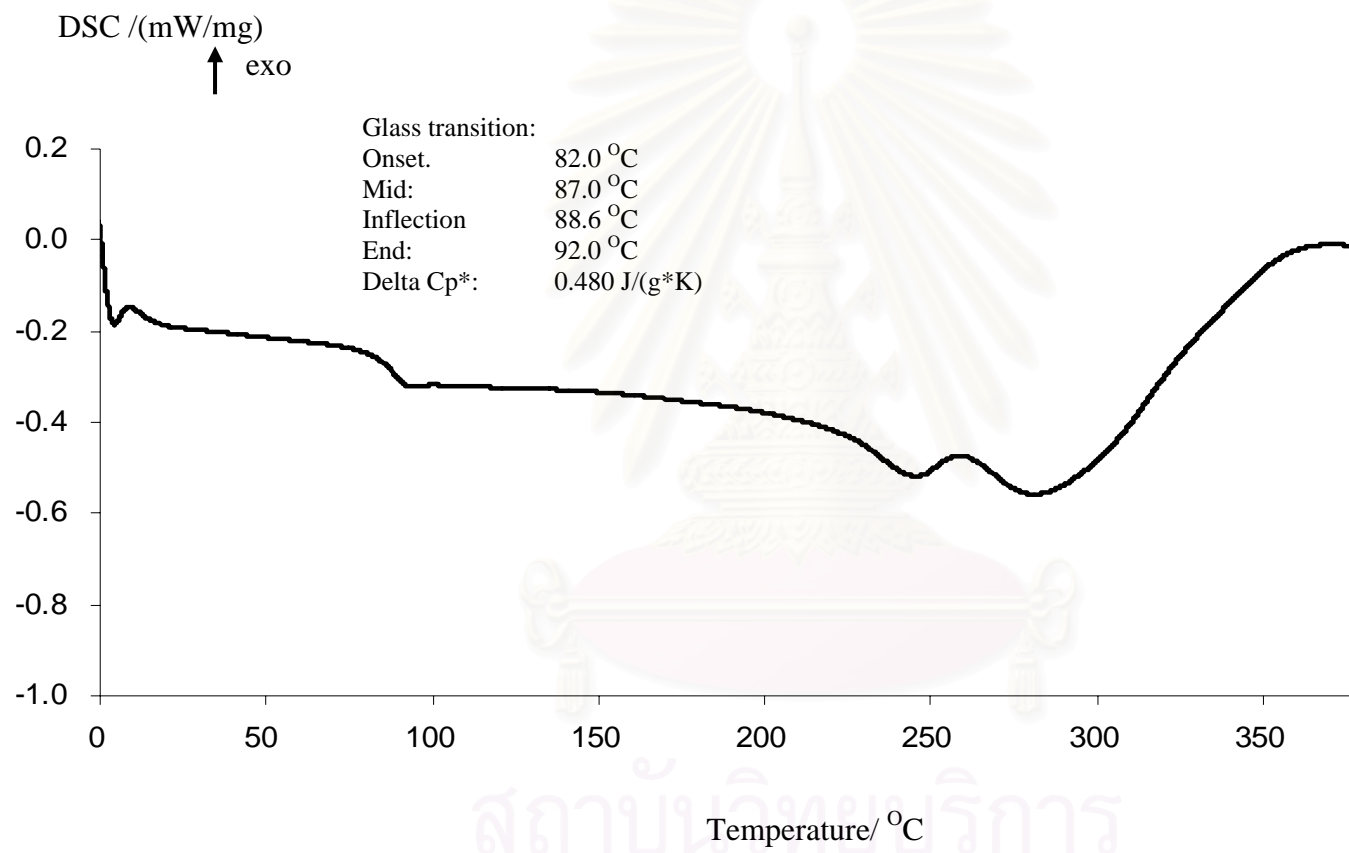


Figure A24 Thermogram of Poly(vinylalcohol-co-vinyl-4-methoxycinnamate), DS 0.44 (PB4)

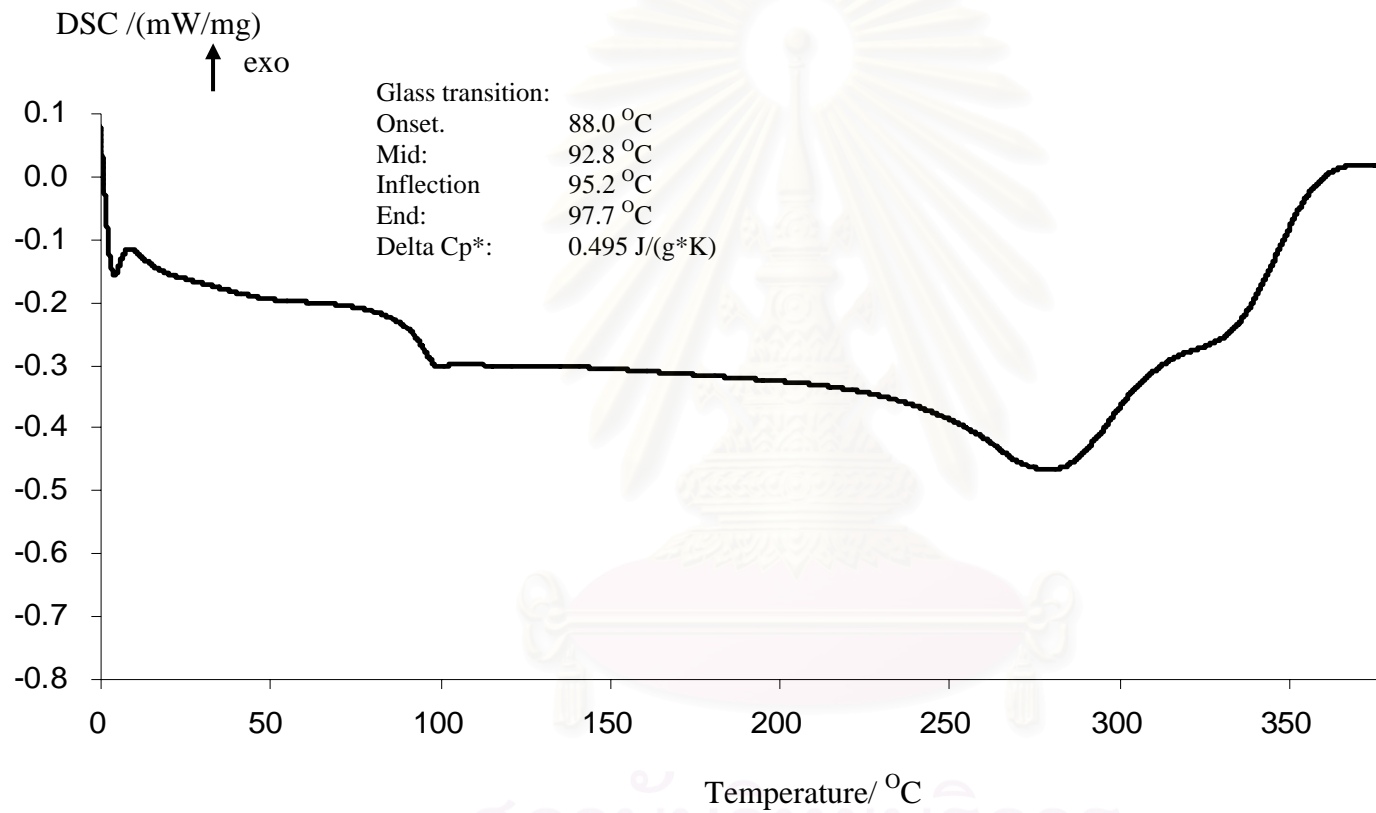


Figure A25 Thermogram of Poly(vinylalcohol-co-vinyl-2,4-dimethoxycinnamate), DS 0.46 (PC)

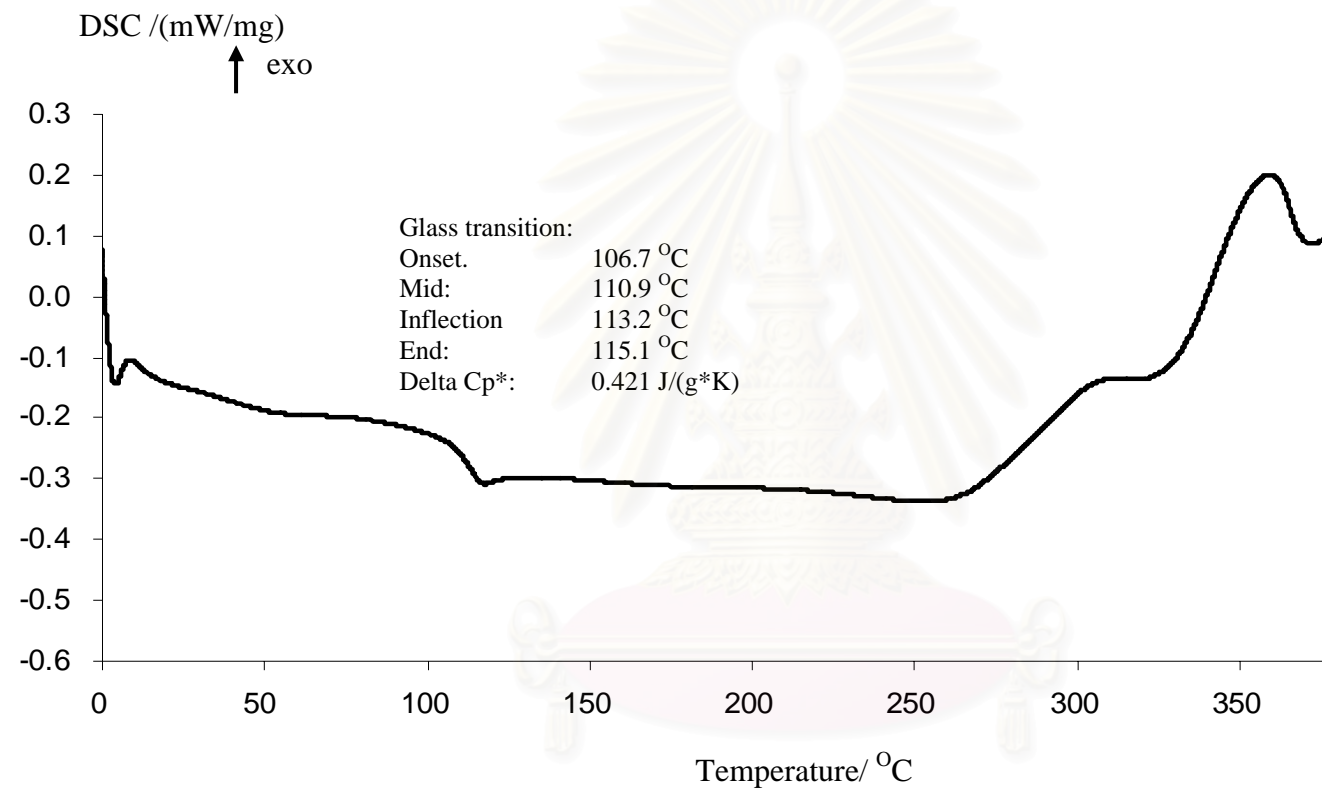


Figure A26 Thermogram of Poly(vinylalcohol-co-vinyl-2,4,5-trimethoxycinnamate), DS 0.53 (PD)

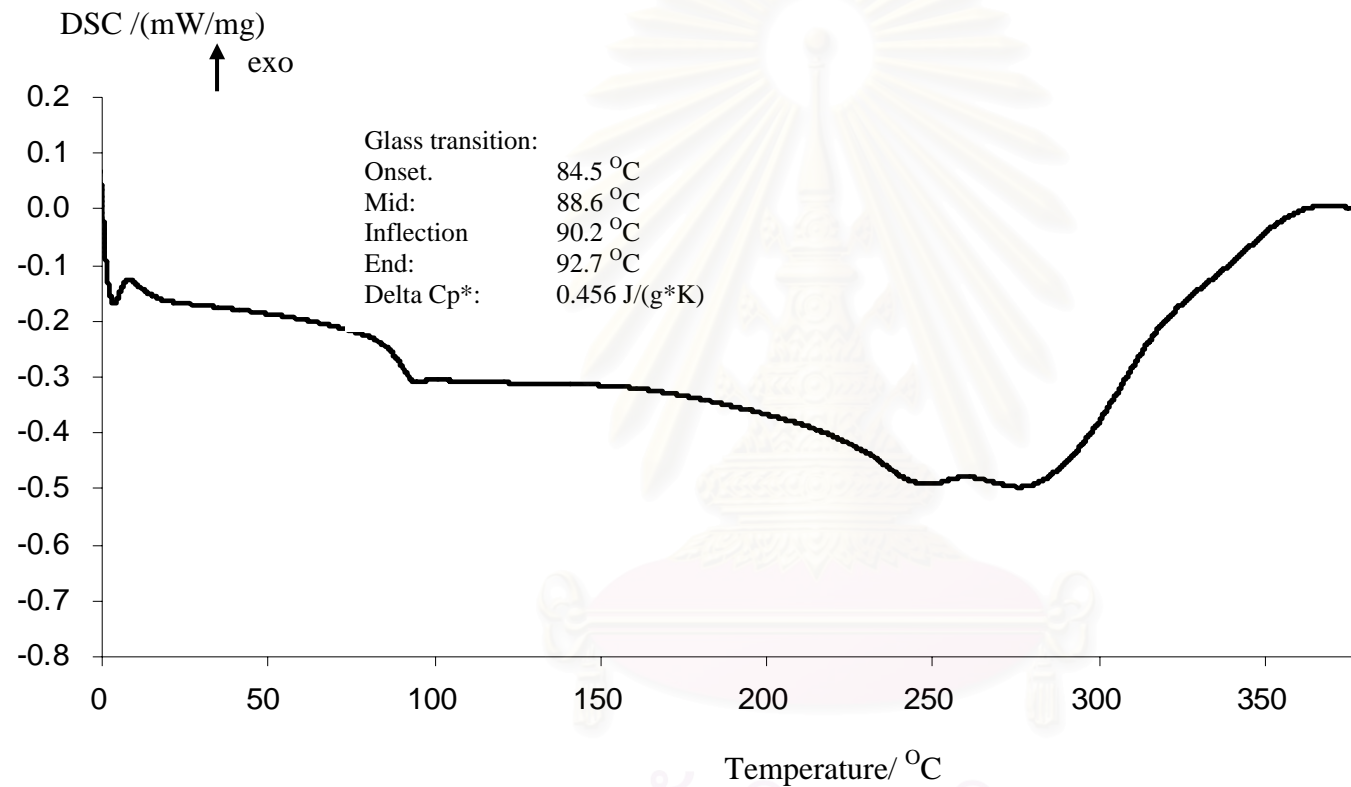


Figure A27 Thermogram of Poly(vinylalcohol-co-vinyl-4-methoxycinnamate) (Mw 50,000 Daltons, DS 0.28) (**P₅B**)

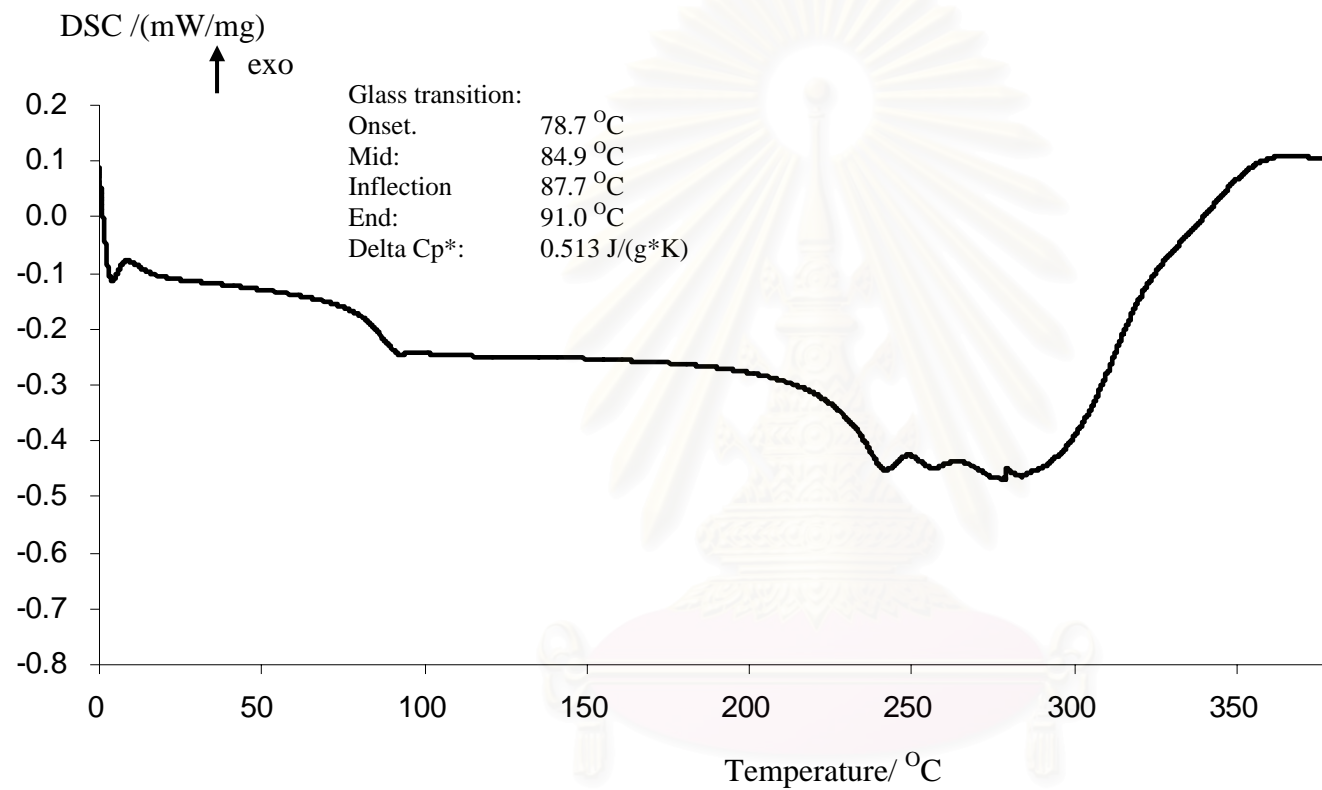


Figure A28 Thermogram of Poly(vinylalcohol-co-vinyl-4-methoxycinnamate) (Mw 10,000 Daltons, DS 0.46) (**P₉B**)

VITA

Ms. Chuleeporn Luadthong was born on February 16, 1978 in Kanchanaburi, Thailand. She got a Bachelor's Degree of Science in Chemistry from Srinakharinwirot University in 2000. After that, she started her graduate study a Master's Degree in Organic Chemistry at Chulalongkorn University and completed the program in 2007.

Her address is 66/146 Romklao Road, Minburi, Bangkok, 10510, Tel. 02-9150183, 081-9305322



สถาบันวิทยบริการ
จุฬาลงกรณ์มหาวิทยาลัย